To the Graduate Council:

I am submitting herewith a dissertation written by Roy Douglas Wilcox entitled "Surface Composition and Interaction of Thermally Treated White Oak with White Sprits." I have examined the final electronic copy of this dissertation for form and content and recommend that it be accepted in partial fulfillment of the requirements for the degree of Doctor of Philosophy, with a major in Polymer Engineering.

Timothy G. Rials
Major Professor

We have read this dissertation
and recommend its acceptance:

John Collier

Billie Collier

Roberto Benson

Simioan Petrovan

David Harper

Accepted for the Council:

Linda Painter

Interim Dean of
Graduate Studies

(Original signatures on file with official student records.)

Surface Composition and Interaction of Thermally Treated White Oak with White Spirits

A Dissertation
Presented for the
Doctor of Philosophy
Degree
The University of Tennessee, Knoxville

Roy Douglas Wilcox
December 2006

Acknowledgements

I would like to express my thanks and appreciation to Dr. Timothy Rials and all the members of my committee for their guidance throughout this research project. Special thanks go to Dr. John Collier for his interdisciplinary leadership role and his invaluable mentoring. Also, thanks go to Dr. Roberto Benson and Dr. Paul Phillips, who is now at the University of Cincinnati, for giving encouragement and direction. For their exceptional technical support, I am grateful to Johnny Jones of the Chemistry Department, University of Tennessee, and Larry Schaffer of Shimadzu, Inc. I would also like to thank Joseph Zimlich, Director of Process Development, and Theodore Lioutas, Vice President of Research and Development, at Brown-Forman for providing samples and enthusiastically promoting an understanding of the science behind the age-old art of spirit production.

In addition, I would like to acknowledge Dr. Nancy Moody, President, and Dr. Michael Clyburn, Provost, of Lincoln Memorial University for the university's professional and financial support. Last but certainly not least, I would like to thank my wife Sally for seeing me through this entire endeavor.

Abstract

The surface composition and energy of two thermally treated white oak stave sources and the acidic composition of their white spirit extracts were studied to determine whether composition of the maturing extract could be attributed to variability in surface composition due to degradation of lignin, cellulose, and extractives with thermal treatment and extraction. The sources were from the Ozarks and Appalachia. Surface composition was determined by X-Ray photoelectron spectroscopy (XPS). Surface energy was obtained from the wicking method of contact angle determination with probe liquids and application of the van Oss geometric mean equation. Acid-base properties and composition of the white spirit extract were identified from titration plots and gas chromatographic analysis of the extract using a column for separating volatile and free fatty acids, esters, and aromatic aldehydes.

XPS results showed a minimum oxygen-to-carbon (O/C) ratio and acid-to-base ratio at 150 ^{o}C for the Appalachian oak and 200 ^{o}C for the Ozark oak. The minimum O/C ratios were compared to theoretical O/C ratios of cellulose (0.83), lignin (0.34), and extractives (0.12). A decrease in O/C ratio was interpreted as an increase in high carbon content extractives and lignin at the surface, whereas an increase was interpreted as either increased oxidation due to thermal treatment or a decrease of these materials at the surface due to extraction. Greater increases were observed in the O/C ratio for the Ozark than for the Appalachian oak upon extraction at higher thermal treatment. The acidic-to-basic composition was defined as the ratio of alcohol (R-OH) and acid (R-COOH) groups to carbonyl (C=O) and aliphatic and aromatic carbon (C-C) groups. At lower thermal treatments the Ozark oak showed little change in acid-to-base ratio. Higher acid-to-base ratios and greater increases in this ratio were observed with the Ozark samples upon extraction at the higher thermal treatments. Surface energy analysis for acidic and basic functional groups present using the wicking method of contact angle analysis and van Oss geometric mean equation showed that the minimum acid-base ratio was obtained at 150 ^{o}C for both oaks. Gas chromatographic analysis showed greater activity upon extraction in the Ozark extract as evidenced by more peaks with greater signal strength.

Table of Contents

1.0 Introduction 1

1.1 Objectives of the Research 4

2.0 Background 5

2.1 Wood Structure 5

2.2 Wood Chemistry and Structural Composition 9

3.0 Surface Chemical Techniques for Analyzing Wood 14

3.1 XPS Curve Fitting 17

3.2 Lewis Acid-Base Properties from XPS Functional Group Composition 21

3.3 Contact Angle and Surface Energy Analysis 22

3.4 Methods for Contact Angle Analysis 25

3.5 The Wicking Method for Contact Angle Analysis 28

3.6 Potentiometric Titration of Alcohol Extracts Using Gran Plot 29

4.0 Materials and Methods 33

4.1 Materials 33

4.2 XPS Method Analysis 34

4.3 Contact Angle Analysis by the Wicking Methods 35

4.4 Fourier Transform Infrared (FTIR) Analysis 36

4.5 Acid-Base Titrations Using a Gran Plot 36

4.6 Gas Chromatography 36

5.0 Results and Discussion 38

5.1 XPS and Charging in Insulating Materials Such as Wood 39

5.2 FTIR of Wood and Functional Group Assignments 40

5.3 XPS Survey Scans and Oxygen-to-Carbon (O/C) Ratios of Thermally Treated White Oaks 42

5.3.1 Mass Loss of White Oak with Thermal Treatment 44

5.3.2 Effect of 60% Aqueous Ethanol Extraction on O/C Ratios 45

5.3.3 Comparison of O/C Ratio Changes with Functional Group Compositional Changes for Thermal Treatments 45

5.3.4 Comparison of O/C Ratio Changes with Functional Group Composition for Thermally Treated and Extracted White Oaks 49

5.3.5 Comparison of Functional Group Changes for Charred White Oak Barrel before and after Extraction for Seven Years 55

5.4 Acid-Base Ratios of Thermally Treated and Extracted Oak....55

5.5 Contact Angle Results and Acid-Base Surface Energy Analysis of Thermally Treated Oak....58

5.6 Analysis of XPS and Surface Energy Acid-Base Ratios 63

5.7 Titration Analysis of White Oak Extract After Six Weeks of Aging 63

5.8 Gas Chromatographic Analysis of White Spirit Extract of the Thermally Treated Oaks....65

5.9 Relationship Between Surface Composition, Surface Energy, and Spirit Extract Composition 77

6.0 Conclusions 80

List of References 83

Appendix 89

Vita 100

List of Tables

Table 1. Peak positions and functional group assignments for XPS of wood. 20

Table 2. Surface free energy parameters of liquids from van Oss and Della Volpe.....23

Table 3. Properties of hexane for pore radius determination in the wicking method. 30

Table 4. Observed FTIR Bands and functional group assignments of Appalachian control. 41

Table 5. Contact angle values of Appalachian and Ozark oak obtained from the wicking method. 59

Table 6. Surface free energy on two oaks using Della Volpe parameters. 60

Table 7. Surface free energy on two oaks using van Oss Parameters.....60

Table 8. Surface energies calculated for water-formamide pair. 61

Table 9. Surface energies calculated for water-ethylene glycol pair. 61

Table 10. Contact angle of alcohols on thermally treated Ozark oak. 62

Table 11: Summary of titration data on Appalachian and Ozark oak.....65

Table 12. Concentrations of components for thermally treated oak extracts.....67

Table A. 1. Appalachian oak XPS Peak Positions……98

Table A. 2. Ozark oak XPS Peak Positions.....99

List of Figures

Figure 1. Cross section of white oak tree trunk (Miller, 1999). 5

Figure 2. Top view of stave with annual rings oriented to the radial plane (stave face). 6

Figure 3. Transverse (A), radial (B), and tangential (C) surface plane of a wood cut (Miller, 1999). 6

Figure 4. Wood cell structure (Palviainen, 2003). 7

Figure 5. SEM Micrograph of Ozark Oak after 2 hours thermal treatment at 200 ^{o}C. 8

Figure 6. Tyloses found in white oak (Wheeler, 1996). 8

Figure 7. Contribution of cell wall components to spirit maturation (Mosedale, 1998). 9

Figure 8. Relative proportions of wood components in cell wall structures (Palviainen, 2003). 10

Figure 9. Structure of a hardwood type lignin (Maga, 1989). 10

Figure 10. Homolysis of lignin to form phenethyl and phenoxy radical (Braun, 2005). 12

Figure 11. Hydrogen abstraction and rearrangement of phenethyl and phenoxy radicals from homolysis of lignin (Braun, 2005). 12

Figure 12. Whiskey lactone (a), vanillin (b), and eugenol (c). 13

Figure 13. XPS spectrum of cellulose (a), lignin (b), and stearic acid (c) (Shchukarev, 2002). 15

Figure 14. Prior to deconvolution of XPS for Appalachian oak control. 18

Figure 15. After deconvolution of XPS for Appalachian oak control. 18

Figure 16. Contact angle of a liquid against a solid surface. 25

Figure 17. Illustration of Wilhelmy slide method for measuring contact angle of a liquid against a uniform rectangular surface. Redrawn from Walinder (2000). 26

Figure 18. Plot of force versus immersion depth for Wilhelmy slide method. 27

Figure 19. Washburn plots for hexane and several other probe liquids against heat treated oak. 30

Figure 20. Gran plot of spirit with 0.1 N NaOH. 32

Figure 21. XPS of white oak before neutralizer use. 38

Figure 22. XPS of white oak using neutralizer. 39

Figure 23. FTIR of Appalachian control with labeled peak positions. 40

Figure 24. FTIR of Appalachian and Ozark Oak at 250 C showing shift in C=O. 41

Figure 25. XPS Survey Scan for atomic ratios of carbon and oxygen. 42

Figure 26. O/C ratio of thermally treated Appalachian Oak.....43

Figure 27. O/C ratio of thermally treated Ozark oak.....43

Figure 28. Mass loss of two oaks versus thermal treatment. 44

Figure 29. O/C ratio of thermally treated Appalachian oak before and after extraction. 46

Figure 30. O/C ratio of thermally treated Ozark oak before and after extraction.....46

Figure 31. O/C Ratio versus C-C+C0 fraction, all samples. 47

Figure 32. Composition of Appalachian oak with thermal treatment.....48

Figure 33. Composition of Ozark oak with thermal treatment. 49

Figure 34. Ozark oak before extraction. 50

Figure 35. Ozark oak after extraction. 50

Figure 36. Appalachian oak before extraction.....51

Figure 37. Appalachian oak after extraction. 51

Figure 38. Heavy char oak before extraction. 53

Figure 39. Heavy char oak after extraction. 53

Figure 40. Appalachian oak composition before and after extraction. 54

Figure 41. Ozark oak composition before and after extraction. 54

Figure 42. O/C ratio of charred white oak before (1) and after (2) extraction.....56

Figure 43. Functional group composition of charred white oak before (1) and after (2) extraction.....56

Figure 44. Acid-base composition of Appalachian oak from XPS.....57

Figure 45. Acid-base composition of Ozark oak from XPS. 57

Figure 46. Acid-base (a/b) ratio of XPS versus surface energy.....64

Figure 47. O/C ratio versus surface energy a/b ratio. 64

Figure 48. Gas chromatogram of flavor standards. 66

Figure 49. Gas chromatogram of Ozark oak control and white spirits after 6 weeks aging. 67

Figure 50. Gas chromatogram of Ozark control after white spirits subtraction. 69

Figure 51. Gas chromatogram of Appalachian control after white spirits subtraction. 69

Figure 52. Gas chromatogram of Ozark 150 °C after WS subtraction. 70

Figure 53. Gas chromatogram of Appalachian 150 °C after WS subtraction. 70

Figure 54. Gas chromatogram of Ozark 200 °C after WS subtraction. 71

Figure 55. Gas chromatogram of Appalachian 200 °C after WS subtraction. 72

Figure 56. Gas chromatogram of Ozark 250 °C after WS subtraction. 73

Figure 57. Gas chromatogram of Appalachian 250 °C after WS subtraction. 73

Figure 58. Gas chromatogram of a mature spirit. 74

Figure 59. Gas chromatogram of charred white oak after extraction. 74

Figure 60. Spider chart of extract components for control. 75

Figure 61. Spider chart for extract components at 150 °C. 76

Figure 62. Spider chart for extract components at 200 °C. 76

Figure 63. Spider chart for extract components at 250 °C. 77

Figure 64. Extract a/b ratio versus surface energy a/b ratio. 78

Figure 65. Extract a/b ratio versus a/b and O/C ratio from XPS. 79

Figure A. 1. XPS scan of Ozark control before extraction. 90

Figure A. 2. XPS of Ozark control after extraction 90

Figure A. 3. Appalachian oak control before extraction 91

Figure A. 4. Appalachian oak after extraction. 91

Figure A. 5. Ozark oak 150 °C before extraction. 92

Figure A. 6. Ozark oak 150 °C after extraction 92

Figure A. 7. Appalachian oak 150 °C before extraction 93

Figure A. 8. Appalachian oak 150 °C after extraction. 93

Figure A. 9. Ozark oak 200 °C before extraction. 94

Figure A. 10. Ozark oak 200 °C after extraction. 94

Figure A. 11. Appalachian oak 200 °C before extraction 95

Figure A. 12. Appalachian oak 200 °C after extraction. 95

Figure A. 13. Ozark oak 250 °C before extraction. 96

Figure A. 14. Ozark oak 250 °C after extraction. 96

Figure A. 15. Appalachian oak 250 °C before extraction 97

Figure A. 16. Appalachian oak 250 °C after extraction. 97

Nomenclature

A	wetted perimeter area, m^2
B	concentration of strong base, M
cosθ	contact angle of liquid solid
E_b	binding energy
E_k	electron kinetic energy
F	force required to partially submerge a smooth plate in Wilhelmy slide, mN
g	gravitational constant, 9.80 ms^2
h	immersion depth in Wilhelmy slide or height rise in wicking experiment, m
hυ	energy of incident photon
$[H^+]$	hydrogen ion concentration, $molesL^{-1}$
K_W	water dissociation constant, $1x10^{-14}$
K	slope of line obtained in wicking experiment with Washburn equation
P	perimeter of the wetted plate in Wilhelmy slide surface tension
R_D	mean hydrodynamic radius in Poiseuille's equation
R_e	mean pore radius in Washburn's equation for wicking rate
v	volume of strong base for titration, ml
V	volume of acid, ml
W_A^{Tot}	work of adhesion total of liquid on a solid surface, mNm^{-1}
W_A^{LW}	work of adhesion due to Lifshitz-van der Waals forces, mNm^{-1}
W_A^{AB}	work of adhesion due to lewis acid-base interactions, mNm^{-1}
γ_{H^+}	hydrogen ion activity coefficient
γ_L^{Tot}	surface tension of liquid-vapor mNm^{-1}
γ_S^{LW}	surface energy of solid due to Lifshitz-van der Waals forces, mNm^{-1}
γ_L^{LW}	surface energy of liquid due to Lifshitz-van der Waals forces, mNm^{-1}
γ_S^{AB}	surface energy of solid due to Lewis acid-base components, mNm^{-1}
γ_L^{AB}	surface energy of liquid due to Lewis acid-base components, mNm^{-1}

γ_S^+	surface energy of solid due to Lewis acidic (electron-acceptor), mNm^{-1}
γ_S^-	surface energy of solid due to Lewis basic (electron-donor), mNm^{-1}
γ_L^+	surface energy of liquid due to Lewis acidic (electron-acceptor), mNm^{-1}
γ_L^-	surface energy of liquid due to Lewis basic (electron-donor), mNm^{-1}
ρ	liquid density, Kgm^{-3}
v	flow velocity, ms^{-1}
η	viscosity, Nsm^{-2}

1.0 Introduction

Oak casks have been used for centuries for flavoring and transporting distilled beverages. Since the maturation of distilled spirits in oak casks requires many years, it represents a significant investment in time and money for spirit manufacturers. Spirit maturation is a complex process involving both extraction and chemical reactions of the distillate with the innermost charred layer as well as the remaining material that makes up the rest of the cask. The distillate contains congener alcohols that undergo reactions either on their own or with the wood. Seasoning, toasting, and charring of the oak modify lignin, cellulose, hemicelluloses, and extractives to form a multitude of compounds that impart aromas and flavors during maturation. Very little is understood about the nature of the thermally treated oak and its influence on oak-derived compounds that contribute to the overall character of the matured spirit. The compositional characteristics of the oak and thermal process conditions are highly variable, making their effects difficult to study (Mosedale, 1998; Maga, 1989).

A number of authors have addressed the change in chemical composition of the maturing distillate with time in order to better understand the maturation process. Reazin (1981) found that the greatest congener change, except for esters, occurs in the first year of aging. He also observed that esters continually increase with maturation time after the first year. In an early study of the effects of barreling proof on the aging of American whiskeys, Boruff and Rittschof (1959) observed that higher alcohol proofs were lower in total extract, acids, and esters. Later, Reazin also observed that higher entry proof results in a decrease in barrel-derived congeners. Conner and Paterson (1993) studied the change in wood extractives from oak cask staves through maturation of scotch malt whisky by analyzing extracted wood samples at 5 mm intervals from the inner char surface to a depth of 25 mm. They noted that aromatic aldehydes and acids were reduced in the first 20 mm of the stave and their maxima shifted towards the center of the stave. In a comprehensive review, Maga (1989) lists numerous studies that summarize compounds identified in the acidic and basic fractions of alcohol soaked oak. Nishimura (1983) investigated the aromatic aldehydes content of heated oak chips. He found that the

aromatic aldehydes content increased with heating temperature, with actual charring resulting in lower amounts, probably due to carbonization of the aromatics. Additional studies have examined the use of pyrolysis-mass spectrometry in assessing whiskey quality with the oak cask (Reid, 1993). Others have looked at how successive use of oak barrels affects the oak-related volatile compounds in wine (Gomez-Plaza, 2004). According to Mosedale and Puech (1998), there is much repetition in the literature with the same compounds being studied by different techniques with limited proof of their organoleptic role. In addition, they assert that relatively few studies have explored the relationship between the role of concentration and composition of oak-derived compounds on the flavor of drinks. One of the dilemmas facing researchers in the field is the amount of resources required to conduct long-term maturation studies. Even though improved separation and identification techniques have helped in compound identification, the large number of compounds formed in the maturation process makes it difficult to establish their roles in spirit quality, which is still primarily assessed by sensory evaluation.

Until now, assessment of the type of compounds formed in the maturing spirit has not been related to the wood surface composition and surface energy. Wood surface composition and energy are dependent on the macromolecular substances present in wood that are in various stages of degradation due to weathering and thermal treatment. The composition of the maturing spirit is, for the most part, a function of the interaction of the white spirit with the functional groups present in the wood. Surface composition and surface energy provide valuable information about the interaction and driving force for removal of acidic and basic compounds. Through evaluation of surface composition and energy, researchers can better understand how thermal treatment affects different oaks and influences the composition of the maturing extract.

Surface spectroscopic techniques, such as X-Ray photoelectron spectroscopy (XPS) and Fourier transform infrared (FTIR) spectroscopy, have been used to investigate functional group composition present in the following types of wood samples:

- a number of wood species before and after extraction (Nzokou, 2005),
- a living tree under tension (Shchucarev, 2002),

- mechanically treated wood (Sinn, Reiterer, 2002; Jaic, 1996),
- weathered composite wood (Stark, 2004),
- inactivated wood from high temperature drying (Sernek, Glasser, 2004), and
- wood charcoal (Nishimiya, 1998).

XPS is particularly well-suited for analyzing subsurface acid-base properties (Shen, 1998). It is also used to study the effect of oxidation treatments on the change in surface composition and wettability of carbon fibers in composite materials (Riviere, 1998). Surface spectroscopic techniques are often applied with contact angle studies to understand the strength of interaction of a fluid or coating with a given surface composition based on its acid-base properties (Jaic, 1996; Gindl, 2002; de Meijer, 2000). Additional studies have assessed the significance of wood acidity from surface energy by comparing it to classical acidity measurements (Gindl, 2002).

Contact angle analysis and FTIR are other surface chemical techniques that can be used to study modifications to the wood surface, subsurface, and bulk composition. The contact angle method provides information about surface wetting characteristics that can be attributed to the acidic and basic surface energy resulting from surface functional group composition. While XPS gives relative functional group composition of the subsurface, FTIR provides qualitative information about functional groups present in the bulk composition (Shen, 1998).

All of these surface chemical techniques are tools for identifying the effect of thermal treatment or other modifications of wood on its surface composition and surface energy (Nishimiya, 1998; Sernek, Glasser, 2004; Liu, Rials, 1998). In addition to surface chemical techniques, gas chromatography can be a useful tool for analyzing the maturing extract to understand the relationships among surface composition, surface energy, and acid-base composition of the maturing extract. Determination of the surface and subsurface functional group composition of thermally treated and extracted white oak provides information about the nature and relative amounts of bonds arising from carbohydrate, lignin, and extractive materials. This information is important because the aroma and flavor compounds derived from wood during thermal treatment arise from degradation of carbohydrates, lignin, and extractives and their interaction with the

maturing spirit (Mosedale, 1998). Comparison of the thermally modified wood's surface composition and acid-base surface energy to the maturing extract's composition and acid-base properties can help to differentiate surface modification effects on raw material sources and the maturing extract.

1.1 Objectives of the Research

This research explores the role that surface functional group composition, acid-base properties, and surface energy of thermally treated white oak plays in the volatile acid, ester, and vanillin formation in a white spirits extract. The primary objective is to determine whether composition of the maturing extract can be attributed to differences in surface composition. These differences are due to degradation of lignin, cellulose and extractives resulting from variations in thermal treatments, white spirit extractions, and white oak sources.

To reach this objective, two thermally treated white oaks identified as from Appalachia and the Ozarks were analyzed to see if they could be differentiated by their surface composition, surface energy, and volatile acid, ester, and vanillin formation. Species differentiation, which would require a large number of samples, is not an objective of this work.

2.0 Background

2.1 Wood Structure

Wood is characterized by a complex hierarchical structure at the macroscopic and cellular level. Figure 1 shows the macroscopic organization of wood from the outer bark (A) to the inner pith (F).

Aged heartwood from white oak is quarter sawn and used to make staves for casks in spirit maturation (Mosedale, 1998). The quarter sawing process results in the early and latewood rings on average being oriented at an ideal 45-degree angle to the radial interior stave face, as shown in figure 2. The three planes of cut wood are shown in figure 3. XPS and FTIR experiments on solid wood should be run on the radial face, which is the same orientation as the inside of the barrel stave.

A) Outer bark-dry dead tissue
B) Inner bark-living tissue
C) Cambium
D) Sapwood
E) Heartwood
F) Pith
G) Wood rays

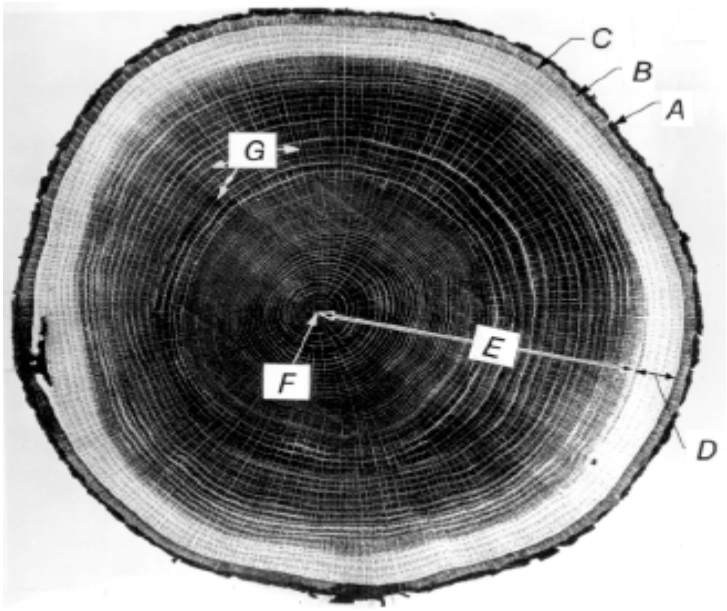


Figure 1. Cross section of white oak tree trunk (Miller, 1999).

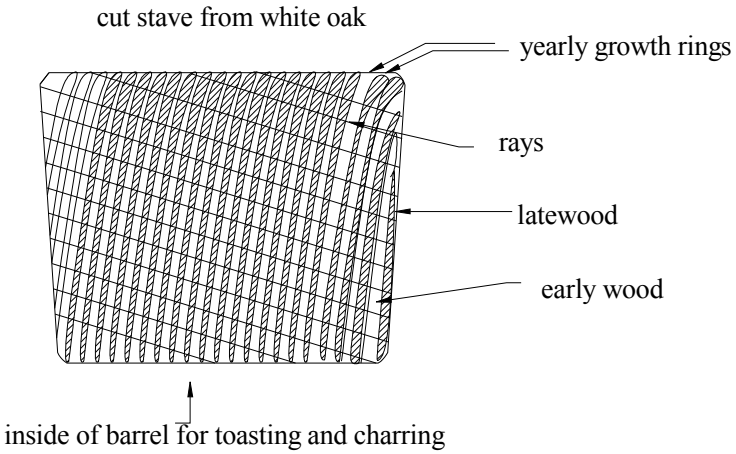


Figure 2. Top view of stave with annual rings oriented to the radial plane (stave face).

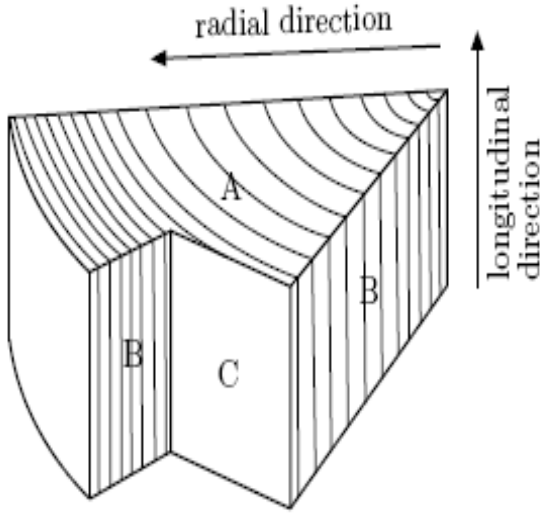


Figure 3. Transverse (A), radial (B), and tangential (C) surface plane of a wood cut (Miller, 1999).

The microscopic cellular structure of wood is an arrangement of cellulose microfibril bundles, as shown in figure 4 illustrating the middle lamella, the primary wall, the outer wall S1, middle wall S2, and inner wall S3. The concentration of cellulose in the cell walls is higher than that between cells. The cellulose molecules are oriented at different microfibril angles in different layers of the wall. Lignin serves as the primary cementing material in the middle lamella and between the cell walls (Palviainen, 2003).

The scanning electron microscopy (SEM) image in figure 5 shows the cellular structure of the Ozark oak after thermal treatment at 200^{o}C for two hours. The middle lamella M is approximately 3 microns in diameter while the S1 outer layer is approximately 0.2-0.3 microns. Cellular features are small compared to the 0.8 mm (800 micron) spot diameter used in XPS analysis. figure 6 shows an additional structural feature found in white oak called tyloses, membranes that form blocking the vessels as the growth cycle ends each year. These sac-like structures inhibit fluid migration from the white oak cask during the maturation process, making white oak the preferred wood for cask fabrication.

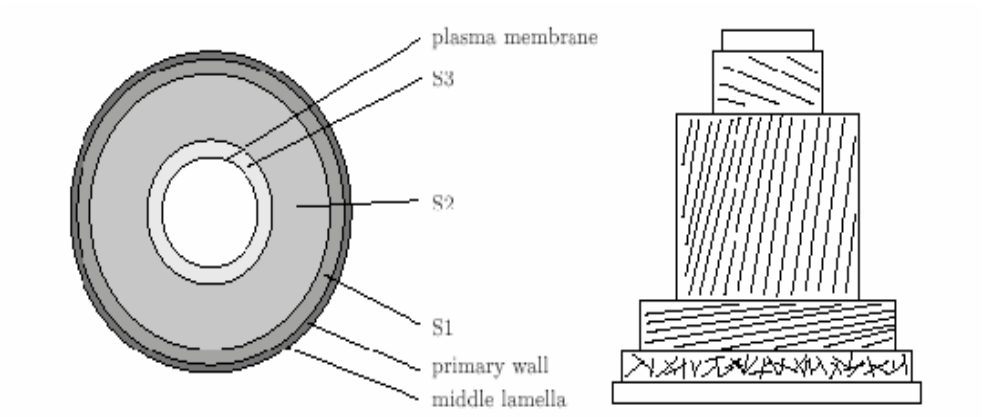


Figure 4. Wood cell structure (Palviainen, 2003).

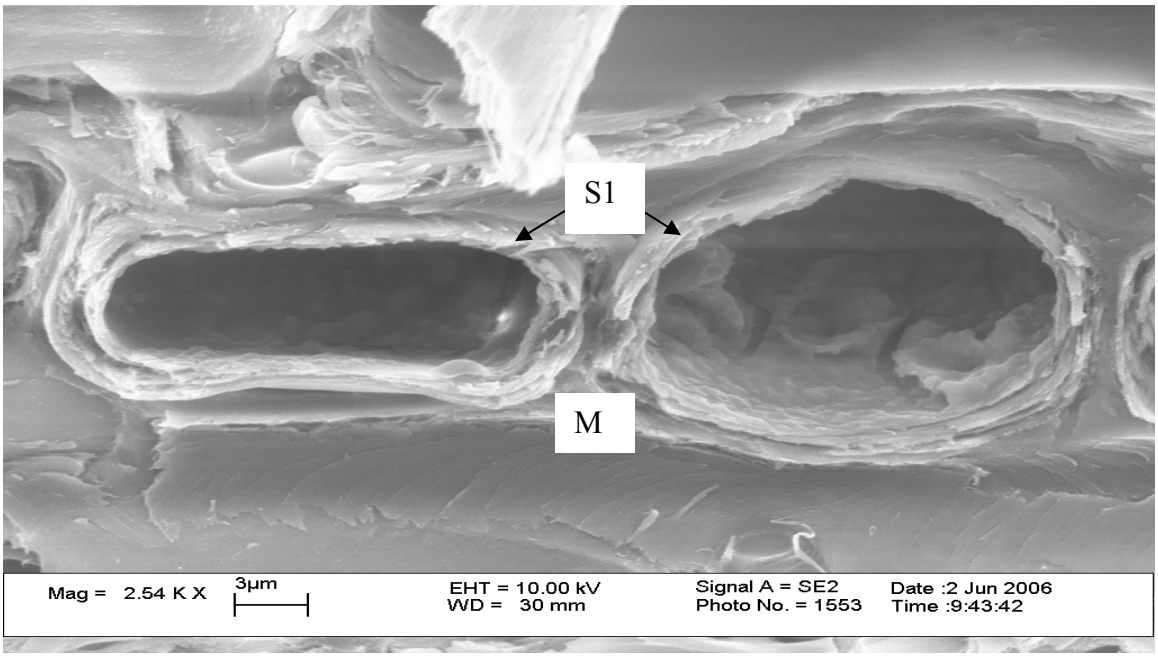


Figure 5. SEM Micrograph of Ozark Oak after 2 hours thermal treatment at 200 °C.

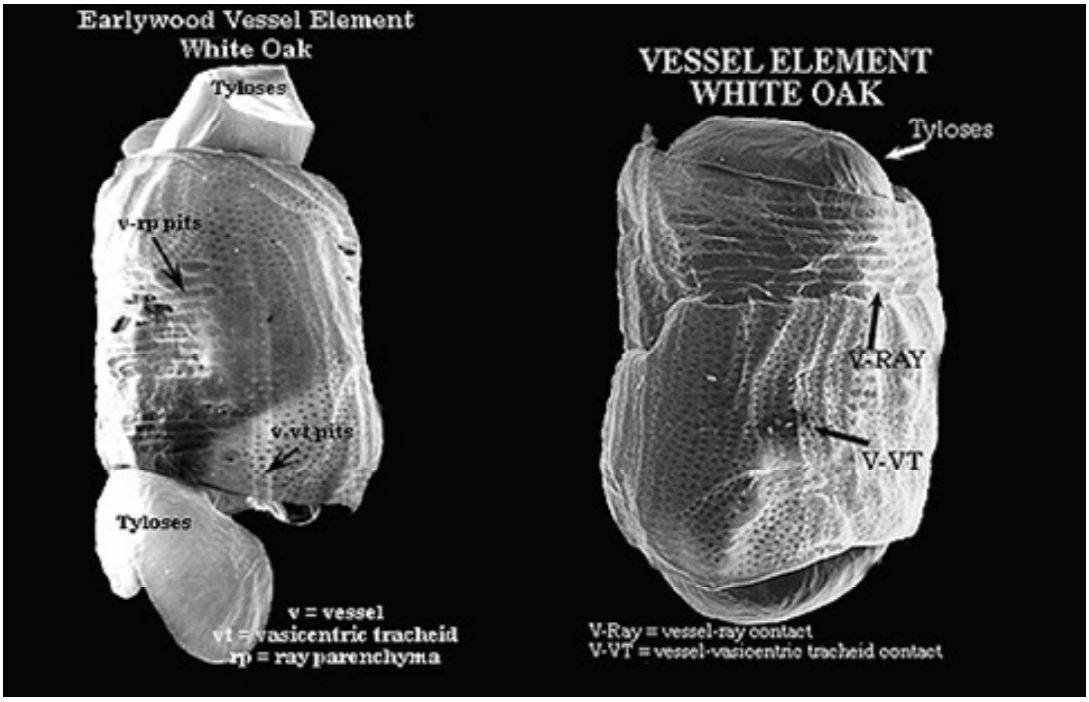


Figure 6. Tyloses found in white oak (Wheeler, 1996).

2.2 Wood Chemistry and Structural Composition

The wood cell is composed of cellulose, hemicelluloses, and lignin in the cell wall, along with extractive and inorganic materials such as minerals. Cellulose is a carbohydrate polymer composed of glucosidic repeat units, whereas hemicelluloses are small macromolecules formed from glucose and other five and six-carbon sugars. Lignin, a complex molecule formed from phenyl-propane precursors, is the glue that binds the cells together (Mosedale, 1998). Figure 7 summarizes oak wood chemical components present in the cell wall and the degradation products formed during spirit maturation that contribute to aroma and flavor.

These composite materials exist at different relative proportions in the different cell wall structures, as shown in figure 8. The central lamellar layer (CML) contains primarily lignin. Softwood and hardwood lignin in figure 9 differ in that softwoods have more syringylpropane units than guaiacylpropane units. The net result is that hardwood has more intermolecular bridging cyclic units than does softwood (Maga, 1989).

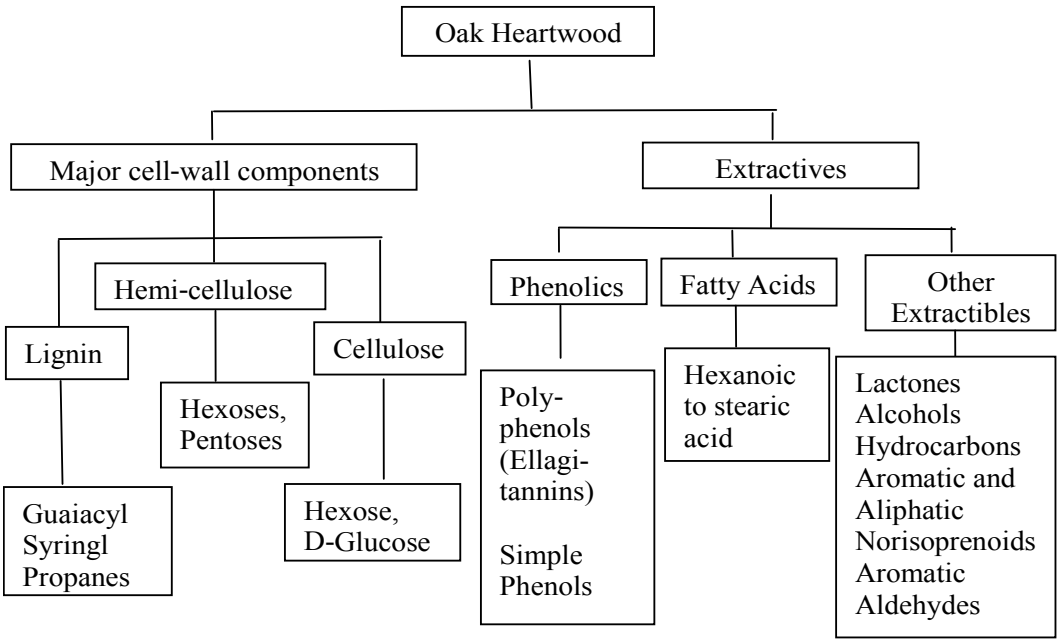


Figure 7. Contribution of cell wall components to spirit maturation (Mosedale, 1998).

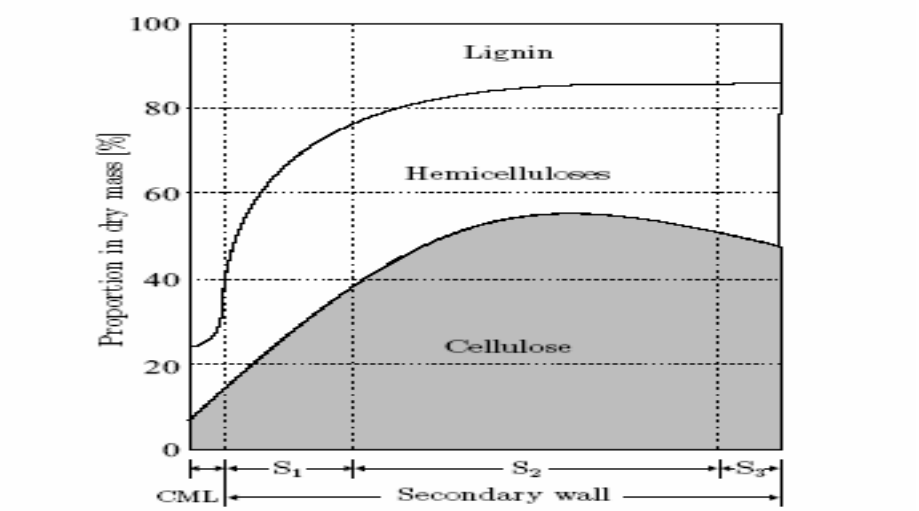


Figure 8. Relative proportions of wood components in cell wall structures (Palviainen, 2003).

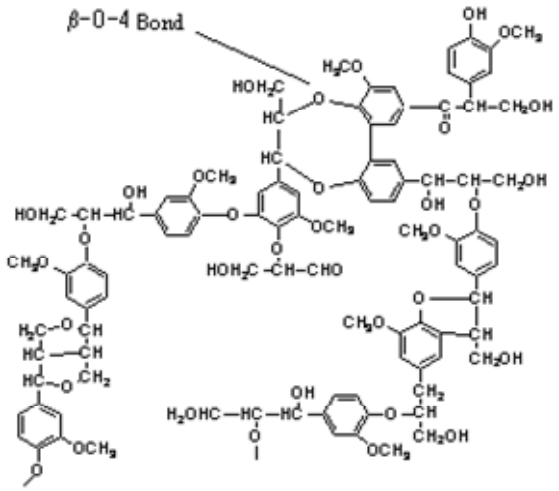


Figure 9. Structure of a hardwood type lignin (Maga, 1989).

In the thermal decomposition of lignin, homolysis of the weakest bond, the β-O-4 bond shown in figure 10, is the most likely candidate for the initial first step (Braun, 2005). The bond dissociation energies of the C-O versus the C-C bonds are approximately 65 and 72 kcal mol^{-1}. This 7 kcal mol^{-1} difference corresponds to a predicted β-O-4 cleavage rate of $>10^3$ at 375 °C (Britt, 1995, 2000). Homolysis of the β-O-4 bond forms the corresponding phenethyl (2) and phenoxy (3) free radicals (Braun, 2005).

Homolysis of the bond and formation of radical intermediates is rapidly followed by hydrogen abstraction and rearrangements to form products as shown in figure 11 (Braun, 2005; Britt, 2000). These types of rearranged products would lead directly to the formation of aromatic aldehydes and alcohols responsible for aromas and flavors in the maturing spirit.

The volatiles identified in a steam-distilled methanol extraction of oak wood shavings gave a number of aliphatic hydrocarbons, aliphatic acids, aromatic hydrocarbons, phenols, furans, lactones, and other aromatics (Nishimura, 1983). The chemical structures of an ester, whiskey lactone, an aromatic aldehyde, vanillin, and eugenol are shown in figure 12. Chemical and thermal oxidation of hardwood lignin result in a variety of compounds, including condensed aromatic molecules with phenolic, carboxylic acid, and carbonyl functional groups. Condensed structures can then interact with ethanol to produce various aromatic aldehydes that provide unique aromas and flavors to the maturing spirit.

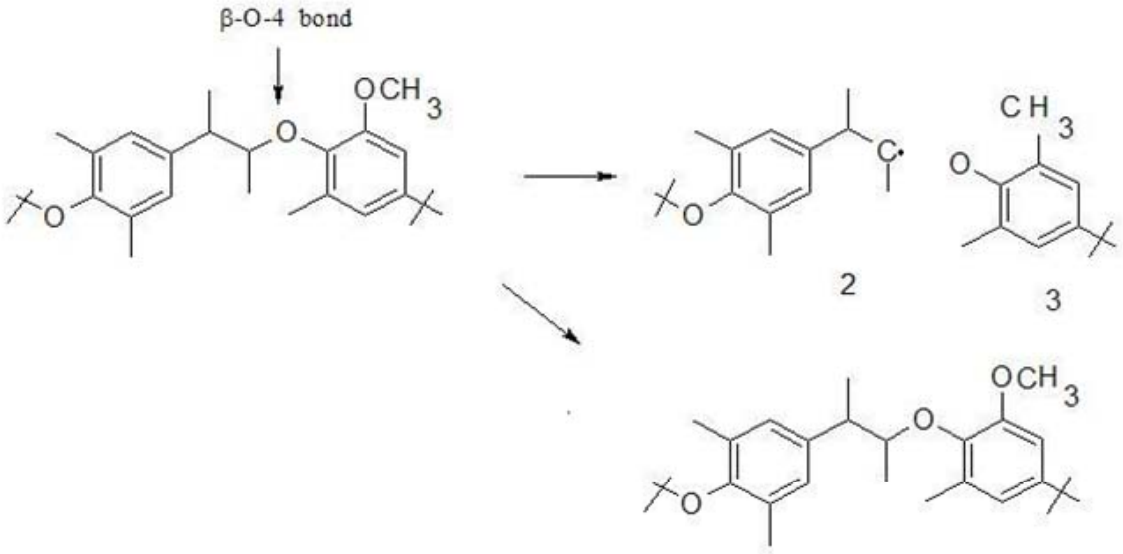


Figure 10. Homolysis of lignin to form phenethyl and phenoxy radical (Braun, 2005).

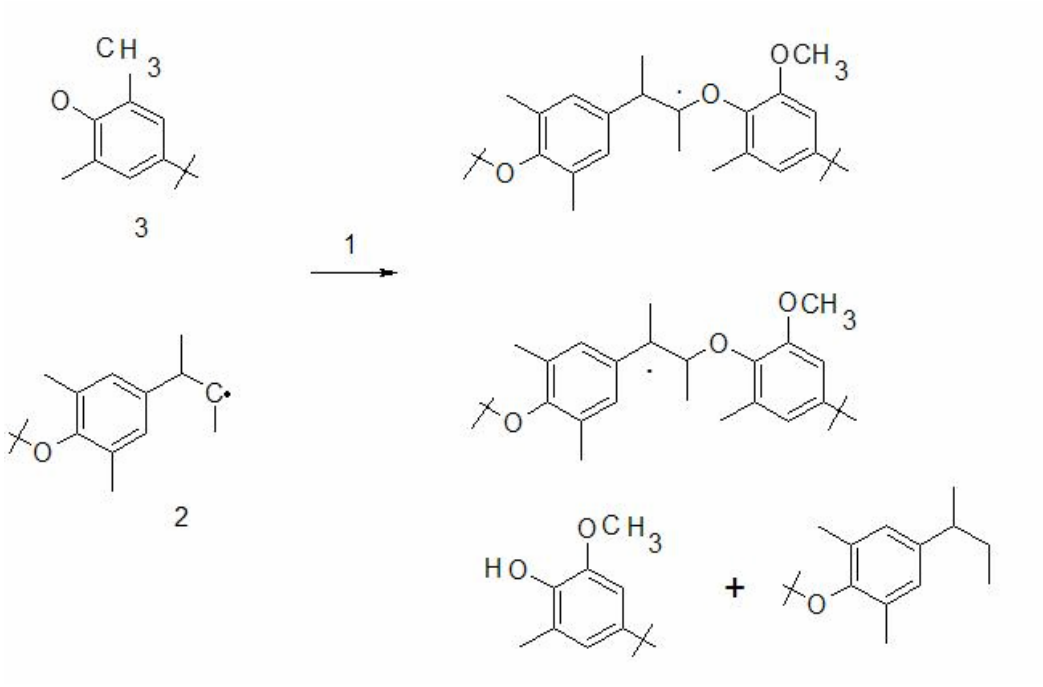
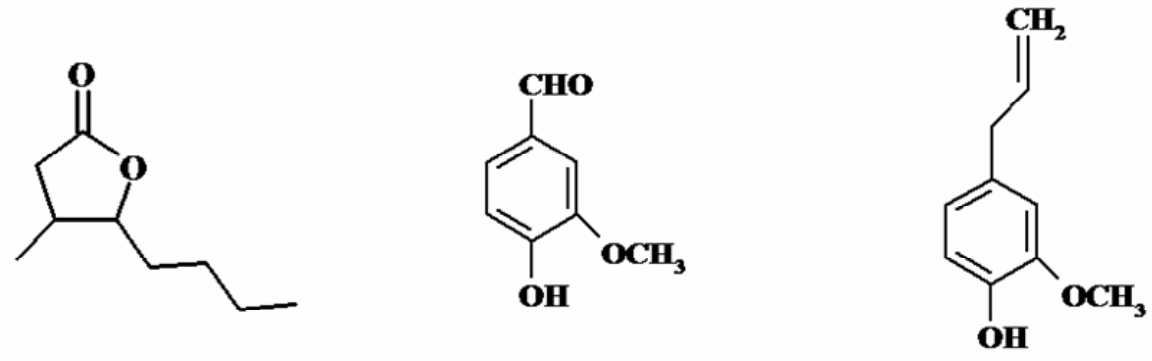


Figure 11. Hydrogen abstraction and rearrangement of phenethyl and phenoxy radicals from homolysis of lignin (Braun, 2005).



(a) (b) (c)

Figure 12. Whiskey lactone (a), vanillin (b), and eugenol (c).

3.0 Surface Chemical Techniques for Analyzing Wood

Two key surface chemical techniques for analyzing the surface structure and wettability of wood are XPS and contact angle. XPS provides information about the relative percent of oxygen-to-carbon and the oxidation state or bond type present. Both types of information are useful in understanding how surface modification and chemical interactions change the surface reactivity. Contact angle data when used with surface composition from XPS and wetting theories, such as those by Fowkes (1983), van Oss (1987), and Zisman (1963), help relate surface property information to adhesive and extractive properties of coatings and solvents with surfaces.

The survey scan in XPS from approximately 0-1000 eV is used to obtain relative atomic concentrations of elements such as carbon and oxygen. The high-resolution carbon and oxygen scan is used to obtain the relative concentrations of the various carbon oxidation states, which include aromatic carbon (C0), aliphatic carbon C-C (C1), alcohol C-OH (C2), carbonyl C=O (C3), and fatty acids COOH (C4). In figure 13 from Shchukarev (2002), a high-resolution XPS carbon scan of cellulose, lignin, and stearic acid shows the peak positions and binding energies associated with the C-C-H (285.3 eV), C-O-H (286.5 eV), O-C-O or C=O functional groups of lignin in 13b. The fatty acid in stearic acid for COOH appears at 289.5 eV in figure 13c. The deconvoluted areas under each curve give the relative concentrations for each oxidation state.

Heat treatment of hardwoods produces charcoals and activated carbons for filtering contaminants. Surface compositional analysis of such activated carbons by XPS can quantify the adsorptivity of various compounds from solution (Baker, 2005). Heat treatment of hardwoods also imparts flavor to distilled beverages through oak barrels (Mosedale, 1998; Doussot, 2000). The barrel aging and maturation process involves the release of flavor molecules as well as the adsorption of undesirable components associated with the oak wood. The XPS technique can be used to characterize quantitatively the wood surface organic functional group composition and its role in the release or adsorption of wood compounds responsible for spirit aromas and flavors.

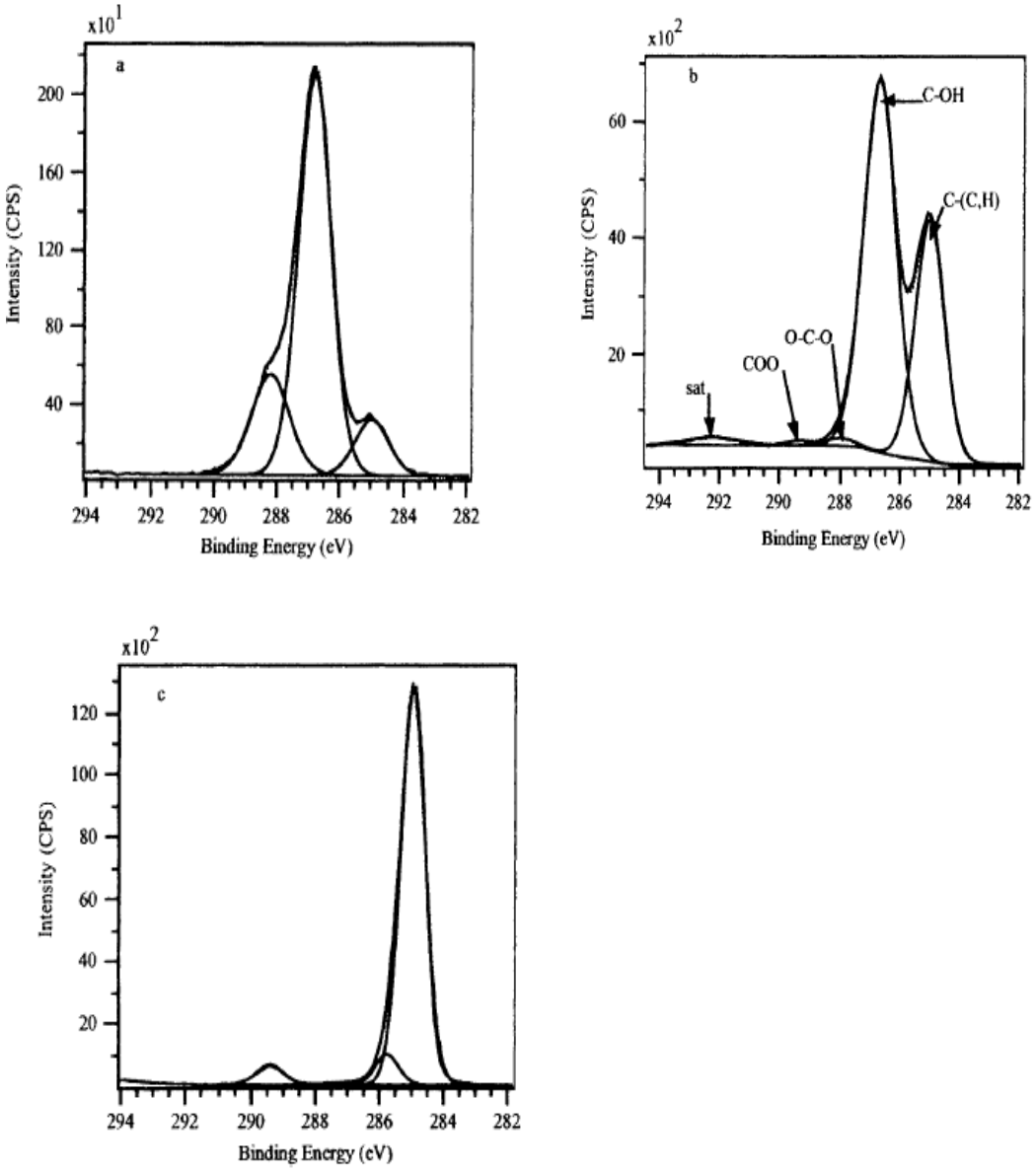


Figure 13. XPS spectrum of cellulose (a), lignin (b), and stearic acid (c) (Shchukarev, 2002).

X-Ray sources in XPS are generated by bombarding a metallic anode with high-energy electrons (10 to 15 KeV). The anode material determines the characteristic x-ray energy and the width of the x-ray line (Riviere, 1998). The most commonly used materials for XPS are Mg and Al with principal photon energies of 1253.6 and 1486.6 eV, respectively. As detailed in Riviere's Handbook of Surface and Interface Analysis (1998), the bombardment of the sample with X-Rays results in a three-step emission process:

1) the electron is promoted from its ground state to the final state above the Fermi level,
2) the electron is transported to the surface, and
3) the electron escapes into the vacuum.

In XPS the kinetic energies of the emitted electrons forming the spectral peaks are measured using an electrostatic charged-particle energy analyzer from which the binding energies of the escaping electrons can be calculated from

$$E_b = h\upsilon - E_k + \Delta\phi \qquad [3.0]$$

where E_b is the binding energy (BE) in the solid, *hv* is the energy of the incident photon, E_k is the electron kinetic energy, and $\Delta\phi$ is the difference in work functions between the sample and detector material assuming there is no electrical charging at the sample surface. Certain procedures are taken to avoid and correct for charging in insulating materials (Riviere, 1998).

The surface specificity of XPS is a result of the fact that the average net distance traveled in a solid by an electron before being inelastically scattered, the attenuation length (AL), is very short. The AL is dependent on the electron KE and the type of material, such as elements, inorganic, or organic compounds. The average depth of the photoelectrons released from the surface is about 4nm. Thus, XPS is highly surface specific.

For insulating materials, differential surface charging can cause what is really a single peak to appear as though it were a mixture of overlapping peaks. Increased sample thickness and surface roughness increase charge effects. In charging, fine structure is often not observed (Riviere, 1998). Calibration to an internal core peak can be effective

in compensating for charging effects. Charging problems can be avoided or reduced by flooding the surface with low-energy electrons from a filament near the surface. The low-energy electrons neutralize the positive charge that develops in an insulating sample when the surface electrons are ejected. In charging, the increased positive charge that develops results in a binding energy shift to higher values since electrons cannot depart the surface as readily. Care must be taken to avoid sample contamination by species emitted from the filament. The neutralizer can be set at the lowest emission settings possible to reduce sample heating by the filament. Peak shifting with increased analysis time is indicative of charging and sample decomposition. Minimizing sample time analysis can also help to avoid charging (Riviere, 1998).

3.1 XPS Curve Fitting

The peaks obtained in XPS follow a Lorentzian-Gaussian distribution. It is necessary to deconvolute the peaks of interest to obtain relative atomic percents of each bond type or carbon oxidation state. In curve fitting a high-resolution scan for the carbon 1s (C1s) core electron, a primary analysis region, deconvolution should follow a consistent pattern. Software, such as XPSPeak, simplifies the process. If a treatment process such as oxidation is conducted, the results need to make sense with respect to the process. Additional supporting information, such as FTIR spectra, is helpful in verifying peak assignments.

Before an XPS curve can be fitted, a baseline must be established. In the narrow region in which high-resolution scans such as carbon are obtained (280-300 eV), the baseline drifts upward to the left. Application of the Shirley correction provides the proper baseline. Once the baseline is established, then peaks can be added. In the current study, an initial peak for carbon was established at 285 eV but was not fixed. The subsequent peaks were given constraints such that 1.4 eV separated the peaks (Nzokou, 2005). The peak addition process was carried out until the primary peak was saturated with subpeaks as shown in figure 14. Figure 15 shows the resulting deconvolution of figure 14.

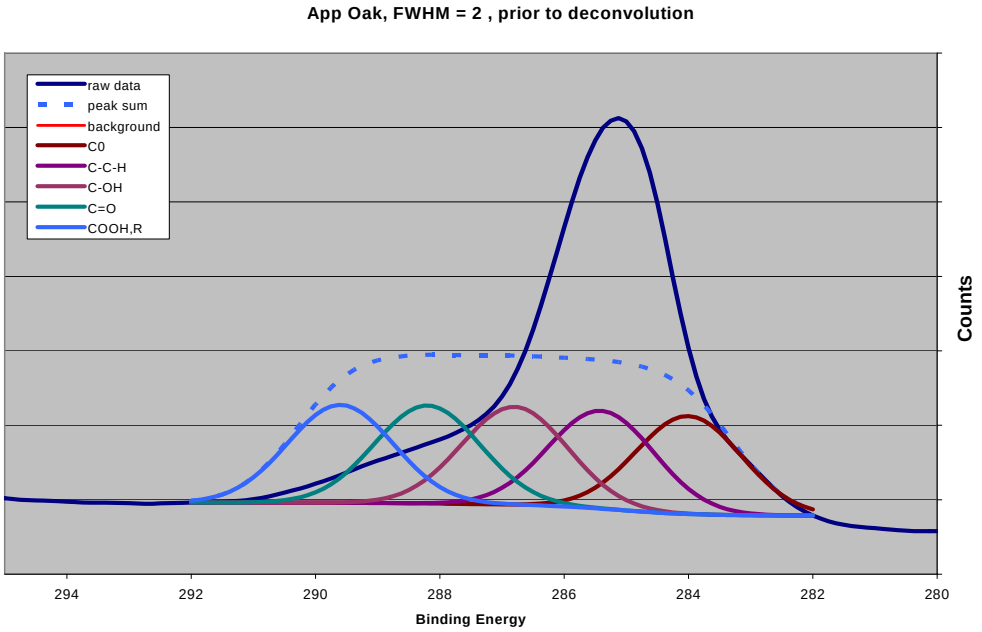


Figure 14. Prior to deconvolution of XPS for Appalachian oak control.

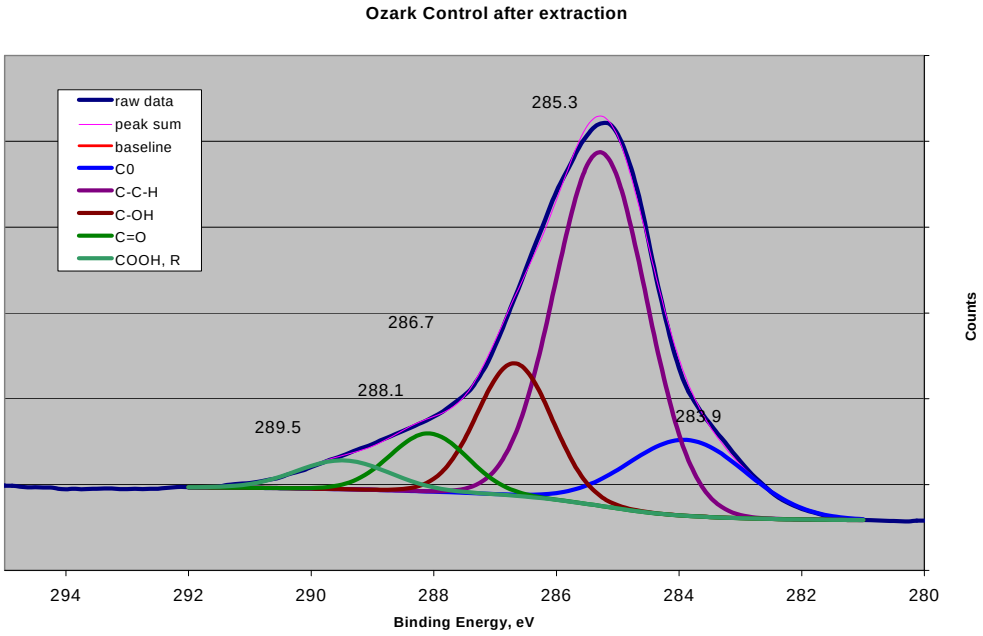


Figure 15. After deconvolution of XPS for Appalachian oak control.

The five peaks shown in figure 14 were assigned a full width at half maximum (FWHM) of 2 but were not fixed. The software varies parameters such as FWHM and the Lorentzian-Gaussian product sum until convergence is obtained. Any subpeaks with substantially different FWHM's were adjusted to obtain as nearly identical FWHM's between peaks as possible. Five peaks were required to obtain a reasonable fit with nearly equivalent FHWM's. The deconvolution procedure resulted in peaks that were obtained at positions closely observed in the literature for wood and polymers and are summarized in table 1 (Nzokou, 2005; Shchukarev, 2002; Sinn, 2001; Briggs, 1992; Nishimiya, 1998; Sernek, 2004). In addition, Briggs and Beamson (1992) provide a catalog of functional group assignments in polymers based on nearest neighbor effects.

XPS and other surface chemical techniques, such as SEM, can provide useful information about surface functional groups present in wood, its microscopic structure, and how various treatments can influence its surface wettability. Nzokou (2005) observed an increase in oxygen-to-carbon (O/C) ratios of several wood species upon extraction with different solvents due to the partial removal of high-carbon content compounds. The increase in O/C ratios was accompanied by a decrease in the C1s peak and an increase in the C2 alcohol peak, indicating a rise in cellulosic and hemicelluloses at the surface. He inferred that these changes would increase surface wettability due to the increased hydrophilic nature of the surface.

Jaic (1996) studied the surface properties of beech and oakwood by XPS, contact angle, and adhesion of a polyurethane coating. Based on low O/C ratios of 0.19, he concluded that the surface contained primarily fatty acid type extractives. He did not observe carbonyl present in oakwood from deconvolution of high-resolution scans and concluded that lignin was masked at the surface. Wettability measurements of the two woods showed that the oak was more hydrophobic, which was consistent with lower pull-off strength of a polyurethane coating.

Table 1. Peak positions and functional group assignments for XPS of wood.

C Peak #	Peak Position	Assignment	Comments
-1	280.6-283	Carbide	Carbon bound to another element, triple bond
0	284.6±0.5	graphite	aromatic and conjugated carbons, naphthalene
1	285.3±0.5	C-C-H	Saturated hydrocarbon, C-C linkages of lignin, cellulose, and extractives
2	286±0.5	CH_2OH, Ar-OH, C-O-C	Alcohol, phenol, ether linkages lignin, cellulose, and extractives
3	288±0.5	C=O	Carbonyl of lignin, extractives
4	289.5±0.5	COOH, COO	Fatty acids and esters from hemicelluloses and extractives
5	291.3-291.7	Plasmon	π transitions from conjugated bonds
O Peak			
0	531.8±0.5	C=O	Carbonyl of lignin, extractives
1	533.3±0.5	C-OH, C-O-C	Alcohol, phenol, ether linkages lignin, cellulose, and extractives
2	534.5-536.5	O, H_2O	Chemisorbed oxygen, adsorbed water

Nishimiya (1998) analyzed the structure of wood charcoal powders with XPS with increasing thermal treatment from none to 2400 ^{o}C. He observed both the graphitic and hydrocarbon peaks along with all other functional groups. He found increased graphitization with increasing temperature. Also, he was unable to obtain useful results with FTIR and NMR at the higher temperatures.

In a recent study, Glasser analyzed the inactivation of yellow poplar and southern pine wood surfaces upon high-temperature drying with XPS, contact angle, and fracture mechanics of adhesively joined surfaces with phenol formaldehyde. He found that the O/C ratio decreased and the C1/C2 ratio (C-C bond to C-OH bond) increased with drying temperatures from 160-180 ^{o}C. He also observed an increase in contact angle with drying temperature but a decrease with time. He found a species dependence both for surface composition and contact angle with lower O/C ratios experiencing greater contact angles (Sernek, Glasser, 2004).

3.2 Lewis Acid-Base Properties from XPS Functional Group Composition

Most studies of wood surface composition and wettability from XPS and contact angle analysis have focused on adhesion of coatings or glues to wood surfaces. Many surface chemistry studies apply the Lewis acid-base concept to the interaction between the material and the surface. The general approach is that Lewis acid-base sites on a surface can form an adduct with Lewis basic and acidic functional moieties of the interacting liquid.

Shen (1998) quantitatively characterized the subsurface acid-base properties of wood by XPS and Fowkes theory. He assigned Lewis acidity to the alcohol and acid groups and Lewis basicity to the carbonyl and carbon-carbon bonds. A Lewis acid is any species with a vacant orbital that can act as an electron pair acceptor. A Lewis base is a compound with an available pair of electrons, either unshared or in a π orbital. In a Lewis acid-base reaction, the unshared pair of the base forms a covalent bond with the vacant orbital of the acid (March, 2001; Sorrel, 1997). Shen obtained acid-base ratios from the Fowkes theory by using acid-base surface energy analysis from dynamic Wilhelmy slide contact angle measurements with probe liquids. Relative acidity can be expressed in terms of the pK_A , or the negative logarithm of the acid dissociation constant, K_A. The acid dissociation constant is an expression of the equilibrium constant associated with dissociation of the weak acid HA into hydrogen ion H^+ and conjugate base A^- according to $HA \rightleftharpoons H^+ + A^-$. The equilibrium constant can be written as $K_A = [H^+][A^-]/[HA]$. Greater dissociation of the weak acid HA results in larger values for K_A and hence smaller values for pK_A, the negative logarithm of K_A. As a reference point, Pk values are for fatty acids (4-5), aromatic alcohols (8-11), water (15.75), aliphatic alcohols and aldehydes (16), ketones (19-20), and aromatic rings (20-23) (March, 2001; Sorrel, 1997). Pk values for conjugated carbons run as high as 43. Shen (1998) observed that the acid-base ratio obtained by contact angle analysis was lower for the wetting measurements compared to XPS. He suggested the difference in values was due to probing depth differences of the two measurements, where the contact angle

measured the outermost surface and XPS measured the subsurface. Holmes-Farley and Whitesides (1987) reported in a series of papers that the contact angle measures the surface to a depth of approximately 1nm while XPS penetrates the subsurface to about 10 nm. The outermost region is accessed by contact angle measurements, the subsurface region by XPS, and the deeper bulk regions by IR, Raman, and UV-Visible spectroscopy.

The significance of the acidity of wood to the surface free energy components of different wood species has been examined by Gindl (2002). In these studies, wood species with varying acid-base surface free energy components, as determined from the sessile drop contact angle method, were compared to both water-soluble and water-insoluble acidity as measured by pH. Significant relationships were found between wood pH and Lewis acid-base surface energy obtained from the geometric mean equation (Gindl, 2002).

3.3 Contact Angle and Surface Energy Analysis

Interaction of wood with its environment, such as moisture vapor, adhesives, or solvents as measured through the work of adhesion from contact angle, arises from attractive intermolecular forces that can be attributed to Lifshitz-van der Waals (LW) and Lewis acid (electron acceptor) Lewis base (electron donor) interactions. Pioneering work by Zisman, Fowkes , van Oss and others in contact angle analysis of polymer surfaces with probe liquids of defined purity has resulted in a geometric mean equation that describes the total work of adhesion as a function of the combined intermolecular forces due to Lifshitz-van der Waals (LW) and acid-base (AB) interactions (Zisman, 1963; Fowkes, 1991, 1983, 1978, 1963; Berg, 1993; van Oss, 1992, 1987; Gardner, 1996). The work of adhesion is described by Young's equation on the left side of 3.1 where cos θ is the contact angle of the liquid against the solid and γ_L^{Tot} is the total surface tension of the liquid. The geometric mean equation describing the total work of adhesion, W_A^{Tot}, as a function of the individual interactions between the solid (S) and liquid (L) attributed to van Oss and Chadhury (1987) is

$$W_A^{Tot} = \gamma_L^{Tot}(1+\cos\theta) = W_A^{LW} + W_A^{AB} = 2\left(\sqrt{\gamma_S^{LW}\gamma_L^{LW}} + \sqrt{\gamma_S^{+}\gamma_L^{-}} + \sqrt{\gamma_S^{-}\gamma_L^{+}}\right) \qquad [3.1]$$

where γ represents the surface energy of the liquid or solid in mN/m, the subscripts S and L represent the solid and liquid components for the individual interactions, and the superscripts LW, +, and – are the Lifshitz-van der Waals, acidic (electron acceptor), and basic (electron donor) components of the surface energy.

Application of the van Oss-Chadhury equation has not been without controversy in that there has been debate about the values for the surface energy components assigned to the probe liquids (Della Volpe, 1997; van Oss 2002). In addition it has been noted that a total of three probe liquids, one for the LW component and two for the AB component, are not adequate for determination of acid-base surface energy values from a statistical viewpoint (Della Volpe, 1997). Papers questioning these assertions and reiterating the original approach were subsequently published by van Oss (2002) and de Meijer (2000). Probe liquid values for $\gamma_L^{Tot}, \gamma_L^{LW}, \gamma_L^{AB}, \gamma_L^{+},$ and γ_L^{-} based on van Oss and Della Volpe are summarized in table 2. Ethanol is also included since ethanol and ethanol-water mixtures were used to evaluate displacement of wood components.

Table 2. Surface free energy parameters of liquids from van Oss and Della Volpe.

Surface free energy parameters, γ_L, mN/m									
	van Oss (1994)					Della Volpe (1997)			
Liquid	γ_L^{Tot}	γ_L^{LW}	γ_L^{AB}	γ_L^{+}	γ_L^{-}	γ_L^{LW}	γ_L^{AB}	γ_L^{+}	γ_L^{-}
Water	72.8	21.8	51.0	25.5	25.5	21.8	51.0	65.0	10.0
Formamide	58.0	39.0	19.0	2.28	39.6	35.6	22.6	1.95	65.7
Ethylene glycol	48.0	29.0	19.0	1.92	47.0	31.4	16.4	1.58	42.5
Diiodomethane	50.8	50.8				50.8			
Ethanol	22.4	18.8	2.6	.019	68				

The following is a summary of how the three components of the solid surface energy ($\gamma_S^{LW}, \gamma_S^+, \gamma_S^-$) were determined from multiple polar probe liquids, which included water, formamide, and ethylene glycol. First, γ_S^{LW} must be determined for the solid surface by using a non-polar probe liquid with only the LW component and no AB component (van Oss, 2002). It should have a relatively high surface tension, such as diiodomethane, so that $\gamma_L^{LW} > \gamma_S^{LW}$. Thus, if the contact angle for the solid surface is obtained in diiodomethane, then the result is

$$W_A^{LW} = \gamma_L^{Tot}(1+\cos\theta) = 2\left(\sqrt{\gamma_S^{LW}\gamma_L^{LW}}\right). \qquad [3.2]$$

For a non-polar liquid of known properties for $\gamma_L^{Tot} = \gamma_L^{LW}$ and contact angle, then γ_S^{LW} can be determined. Once γ_S^{LW} is found using equation 3.2 , then $2\left(\sqrt{\gamma_S^{LW}\gamma_L^{LW}}\right)$ is determined for a series of acid-base probe liquids where the parameter for γ_L^{LW} for each acid-base probe liquid is known (Table 2). From equation 3.1, then

$$W_A^{AB} = W_A^{Tot} - W_A^{LW} \qquad [3.3]$$

is obtained. By transformation of equation 3.1, when γ_S^{LW} is known, the equation

$$W_A^{AB} = 2\left(\sqrt{\gamma_S^+\gamma_L^-} + \sqrt{\gamma_S^-\gamma_L^+}\right) \qquad [3.4]$$

can be rearranged to equation 3.5

$$\frac{W_S^{AB}}{2\sqrt{\gamma_L^-}} = \sqrt{\gamma_S^+} + \sqrt{\gamma_S^-}\left(\sqrt{\frac{\gamma_L^+}{\gamma_L^-}}\right). \qquad [3.5]$$

A plot or least squares regression of the left hand side versus the right gives an intercept of $\sqrt{\gamma_S^+}$ and a slope of $\sqrt{\gamma_S^-}$. Thus, if the solid surface is unknown, then by using multiple acid-base probe liquids of known values for $\gamma_L^{Tot}, \gamma_L^{LW}, \gamma_L^+,$ and γ_L^-, the solid surface energies due to the acidic and basic components, γ_S^+ and γ_S^- can be determined.

Many studies have demonstrated that the wettability and surface energy of wood are important parameters for understanding its interaction with adhesives (de Meijer, 2000; Walinder, 2000; Shen, 1998; Gardner, 1996). Other studies have explored the significance of wood acidity relative to the Lewis acid-base components of the surface free energy (Gindl, 2002). It has been noted that even though surface energy methods indicate that the basic component dominates over the acidic component in wood, classical methods for determining acidity, such as pH, show wood to be acidic. This contradiction between surface energy and classical acidity has been explained by an oxidative gradient that exists between the surface and the bulk (Shen, 1998).

3.4 Methods for Contact Angle Analysis

Contact angle analysis of a liquid against a solid surface is used to determine the solid surface energy through various approaches. Three methods available for determining contact angle of wood are the sessile drop, the Wilhelmy slide, and the wicking method. The contact angle of a liquid drop against a solid surface is represented in Figure 16. The equilibrium contact angle is represented by the acute angle, θ_e . The surface tensions of the interfaces are γ_{LV} for liquid vapor and γ_{SV} for the solid-vapor.

De Meijer (2000) has compared the three methods for the surface energy determination of wood. In the sessile drop method, the droplet angle against the wood surface is monitored with time. The angle obtained by the sessile drop method is dependent on time and whether it is measured along or with the grain.

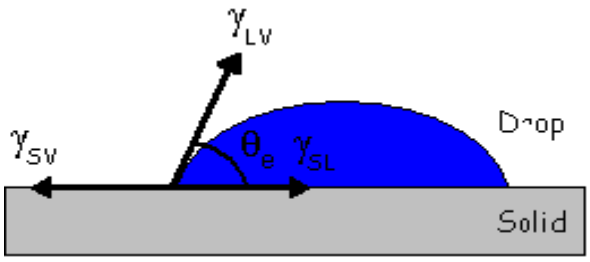


Figure 16. Contact angle of a liquid against a solid surface.

The contact angle measurement by the Wilhelmy slide method is based on a force balance of a rectangular plate as it is immersed in a liquid (Walinder, 2000). The force, F, required to submerge partially a smooth plate in a liquid is given as

$$F = P\gamma\cos\theta - \rho Ahg \qquad [3.6]$$

where P is the perimeter of the wetted plate, γ is the surface tension of the liquid, θ is the liquid-solid contact angle, ρ is the liquid density, and g is the gravitational constant. Figure 17 illustrates the force balance and wetted surface perimeter associated with the Wilhelmy slide method for contact angle determination.

In a Wilhelmy experiment for dynamic contact angle determination, a rectangular plate of known dimensions of width and thickness is immersed in a liquid of known surface tension and the force is monitored as a function of the advancing immersion depth. The plate is then retracted and the force is monitored as a function of the receding immersion depth. By conducting a regression analysis of the force versus the immersion depth, the intercept yields Pγcosθ and the advancing contact angle can be calculated.

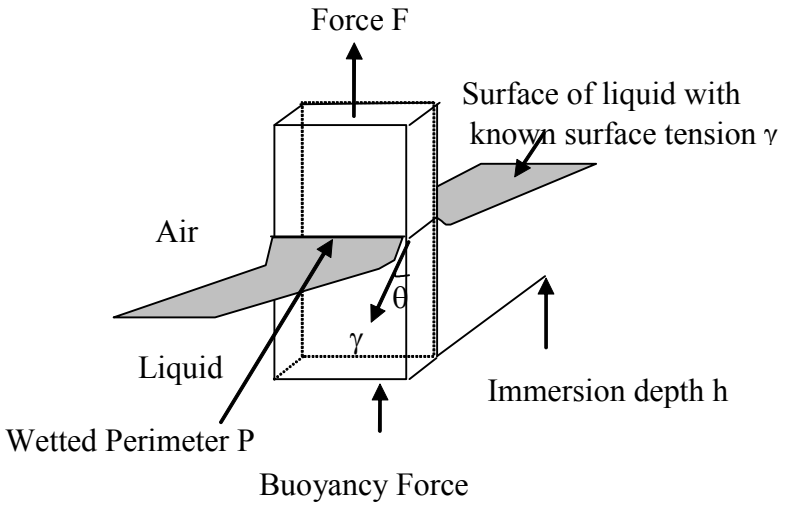


Figure 17. Illustration of Wilhelmy slide method for measuring contact angle of a liquid against a uniform rectangular surface. Redrawn from Walinder (2000).

An example of this experiment is shown in figure 18. Lines 3 and 4 represent the advancing and receding cycles used to calculate the advancing and receding contact angles. If the weight of the plate changes during an experiment due to wicking, then equation 3.6 must include a term $F_w(t)$, which is the force due to wicking and sorption at time t. The difference between 5, the force after the plate has been withdrawn from the liquid, and 1 is the force due to liquid adsorbed by the plate. The Wilhelmy method in wood is best used to obtain an initial advancing contact angle, due to problems associated with completely removing the plate and backing out the liquid amount sorbed.

The dynamic Wilhelmy slide method gives an advancing and receding contact angle by measuring a force balance with immersion depth (Gardner, 1996; Walinder, 2000). In this method, adsorption of the wetting liquid into the wood gives a contact angle that decreases upon wetting. Nevertheless, de Meijer (2000) reported consistent results in surface energy determination from contact angle analysis using the sessile drop and Wilhelmy slide method, with values ranging from 30-50 mJm^{-2}.

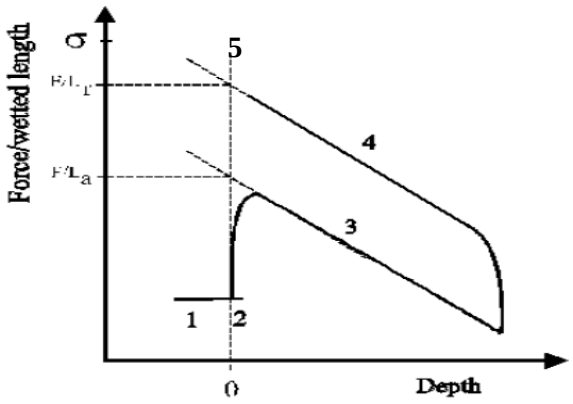


Figure 18. Plot of force versus immersion depth for Wilhelmy slide method.

3.5 The Wicking Method for Contact Angle Analysis

In the wicking method, the contact angle of the liquid is determined from the rate of rise of a liquid through a porous solid using the Washburn equation. De Meijer (2000) conducted wicking studies using only non-polar liquids because of swelling interaction with polar liquids. Walinder (2000) observed that in the wicking method the slope is linear over a certain time range for polar liquids and used the data in this range in accordance with the Washburn equation for capillary rise to obtain contact angle. Both Walinder and de Meijer observed higher contact angles with probe liquids using the wicking method compared to other methods. The wicking method cannot be used if the liquid does not wet the solid (i.e. $\theta > 90$) or if the uptake velocity is too low to be measured. Low velocities that occur with highly swelling clays and or with viscous probe liquids also prevent application of the wicking method (van Oss, 2002).

Measurements of contact angle on wood by the sessile drop and Wilhelmy slide are highly dependent on geometric factors such as surface roughness and orientation with respect to the grain (de Meijer, 2000). For this reason, the wicking method of -60+80 mesh sized wood particles was selected for contact angle determination of thermally treated white oak. The wicking method is based on the capillary rise rate of liquid through a packed column bed. The wicking method uses Washburn's equation, which is based on Poiseuille's law describing liquid flow through a capillary (Sielbold, 1997; Walinder, 2000; de Meijer, 2000):

$$v = \frac{R_D^2}{8\eta}\frac{\Delta P}{l} \qquad [3.7]$$

The Washburn equation is

$$h^2 = \frac{R_e \gamma_L \cos\theta}{2\eta} = Kt \qquad [3.8]$$

where h is height rise at time t, R_e is the mean pore radius, λ_L is the liquid surface tension, η is the viscosity, and K is the slope of the line obtained from a plot of h^2 versus t. Because both the pore radius, R_e, and the contact angle, θ, are unknown, it is

necessary to determine the pore radius with a completely wetting, non-polar liquid such as hexane where cos θ equals 1. Once the pore radius is obtained, then the contact angle can be determined. Packing of the column should be precisely controlled and a packing density determined. The packing methodology will be discussed in detail in the methods section. An example for the determination of the pore radius for a heat treated wood sample is shown in table 3. The resulting equation is

$$R_e = \frac{K \cdot 2 \cdot \eta}{\gamma_L \cdot \cos\theta} = 1.74\mu \,. \qquad [3.9]$$

Figure 19 shows the plots of h^2 versus t for hexane and several probe liquids for a thermally treated oak. The slopes were obtained from the linear portion of the plot where the Washburn equation is obeyed.

3.6 Potentiometric Titration of Alcohol Extracts Using Gran Plot

For alcohol systems containing many weak mono and diprotic acids or multiple acid species, determination of total titratable acidity can be better represented by a Gran plot that is used for determining the total acidity of wine (Rudan-Tasic, 1998). Normally, titration endpoints are taken as reaching an equivalency of $\left[H^+\right] = \left[OH^-\right]$ at a pH of 7.0 to 8.2. In a titration where pH is monitored, a volume of acid, V, is titrated with a volume v of strong base of B concentration. For individual acids, the equivalence point occurs at a sharp break in the titration curve of pH versus volume of base. With mixtures of acids, and both monoprotic and diprotic acids present, a clear break is not obtained. Often derivatives are used to obtain the endpoint, but sometimes it is difficult to determine where that endpoint occurs in systems of mixtures. A Gran plot is a graphical method that allows localization of the endpoint using data from before or after the endpoint (Crouch, 2004). With multiple weak monoprotic and some diprotic acids present that form conjugate bases, the pH for the true endpoint for different alcohol systems will vary. Moreover, the total acidity, which reflects the strong base required to reach the endpoint, will vary if the true endpoint is reflected by various pH values.

Table 3. Properties of hexane for pore radius determination in the wicking method.

Hexane	Surface tension, γ	18.0 mN/m
	Viscosity, η	3.26×10^{-4} Nsm^{-2}
From wicking experiment	Slope, K	$0.48\ cm^2s^{-1} = 4.8 \times 10^{-5} m^2s^{-1}$

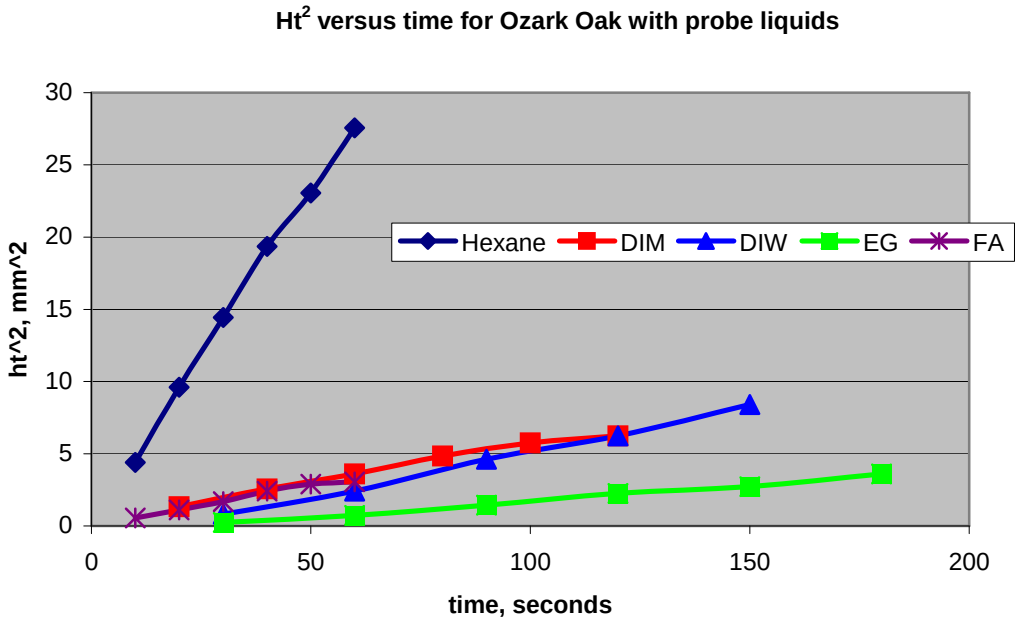


Figure 19. Washburn plots for hexane and several other probe liquids against heat treated oak.

Since alcohol systems are a complex mixture of weak acids that hydrolyze upon titration to form conjugate bases, Rudan-Tasic (1998) applied the Gran plot for the endpoint determination in the alkaline range or beyond the normal equivalence point. In the range beyond the normal endpoint v_e, v $\geq$v$_e$, where v represents titration volume, the hydrogen ion concentration is given by

$$\left[H^+\right] = \frac{K_W}{\left[OH^-\right]} = \frac{K_W\left(V+v\right)}{B\left(v-v_e\right)} \qquad [3.10]$$

where K_w is the water dissociation constant and B is the concentration of strong base. Using the relationship between hydrogen ion activity and pH of $\alpha_{H^+} = \left[H^+\right]\gamma_{H^+}, \gamma_{H^+} = 10^{-pH}$ where γ_{H^+} is the activity coefficient of hydrogen ions, equation 3.10 above leads to the equation below

$$\left[H^+\right] = \frac{10^{-pH}}{\gamma_{H^+}} = \frac{K_w(V+v)}{B\left(v-v_e\right)}. \qquad [3.11]$$

By measuring pH directly and defining a function Φ' as

$$\Phi' = \frac{B\left(v-v_e\right)}{K_w\gamma_{H^+}} = \left(V+v\right)\cdot 10^{pH} \qquad [3.12]$$

for K_w and γ_{H^+} constant, then Φ' is a linear function of v_e so that when Φ' is 0, v is equal to v_e. Thus, in plotting Φ' versus v by extrapolation of the line to the abscissa, the volume to reach the equivalence point to include the alkaline range can be obtained. Figure 20 shows a plot of pH and Φ' versus volume for an aged spirit.

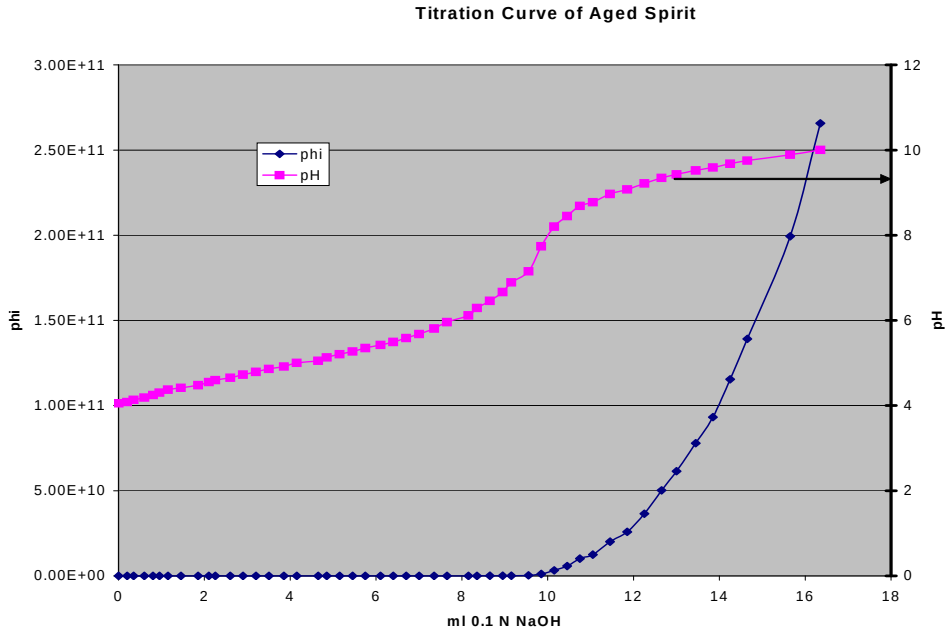


Figure 20. Gran plot of spirit with 0.1 N NaOH.

4.0 Materials and Methods

4.1 Materials

White oak staves identified as being from the Ozarks and Appalachia were obtained from a cooperage in Kentucky. The staves were taken from a fabricated cask that had not been thermally treated and identified as Appalachian 1 and 2 and Ozark 3. The original samples were received as pieces 3.25 x 5/8 x 7 5/8 inches in dimension. These pieces were cut perpendicular to the grain in 5 cm length strips and then cut with a chisel parallel to the grain to produce pieces 5x2x1 cm in dimension with the 2 cm face dimension being the radial plane. For each sample listed above, 32 pieces were prepared for thermal treatment studies. Sample masses were initially recorded, then wrapped in aluminum foil, and heated in a ceramic kiln for two hours at 150, 200, and 250 ^{o}C. The samples were removed from the oven, and final masses recorded for mass loss experiments. These samples were stored in sealed plastic bags in aluminum foil and later used for XPS, FTIR, contact angle and extraction studies with 60% aqueous ethanol (white spirits).

For extraction studies, the control and thermally treated wood strips were placed in amber bottles containing 50 ml of white spirits. The volume-to-mass ratio averaged from approximately 5.5 to 6.5 to one. All sample masses were recorded so that subsequent experiments could be referenced to volume to sample mass ratios. Samples were extracted for six weeks and then a section was split along the grain so that for XPS analysis, the radial plane could be analyzed. Five milliliter aliquots were withdrawn at this point and stored in sealed GC head space vials for titration and GC analysis.

For contact angle studies by the wicking method, high purity hexane, HPLC grade water, diiodomethane and formamide obtained from Aldrich chemical were used. For extraction studies, white spirits (60 % aqueous ethanol) obtained from a spirit manufacturer were used.

4.2 XPS Method Analysis

XPS was conducted using a Perkin Elmer PHI 5400 X-Ray Photoelectron Spectrometer with a 0.80 mm spot diameter. Samples of approximately 0.8x0.8x0.4 mm were placed in a stainless steel sample holder with the radial face positioned at 90 degrees to the Al Kα X-ray source. For XPS high-survey and high-resolution carbon and oxygen scans, the sample was analyzed on the radial face. Three high-resolution carbon scans were run on each sample at a separation distance of 1mm and the deconvolution results averaged. For the survey scans, two separate spots were analyzed.

A low-energy electron neutralizer was used to minimize charging of the insulating wood samples. Low-energy electrons are used to flood the sample so that for insulating samples, build up of positive charge resulting in increased binding energy is minimized. Consequently, the obtained peak positions are equivalent to published literature values. Other methods of reducing charging are to use very thin samples and minimize analysis time. Both of these approaches were considered inadequate for obtaining information about real sample configurations and sufficient counts for high-resolution scans. Emission control was set at 17 mA and electron energy was set at 6.8 V dc bias. Maximum values for these parameters are 22 mA and 170 V dc bias with the instrument. Electron energy values that are excessive can reduce filament life and increase contamination due to re-condensation of organic matter.

All spectra were run at a pass energy of 89.9 eV and 300 watts power. For low resolution survey scans of the elements, acquisition was obtained using 0.5 eV/step, 10 msec per scan, and 25 sweeps from 0-1000 eV. For high-resolution carbon and oxygen scans, surveys were conducted from 280-300 eV and 525-545 eV respectively. A 0.125 eV per step, 50 msec/sweep and 100 sweep profile was used to ensure sufficient data resolution for deconvolution analysis. Deconvolution was conducted using XPSPeak 4.1 software. The deconvolution procedure consisted of obtaining a Shirley background due to an upward rise in the energy from low to high binding energy. Peaks were added until the raw intensity data were saturated with peaks at 1.0 FWHM with 1.4 eV between peaks. The Lorentzian-Gaussian peak percent as well as the FWHM were allowed to

float during the optimization process, resulting in de-convoluted peaks with the overall best fit as shown in figures 14 and 15 in section 3.1.

4.3 Contact Angle Analysis by the Wicking Methods

Contact angles were obtained by the wicking method, which applies the Washburn equation to the capillary rise rate of probe liquids through uniformly sized wood particles as described in section 3.5. Powdered wood particles were obtained by cutting the 5x2x1 cm blocks prepared in thermal treatments with a chisel so that pieces of approximately 5x0.3x0.2 cm resulted. The smaller pieces were passed once through a Wiley mill with a 60-mesh screen. The collected powder was then passed through a 60-mesh and 80-mesh screen. Samples that passed through the 60-mesh and retained on the 80-mesh screen were then used for column packing and wicking experiments. Glass tubes of approximately 3 mm inner diameter (id) and 10 cm length were used to pack the porous wood using the following procedure. A small cotton plug was placed in the bottom of the tube and a small powder funnel was fitted around the top end. A fixed quantity of wood was placed in the powder funnel and a vibrating tool was used to vibrate the top portion of the glass tube so that the powdered wood would fall uniformly into the tube. Initial and final masses were obtained on all tubes and a packing density calculated.

High purity probe liquids hexane, diiodomethane, HPLC-grade water, and formamide obtained from Aldrich were used as probe liquids. Hexane, a non-polar solvent, was used to obtain particle size. Diiodomethane was used to obtain the non-polar or Lifshitz-van der Waals surface energy. Distilled water and formamide were used to obtain the acid-base contributions to the surface energy using the van Oss three liquids approach.

The capillary rise rate was measured by placing a mark approximately 1 cm above the bottom of the tube. An mm rule was placed behind the glass tube, which was then placed into the liquid. Timing began at the 1 cm mark and height rise readings were taken at selected time intervals based on the liquid being used. One individual called out the time and the other called out the height. All data were manually recorded in a

notebook and transferred to Excel for analysis. Four replicates were made for each fluid for each thermal treatment and for each oak. Once the pore radius was determined using hexane, the contact angle was then determined for each probe liquid using the Washburn equation.

4.4 Fourier Transform Infrared (FTIR) Analysis

FTIR was run on the radial plane of the thermally treated samples using a Nicolet FTIR Spectrometer from 400-4000 cm^{-1}. Peak assignments were taken from a review by Coates (2002) in the *Encyclopedia of Analytical Chemistry*.

4.5 Acid-Base Titrations Using a Gran Plot

Titrations were conducted using a Vernier probe system where pH was monitored with addition of a 0.02 normal sodium hydroxide. The sodium hydroxide was standardized with potassium hydrogen phthalate. The Vernier probe allowed determination of stable pH at each volumetric addition. The titration curve was analyzed using a Gran plot for the determination of Ka (acid dissociation constant) and equivalent acid content in the extracted liquid per gram of solid.

4.6 Gas Chromatography

A Shimadzu GC 17A with an automatic flow controller (AFC) with flame ionization detector (FID) was used to separate the volatile acids, esters, and aromatic aldehydes from aqueous ethanol (60% white spirit) extracts of all thermally treated white oak samples. By using a bonded polyethylene glycol (PEG) capillary column, flavor compounds in distilled spirit products can be quantified in a single splitless injection. A Stabilwas-DA column with an acidic functionality added to the PEG stationary phase reduces adsorption of acidic components and significantly reduces peak tailing. A 30 m long, 0.25 mm diameter Restek Stabilwax-DA column for free underivatized acids was used to separate the material extracted from the thermally treated 5x2x1 cm samples after six weeks. For separation of components a 4mm id splitless liner with wool was used. Injection temperature was 240 ^{o}C with hydrogen as the carrier gas and nitrogen as the

make up gas. Oven temperature was controlled at 70 ^{o}C, followed by raising the temperature to 240 ^{o}C at 12 ^{o}C min^{-1} where it was held for 3 minutes. A linear flow velocity was maintained at 40 cm/sec with the GC-17A AFC.

5.0 Results and Discussion

In wood, which is an insulating material unable to conduct electrons freely, charging can become a serious issue. When insulating materials are bombarded with high-energy radiation, departing electrons leave a positive charge that results in a shift in binding energy. Charging problems can be minimized by using thin films and a low-energy electron neutralizer that is available on XPS instruments. The low-energy electrons neutralize the positive charge, thus allowing ejected electrons to flow more freely to the energy analyzer on the XPS unit. Since a positive charge holds electrons more tightly, a greater binding energy is observed, making it difficult to establish peak positions with functional groups. Figure 21 shows a high-resolution carbon scan of white oak without using a neutralizer of a wood sample approximately 0.5x0.5x0.5 cm in dimension without thermal treatment.

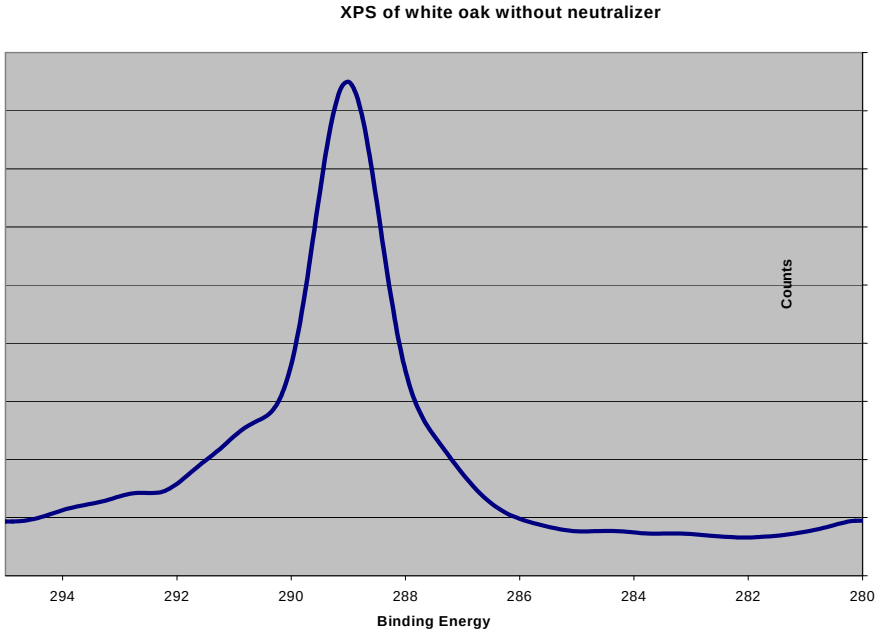


Figure 21. XPS of white oak before neutralizer use.

5.1 XPS and Charging in Insulating Materials Such as Wood

Application of the low-energy neutralizer in figure 22 shows a shift in peak positions, giving a spectrum that is more in line with a high carbon containing material such as wood. Note that the spectrum in figure 22 covers binding energies from around 283 to 291 eV, whereas figure 21 goes from 286 to 295 eV. For the spectrum in figure 22, the whole range of functional groups present in wood is accounted for based on published values for the specific wood and organic functional groups. Typical XPS deconvolutions obtained in this study appear like figure 15 in section 3.1. Note that the peak positions are very similar to those shown in table 1. The non-neutralized data in figure 21 show that a carbon peak at 285 eV is not present and charging has resulted in a binding energy shift.

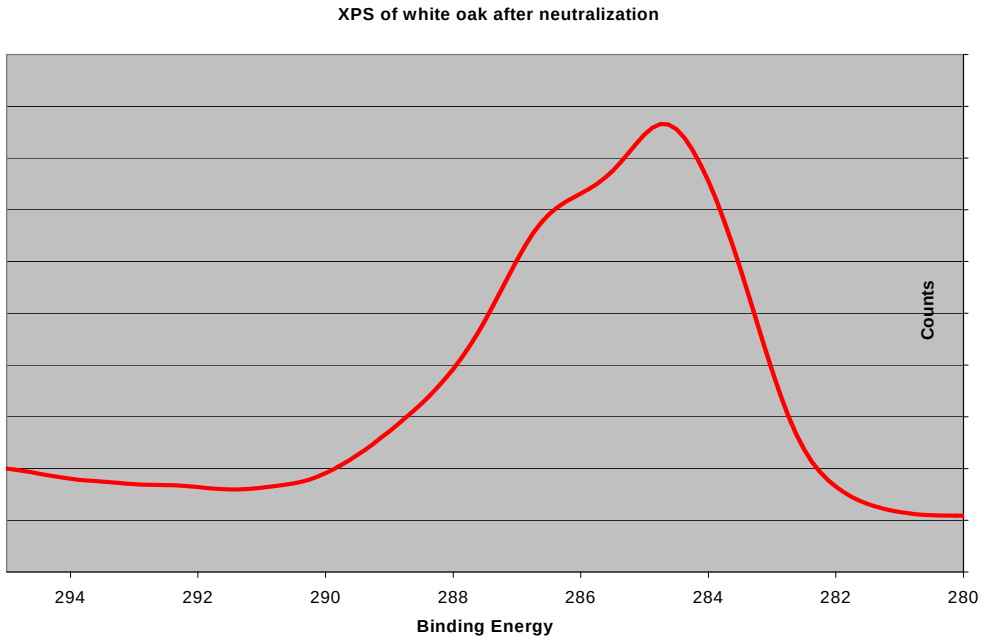


Figure 22. XPS of white oak using neutralizer.

5.2 FTIR of Wood and Functional Group Assignments

A typical FTIR with ATR cell obtained on the Appalachian white oak control with peak positions is shown in figure 23. Assignment of peak positions to functional groups can best be accomplished by comparing several bands available for each group. Using peak assignments described by Coates (2002), it is possible to assign functional groups that are consistent with the deconvolution procedure used for XPS spectra. Table 4 summarizes peak positions obtained from FTIR analysis of the Appalachian oak control with peak positions and assignments from Coates' reference article. The assignments show the presence of both aromatic and aliphatic hydrocarbons, phenols, alcohols, ethers, aldehydes, ketones and carboxylate salts. It is very difficult to separate types of carbonyls using the 1700-1750 peaks due to overlap between types of carbonyls. The FTIR spectra obtained for the thermally treated oaks varied somewhat in peak positions with shifting to lower frequencies for the carbonyl band with higher thermal treatments for the Appalachian oak but not the Ozark oak, as shown in figure 24 at the 250 °C thermal treatment.

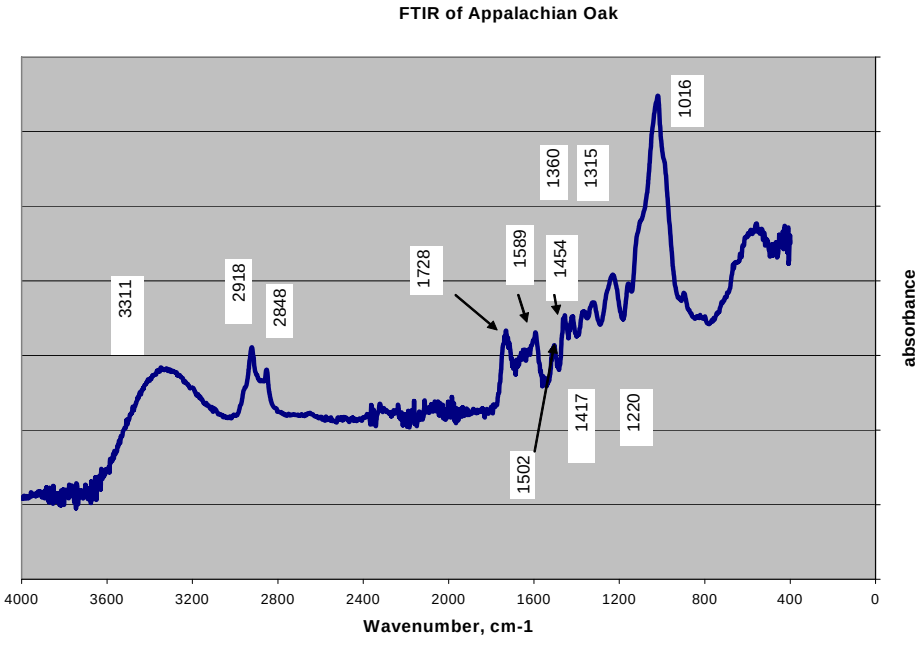


Figure 23. FTIR of Appalachian control with labeled peak positions.

Table 4. Observed FTIR Bands and functional group assignments of Appalachian control.

FTIR Bands observed	Description	Range of wavenumbers for assignment
3311	Polymeric OH stretch	3400-3200
2918	Methylene C-H asymetric stretch	2935-2915
2848	Methylene C-H asymetric stretch	2865-2845
1728	aldehydes, ester, ketone, carboxylic acid	1740-1725,1750-1725,1725-1705,1725-1700
1589	carboxylic acid salt	1610-1550
1502	Aromatic ring stretch	1510-1450
1454	Methyl CH3 stretch, Methylene C-H bend	1470-1430, 1485-1445
1417	carboxylic acid salt	1420-1300
1315	carboxylic acid salt	1420-1300
1220	aromatic ethers, phenol C-O stretch	1270-1230,1200
1018	cyclohexane ring vibrations	1055-1000

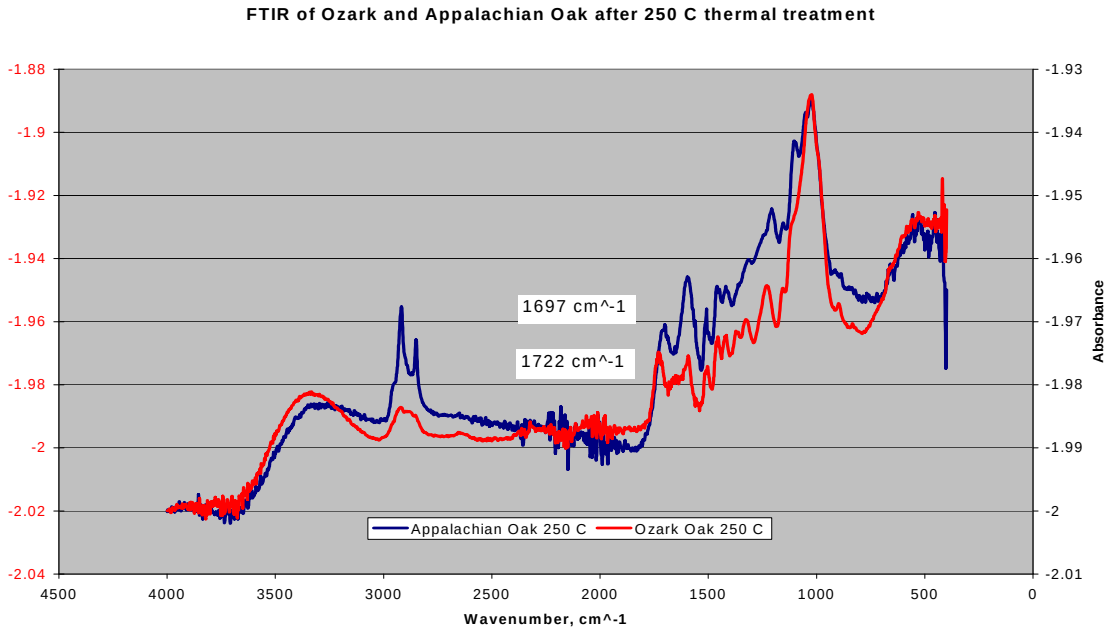


Figure 24. FTIR of Appalachian and Ozark Oak at 250 C showing shift in C=O.

5.3 XPS Survey Scans and Oxygen-to-Carbon (O/C) Ratios of Thermally Treated White Oaks

An XPS survey scan for thermally treated oak is shown in figure 25. The derived oxygen-to-carbon ratio from thermal treatments before and after extraction is useful for comparing the relative contributions of extractives, lignin, and cellulose at the surface. The theoretical O/C ratio for extractives is about 0.10, lignin 0.33, and cellulose 0.83 (Li, 2004). An O/C value of a synthesized lignin dimer of 0.19 was also reported by Li.

Figures 26 and 27 show the change in the O/C ratio of thermally treated Appalachian and Ozark oak. Initial O/C ratios of 0.22 and 0.28 indicate the surface is rich in extractives and lignin. The reduction in O/C ratio of the Appalachian oak at 150°C is indicative of an increase of extractives or perhaps some form of dimer lignin at the surface while the subsequent increase with temperature shows increased oxidation and a more lignin-rich surface. For the thermally treated Ozark oak in figure 27, the O/C ratio decreases to a minimum at the 200 ^{o}C and increases at 250 ^{o}C due to increased oxidation. Functional group analysis from high-resolution carbon scans will later clarify O/C ratio changes with compositional changes from thermal treatment of the two oaks.

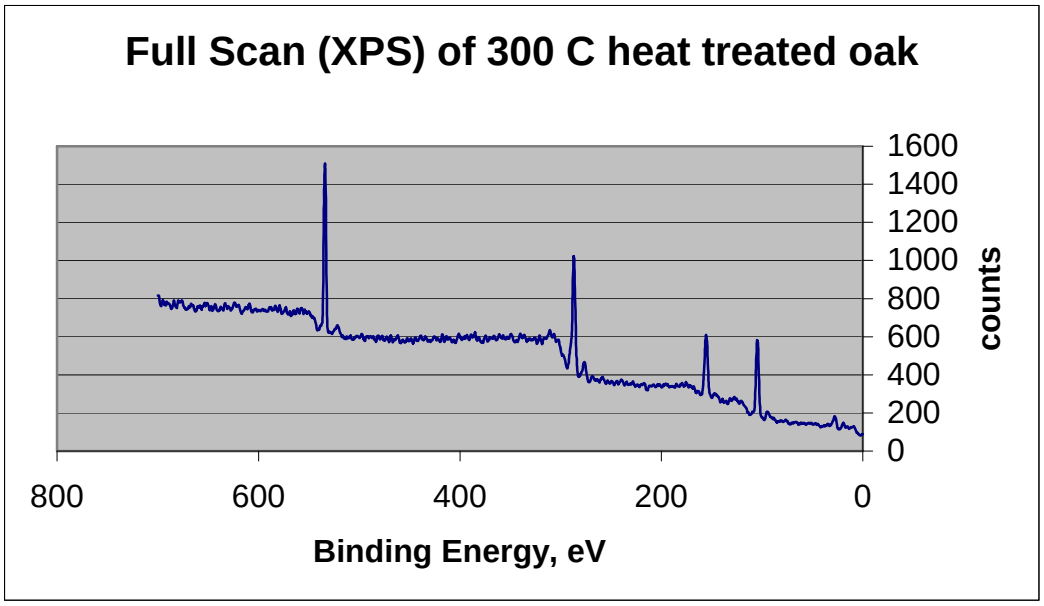


Figure 25. XPS Survey Scan for atomic ratios of carbon and oxygen.

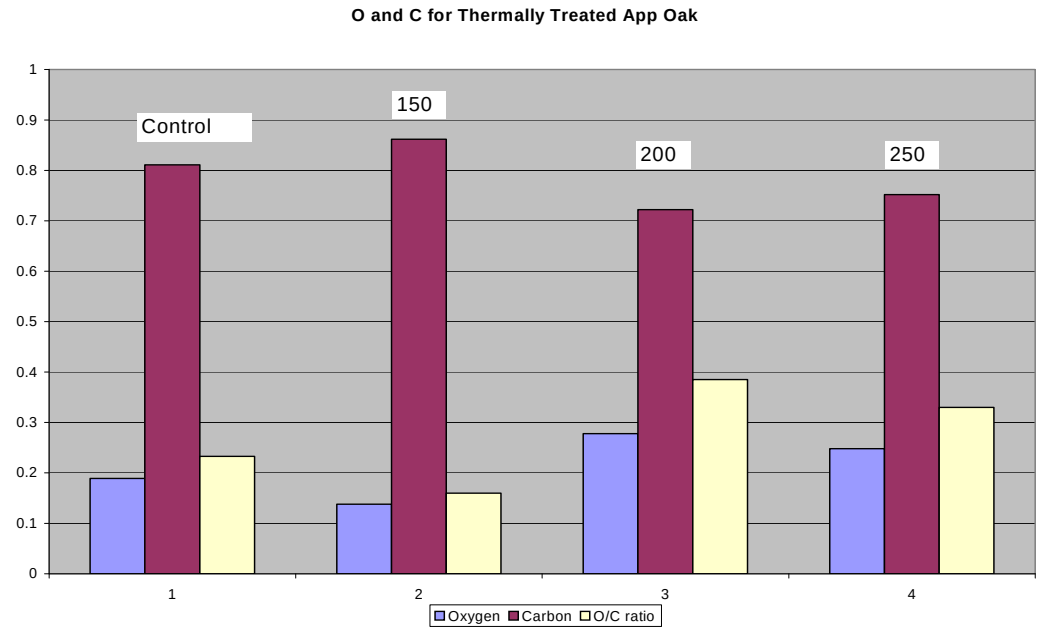


Figure 26. O/C ratio of thermally treated Appalachian Oak.

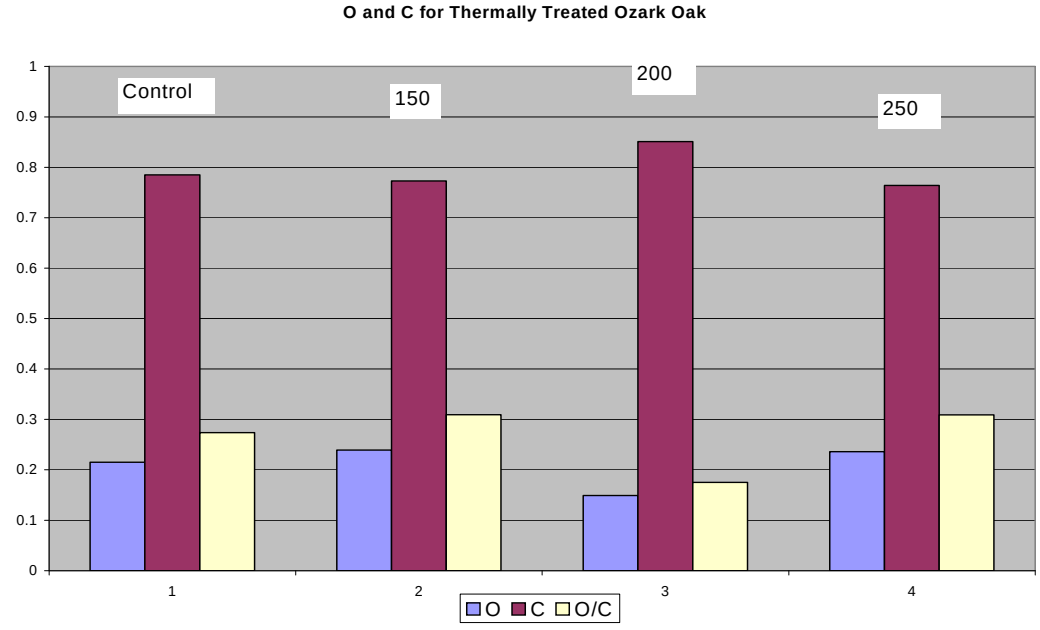


Figure 27. O/C ratio of thermally treated Ozark oak.

5.3.1 Mass Loss of White Oak with Thermal Treatment

The results in figure 28 show the average mass loss of 8 samples at each temperature of Appalachian 1, Appalachian 2, and Ozark 3. The mass loss is consistently greater for the samples identified as Appalachian 1 and 2 than it is for Ozark 3. Error bars indicate reproducible behavior between the two Appalachian stave boards. The results indicate that the Appalachian oak is more oxidized at lower temperatures than the Ozark oak as previously shown in the O/C ratio of the thermally treated oaks. In addition, the presence or formation of aliphatic versus aromatic carbon and aliphatic and aromatic acids and esters obtained from high-resolution carbon and oxygen scans will provide clues to the variation in surface composition due to thermal treatment and materials available during extraction and maturation with aqueous ethanol.

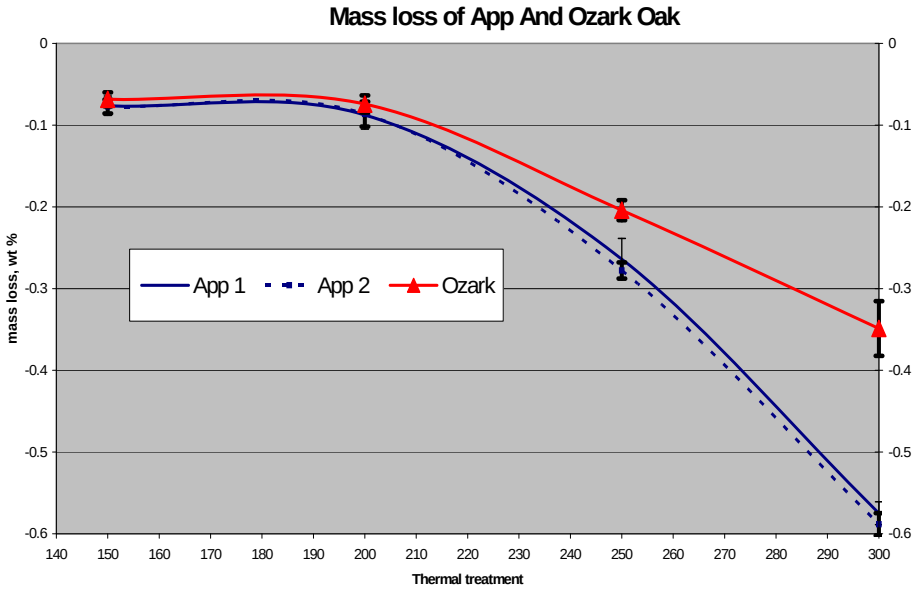


Figure 28. Mass loss of two oaks versus thermal treatment.

5.3.2 Effect of 60% Aqueous Ethanol Extraction on O/C Ratios

The effect of aqueous ethanol (60% white spirits) on the O/C ratio of the Appalachian and Ozark oaks after six weeks of extraction is shown in Figures 29 and 30. The increase in the O/C ratio of the extracted surface for the Appalachian oak control and sample treated at 150 ^{o}C is due to high carbon content extractives that include volatile and free fatty acids and possibly esters being removed. The O/C ratio of the extracted Ozark oak undergoes less change for the same conditions, indicating less removal of the high carbon containing materials such as fatty acids, probably due to less material present. The decrease in the O/C ratio of the Appalachian oak extract at 200 ^{o}C implies more surface adsorption of high carbon content compounds and de-sorption of compounds containing higher oxygen contents such as hemicelluloses. No change in the O/C ratio is observed for the Appalachian oak at 250 ^{o}C thermal treatments. The Ozark oak behaves differently upon extraction in that it remains relatively stable without thermal treatment and at 150 ^{o}C. At 200 ^{o}C and 250 ^{o}C, the O/C ratio increases upon extraction for the Ozark oak, indicating removal of higher carbon content compounds such as lignin and extractives.

5.3.3 Comparison of O/C Ratio Changes with Functional Group Compositional Changes for Thermal Treatments

In the high-resolution carbon scans from 280-300 eV, it was necessary to fit the de-convoluted curve using a C0 peak located approximately -1.5 eV from the C1 285 peak for carbon as shown in figure 15 in section 3.1. Peak positions in this region have been attributed to graphite and other aromatic materials such as naphthalene. Aromatic material is present in lignin, and condensed aromatics have been shown to appear at 283.5 eV where this peak is appearing (NIST database, 2003). The peak obtained at this position remained constant with time, indicating that electron neutralization was effective in controlling charging.

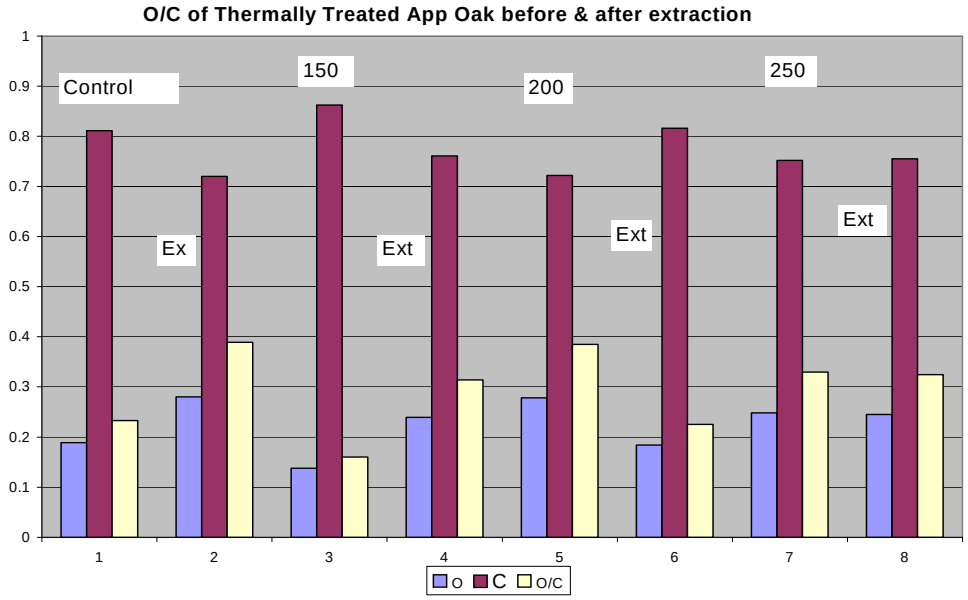


Figure 29. O/C ratio of thermally treated Appalachian oak before and after extraction.

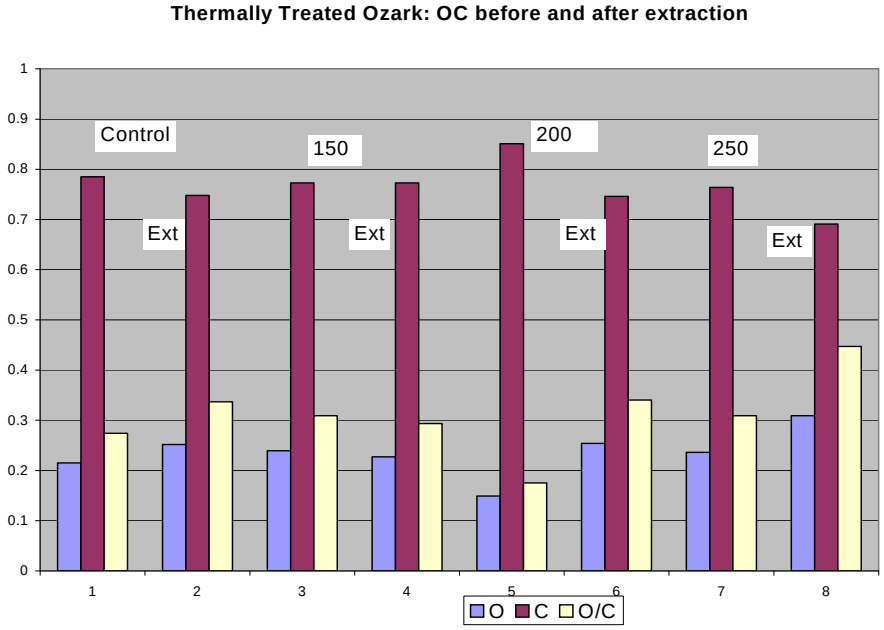


Figure 30. O/C ratio of thermally treated Ozark oak before and after extraction.

Some subpeak positions have been attributed to sample contamination. Sample contamination with carbon of high O/C ratio materials, such as cellulose, has been shown to be a problem in that the theoretical and measured O/C ratio varied from 0.83 to 0.62. Higher carbon content materials such as lignin were found to have nearly identical theoretical and measured O/C ratios by XPS, indicating less of a contamination problem on higher carbon content surfaces (Li, 2004). A comparison of the O/C ratio from the survey scan to an O/C ratio calculated from the high-resolution carbon scan using molar fractions of O/C for C-OH, C=O and COOH gave a linear correlation of 0.85 whether the C0 peak was included or not. Also, a plot of the O/C ratio versus the total carbon content due to aliphatic (C1) and aromatic (C0) in figure 31 shows a linear relationship with a 0.85 correlation between two separate measurements of carbon content by survey and high-resolution scans. Any filament heating would be greater with the high-resolution scan than the survey scan due to greater analysis time. Since both hydrocarbon and aromatic carbon groups are of interest in wood thermal treatment and charring, results will be reported with the C0 peak.

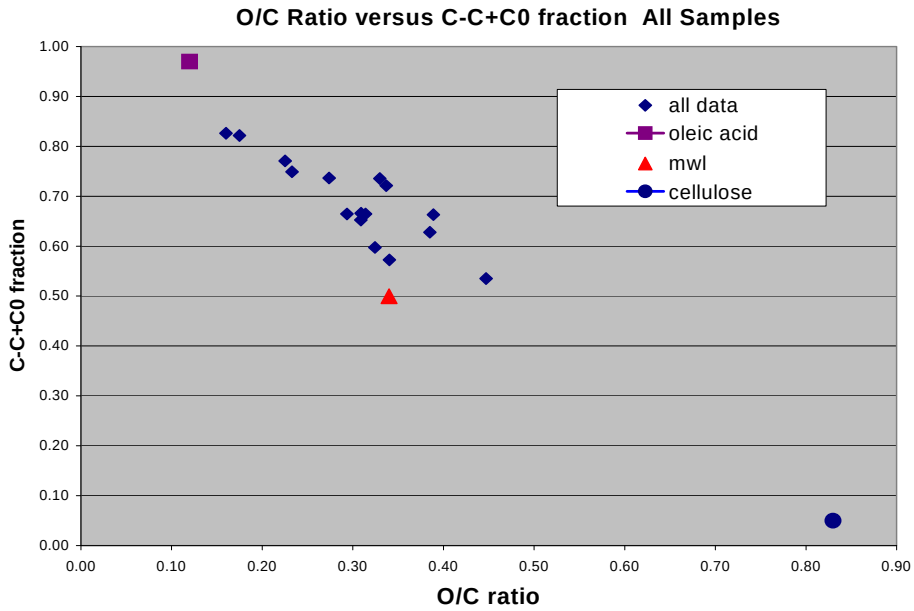


Figure 31. O/C Ratio versus C-C+C0 fraction, all samples.

The results in figure 32 and 33 show the functional group composition change with thermal treatment for the two oaks. For the Appalachian oak, the carbon level reaches a maximum at 150 ^{o}C compared to 200 ^{o}C for the Ozark oak while the C-OH and C=O functional groups reach a minimum at those respective temperatures, indicating that the surface is reaching a maximum in hydrophobicity at those temperatures. These results are consistent with the minimum O/C values previously reported in Figures 26 and 27. Increased C-OH and C=O levels are observed beyond the minimum O/C ratio for both oaks and are indicative of increased oxidation and formation of aromatic groups in the C0 peak. The Ozark oak clearly shows increased levels of oxygen containing functional groups at the highest thermal treatment (250 ^{o}C) relative to the Appalachian oak although its O/C level is not higher, as illustrated in Figures 26 and 27.

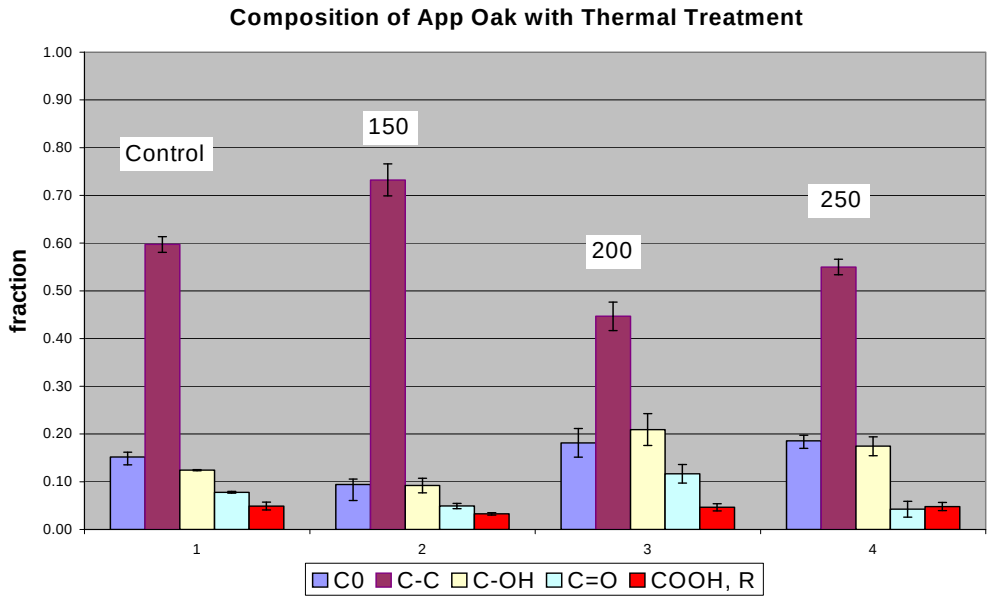


Figure 32. Composition of Appalachian oak with thermal treatment.

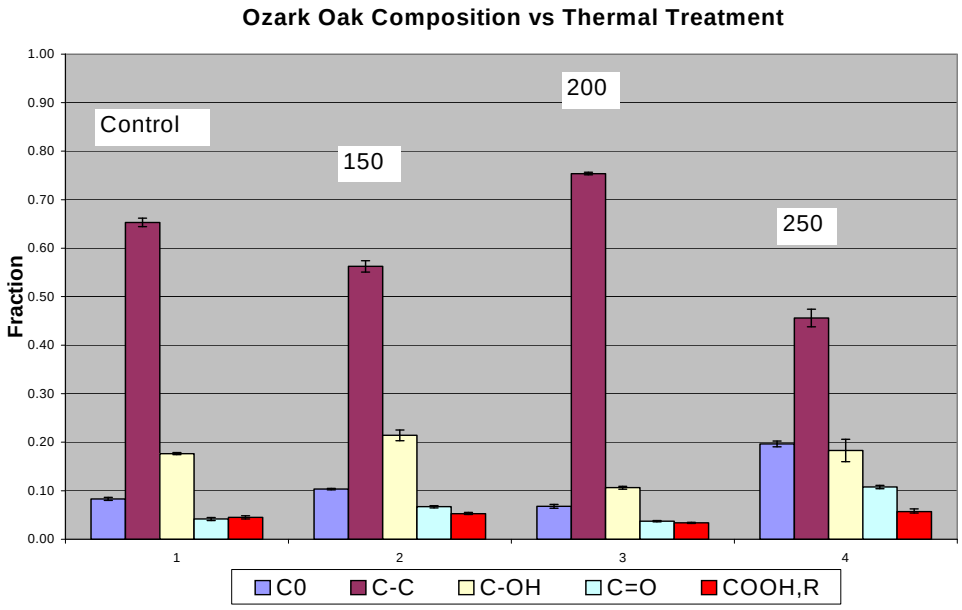


Figure 33. Composition of Ozark oak with thermal treatment.

5.3.4 Comparison of O/C Ratio Changes with Functional Group Composition for Thermally Treated and Extracted White Oaks

XPS data for relative amounts and peak positions are important in evaluating compositional changes in thermally modified and extracted oak. Functional group composition is important to the wood wetting characteristics and ability of a solvent to interact with a surface and remove components. As discussed previously, the ratio of Lewis acidic alcohol and fatty acid groups to Lewis basic groups such as carbonyl and carbon-carbon bonds provides a method to investigate acid-base interactions between the solvent and surface.

Evaluation of functional group composition in XPS relies on assigning and understanding peak position shifts due to the influence of oxidation state on core electron binding energy. Shift of the main carbon peak from 285.3 for saturated hydrocarbons to 284.6 ±0.5 is indicative of the formation of graphitic or aromatic carbons. Figures 34-37 summarize the deconvolution curves and peak positions for the control samples for the two oaks before and after extraction. These results show that the Ozark oak carbon peak is more aromatic than the Appalachian oak based on peak positions of 284.9 and 285.2.

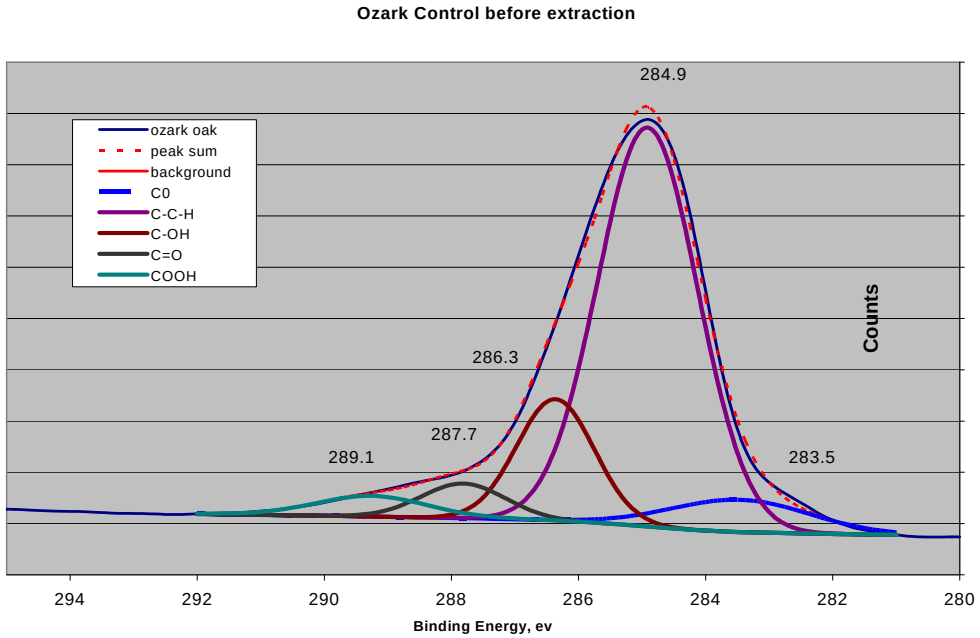


Figure 34. Ozark oak before extraction.

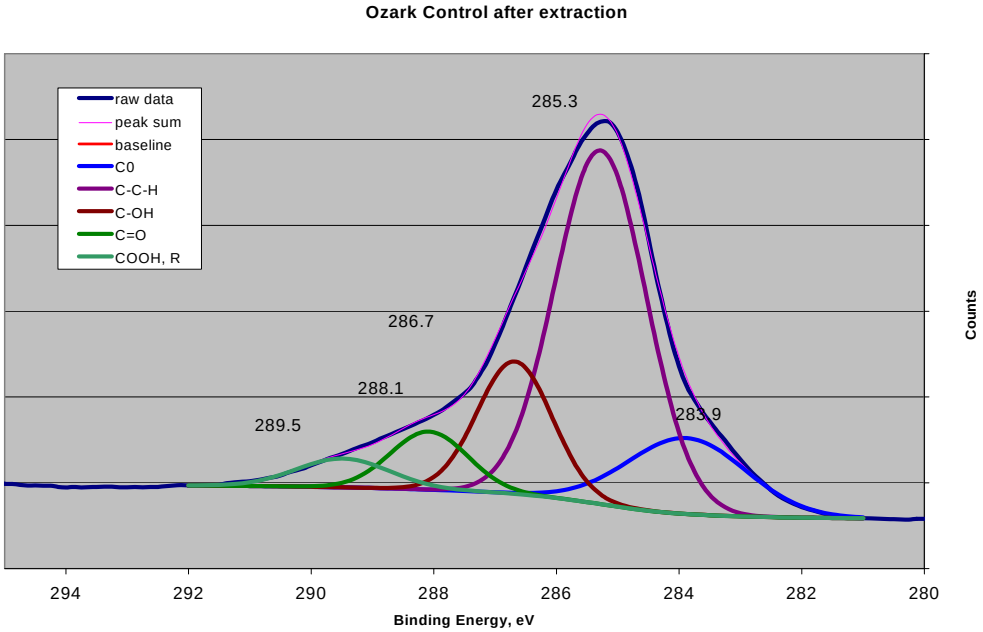


Figure 35. Ozark oak after extraction.

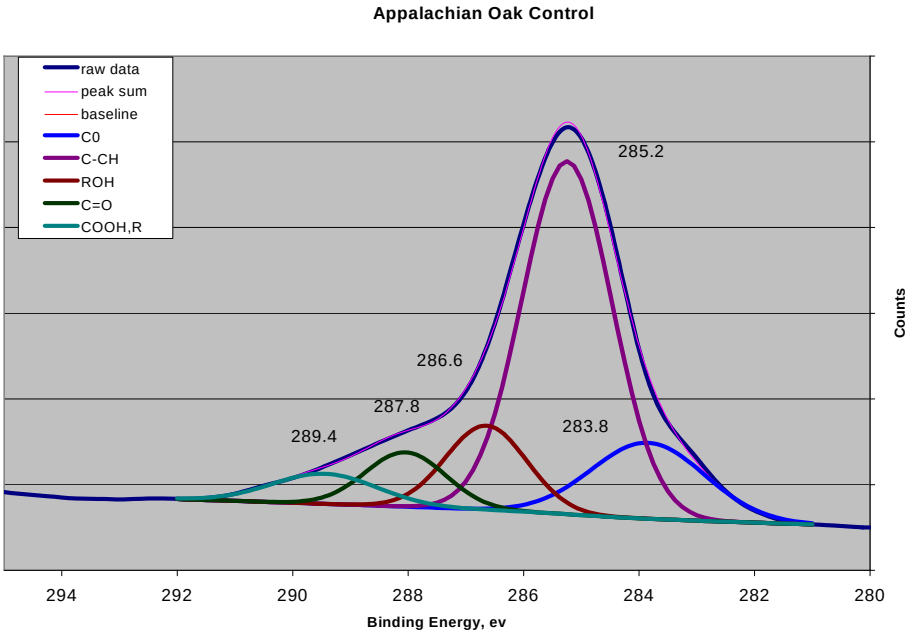


Figure 36. Appalachian oak before extraction.

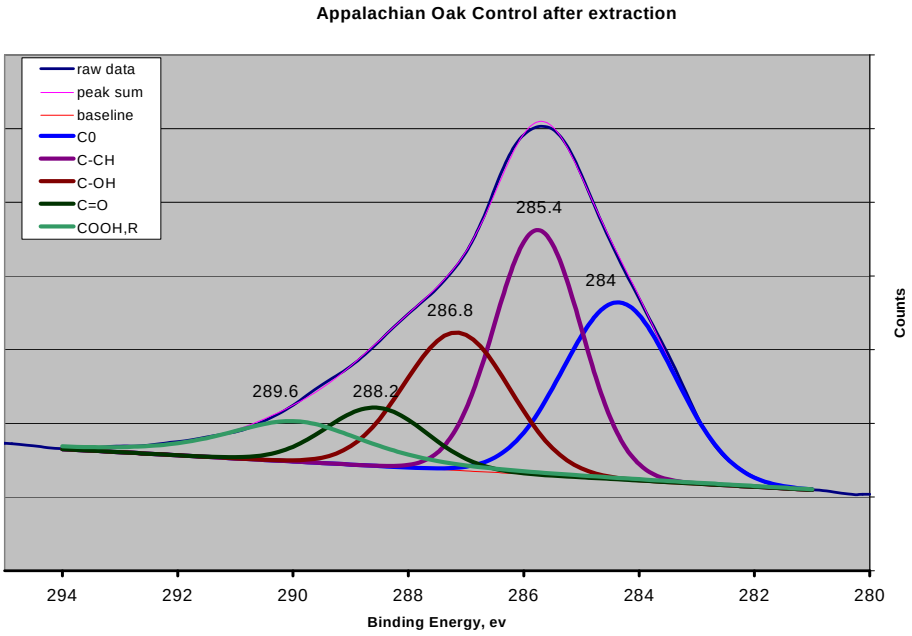


Figure 37. Appalachian oak after extraction.

Figures 38 and 39 show a white oak stave sample that has been subjected to heavy charring before and after seven years extraction. The heavy char samples show the carbon peak at 284.6 and 284.3 before and after extraction with a subsequent shift downward of other peaks due to the aromatic delocalization effect on the binding energy.

The remaining deconvolution curves for the two oaks with all thermal treatments before and after extraction with peak positions are summarized in Figures A.1-A.16 in the appendix. The peak positions and relative area percents are also summarized in tables A.1 and A.2 in the appendix. The surface functional group composition of the thermally treated and extracted Appalachian and Ozark oaks is summarized in Figures 40 and 41.

For the Appalachian oak control and thermally treated oak at 150 ^{o}C in figure 40, the C1 content is reduced and the C2 (OH) and C3 (C=O) contents are increased at the surface upon extraction, which is consistent with the increased O/C ratio upon extraction shown earlier in figure 29. Removal of high carbon content extractives would result in more COH containing cellulosic and C=O containing lignin-type structures at the surface. The C1 peak position for the Appalachian oak of 285.2 is indicative of saturated hydrocarbon present although the aromatic C0 peak increase supports the observed increase in lignin-type material accumulating at the extracted surface in the control and 150 ^{o}C treatment. At the 200 ^{o}C thermal treatment, the saturated C increases, while the aromatic C, COH and C=O peaks decrease, indicating a depletion of lignin-type materials at the surface. This pattern is consistent with reduced O/C from 0.38 to 0.22 in figure 29 for the 200 ^{o}C treatment. For the Appalachian oak at the 250 ^{o}C thermal treatment, the aliphatic carbon is reduced upon extraction, and a slight increase in aromatic carbon and alcohol groups is observed as shown in figure 40. Also, more C=O and COOH are observed at the 250 ^{o} C treatment upon extraction.

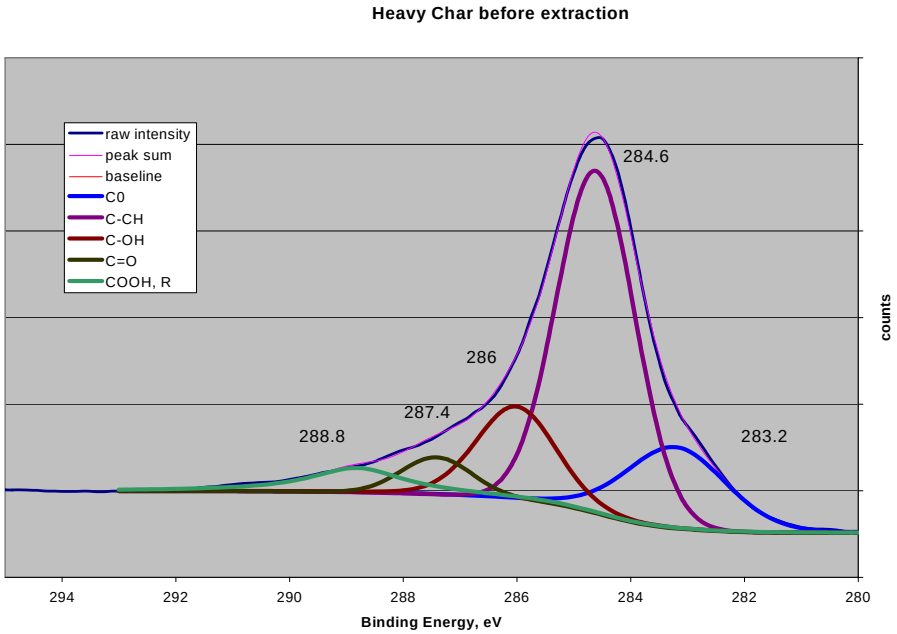


Figure 38. Heavy char oak before extraction.

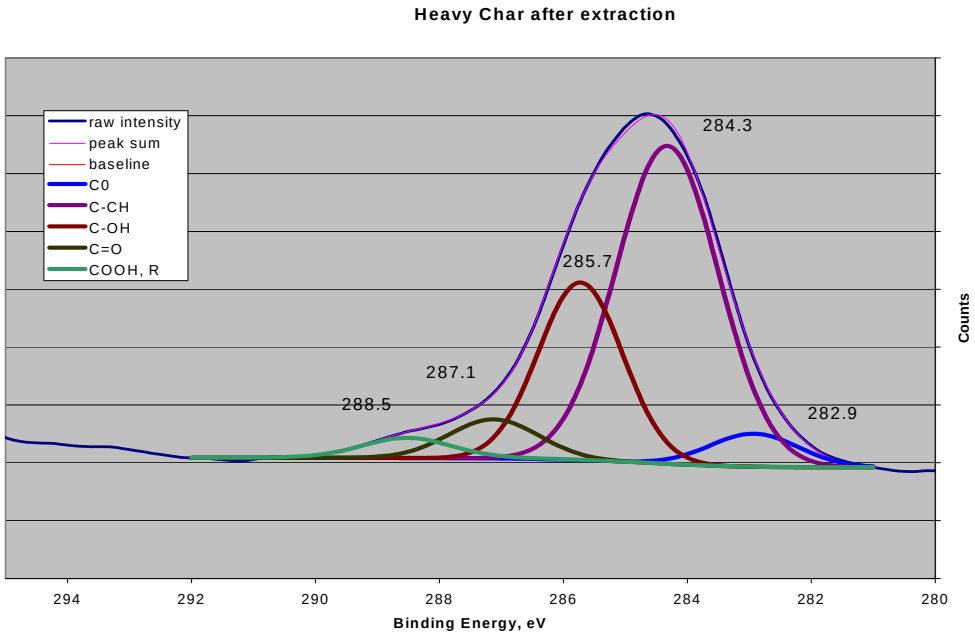


Figure 39. Heavy char oak after extraction.

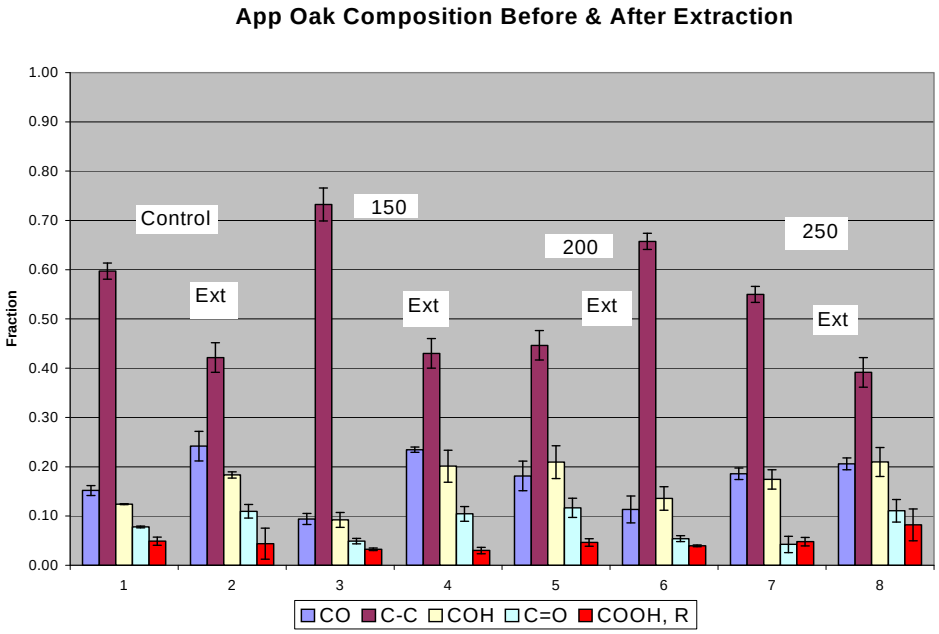


Figure 40. Appalachian oak composition before and after extraction.

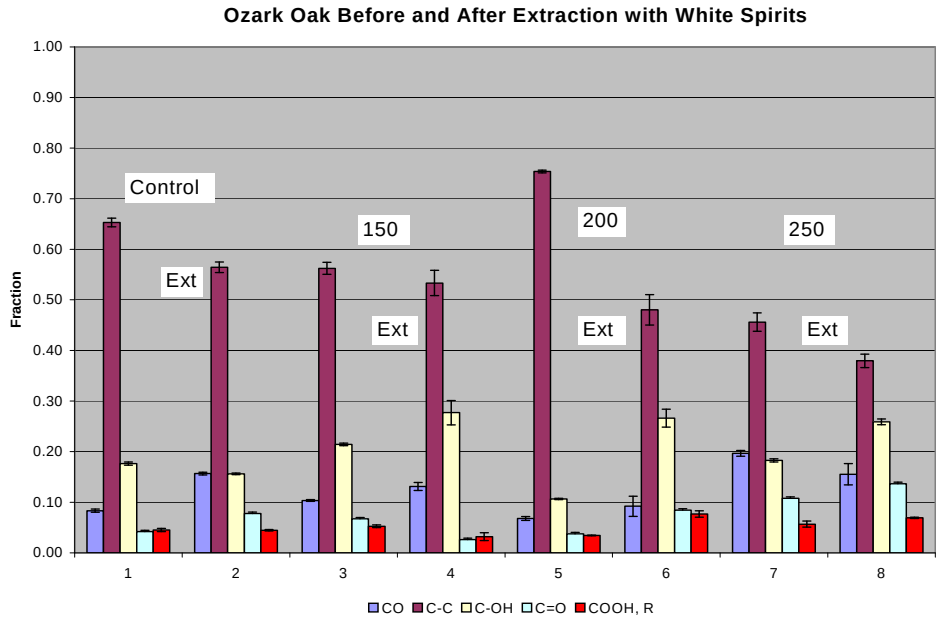


Figure 41. Ozark oak composition before and after extraction.

For the Ozark oak control and the 150 ^{o}C treatment in figure 41, the C1 peak decreases slightly upon extraction while slight increases in C=O are observed in the control and COH at the 150 ^{o}C treatment. Slight changes upon extraction for the Ozark control and 150 ^{o}C treatments are consistent with the nearly constant O/C ratios shown earlier in figure 30. At the 200 ^{o}C thermal treatments, C1 decreased and COH and C=O increased upon extraction, corresponding to a change in O/C ratio of 0.18 to 0.33 as shown in figure 30. At the 250 ^{o}C treatment, decreased C1 and increased C-OH, C=O, and COOH were observed, corresponding to an O/C ratio increase of 0.31 to 0.44 in figure 30.

5.3.5 Comparison of Functional Group Changes for Charred White Oak Barrel before and after Extraction for Seven Years

The results in Figures 42 and 43 show the change in O/C ratio and composition for a charred white oak stave before and after extraction. The O/C ratio increases upon extraction with white spirits, which is consistent with previous observations on thermally treated white oak. The aromatic carbon (C0) decreases and the alcohol (C1) increases, indicating that aromatic alcohols are probably being removed from the charred layer during extraction.

5.4 Acid-Base Ratios of Thermally Treated and Extracted Oak

The acidity in the acid-base ratio depends on the alcohol (C2) and acid content (C4) due to their electron accepting capacity and lower pK_A values. The basicity is dependent on the contribution of carbon (C0, C1) and carbonyl (C3) because of their electron donating capability and higher pK_A values. The aldehyde form of carbonyl is comparable to the aliphatic alcohol in terms of the pK_A (16 for both) value whereas the ketone, which is more prevalent in lignin, has a pK_A around 19-20 (March, 2001).

The acid-base ratio of the Appalachian oak increases more upon extraction for the control oak and thermally treated oak at 150 ^{o}C , while the Ozark oak remains more stable for the same treatment conditions, as shown in Figures 44 and 45.

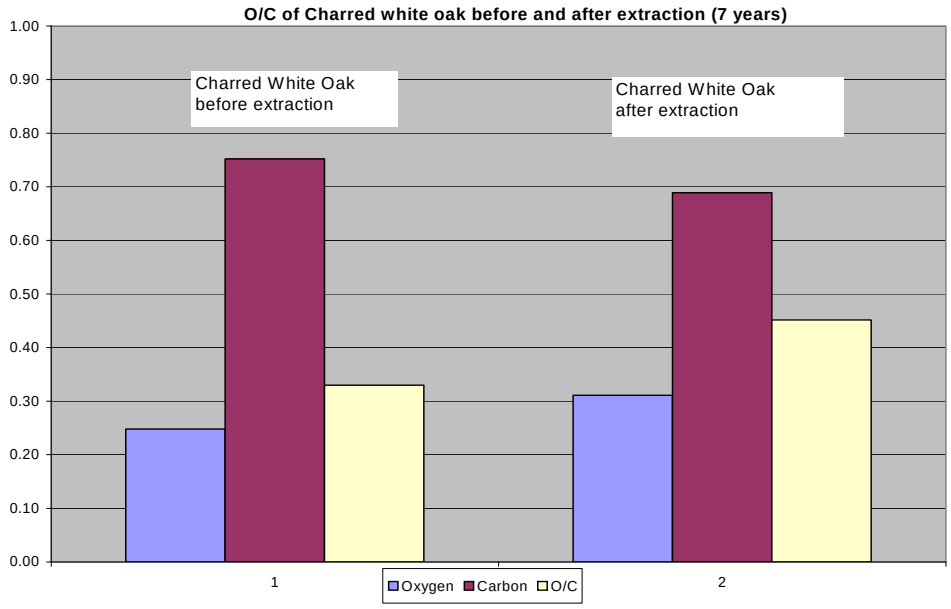


Figure 42. O/C ratio of charred white oak before (1) and after (2) extraction.

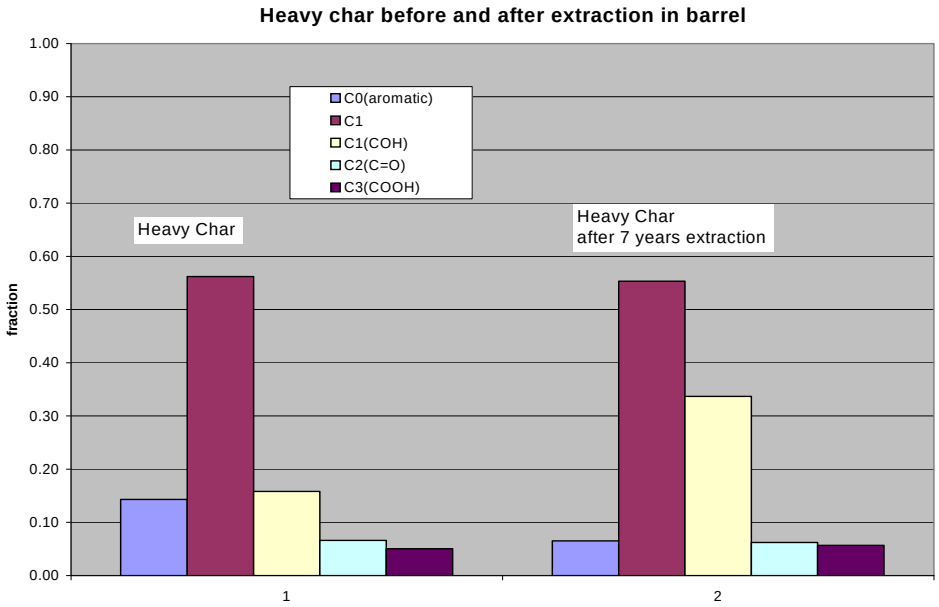


Figure 43. Functional group composition of charred white oak before (1) and after (2) extraction.

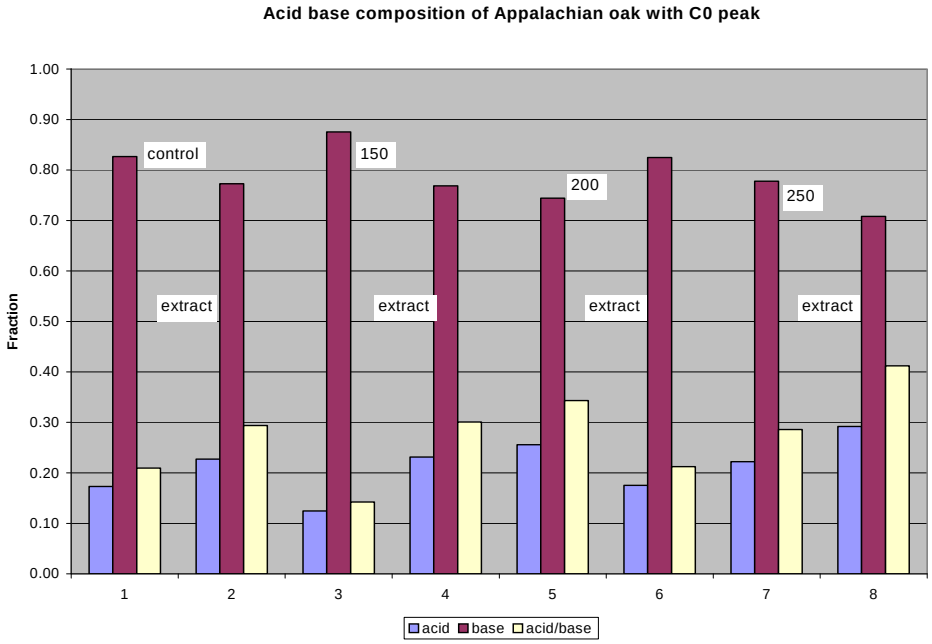


Figure 44. Acid-base composition of Appalachian oak from XPS.

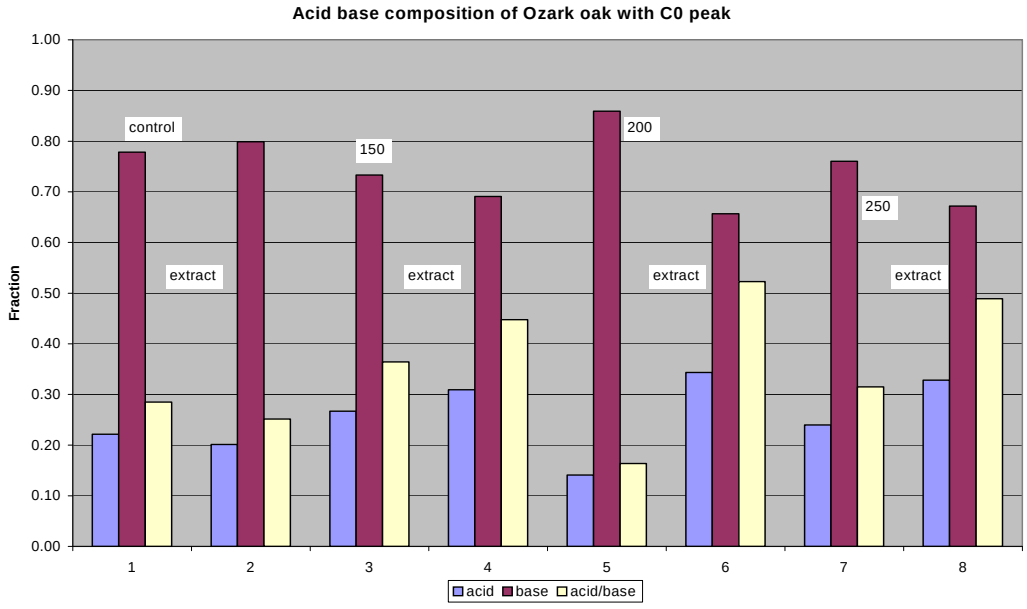


Figure 45. Acid-base composition of Ozark oak from XPS.

For the unextracted samples, the Appalachian oak undergoes a minimum in acid-base ratio at 150 ^{o}C while a similar minimum is obtained in the Ozark oak at 200 ^{o}C.

The thermal treatment to obtain minimum acid-base ratios for the two oaks corresponds to minimum O/C ratios discussed previously. The acid-base ratio is higher for the Ozark oak at its minimum when compared to the Appalachian oak's minimum. Also, the Ozark oak has a higher acid-base ratio than the Appalachian oak for the unextracted samples at all thermal treatments. The higher acid-to-base ratio for the Ozark oak is a direct result of an increase in the C-OH and COOH electron acceptor groups relative to the electron donor groups. The acid-base ratio is also higher for the extracted Ozark oak at all thermal treatments with the exception of the control. These results indicate that the Ozark oak has more active acidic sites relative to basic sites than does the Appalachian oak. The increased concentration of these sites in the Ozark oak increases the activity of the aqueous ethanol white spirits towards the wood, resulting in increased concentration of acidic compounds migrating from the bulk of the sample to the surface.

5.5 Contact Angle Results and Acid-Base Surface Energy Analysis of Thermally Treated Oak

The pore radii obtained from wicking rates with hexane are summarized in table 5 for the two oaks. Contact angles obtained with the probe liquids water, formamide, ethylene glycol, and diiodomethane are also summarized in table 5. Similar contact angles were obtained with water for the two oaks with the exception that the Appalachian oak thermally treated at 250 ^{o}C did not wick water. A contact angle of greater than 90^{o} is implied.

Table 5. Contact angle values of Appalachian and Ozark oak obtained from the wicking method.

		Pore Radius, Re, μ (std)	Contact Angles			
Sample	Treatment	Hexane	Water	Formamide	Ethylene Glycol	Diiodo methane
App	Control	1.71 (.06)	85.3 (.6)	64.6 (5)	46.2 (5.3)	67.3 (3.2)
	150	1.61 (.1)	82.6 (.7)	59.5 (1.5)	59.8 (10)	67.2 (.8)
	200	1.64 (.06)	85.3 (.5)	55.3 (2.4)	47 (7)	65.4 (2)
	250	1.79 (.2)	Did not wick	35.7 (5.6)	22.6 (5)	62.8 (4)
Ozark	Control	1.67 (.09)	84.3 (.4)	59.2 (6)	30 (3)	70 (0.9)
	150	1.57 (.05)	82.8 (.5)	75 (1.5)	45(17)	67.8 (.8)
	200	1.77(.12)	86.7 .25)	65.7(6)	22.3(2.5)	67 (3)
	250	1.88 (.13)	89.3 (.3)	61.6 (4.5)	<20	63 (1.5)

The acid-base probes formamide and ethylene glycol behaved quite differently towards the two oaks, and this behavior is reflected in the acid-base surface energy calculations summarized in tables 6 and 7 using Della Volpe (1997) and van Oss (1987) parameters. Better correlation coefficients were obtained using the Della Volpe parameters for the van Oss geometric mean equation. It has been pointed out by van Oss that surface energy should be determined using only two acid-base probe liquids, with water being one and the other selected from formamide or ethylene glycol. The method described by van Oss (2002) and de Meijer (2000) was used to calculate the acid-base surface energies from the contact angle data in table 5 for the water-formamide and water ethylene glycol pairs and is summarized in tables 8 and 9. The acid-base surface energy values in tables 6 and 7 show that a minimum was obtained at the 150 ^{o}C thermal treatment for both oaks as compared to 150 ^{o}C for the Appalachian and 200 ^{o}C for the Ozark oak from XPS data. It would appear that the XPS data are providing information about a different region than surface energy obtained from the wicking method of contact angle analysis.

Table 6. Surface free energy on two oaks using Della Volpe parameters.

Surface free energy parameters obtained on two thermally treated oaks by the wicking method using Della Volpe parameters							
mNm^{-1}	γ_S^{Tot}	γ_S^{LW}	γ_S^{AB}	γ_S^+	γ_S^-	γ_S^+ / γ_S^-	r^2
App Control	28.7	24.4	4.25	2.2	2.1	1.01	0.99
150	28.7	24.4	4.23	1.4	3.1	0.46	0.99
200	29.9	25.5	4.45	3.0	1.6	1.82	0.99
250	29.8	27.0	2.81	5.8	0.05	120*	0.99
* θ>90 in	water						
Ozark Control	27.8	22.9	4.9	2.3	2.6	0.89	0.88
150	29.2	25.3	3.9	1.2	3.2	0.36	0.98
200	29.1	24.6	4.5	4.2	1.2	3.44	0.83
250	29.0	25.7	3.3	2.8	1.0	2.85	0.81

Table 7. Surface free energy on two oaks using van Oss Parameters.

Surface free energy parameters obtained on two thermally treated oaks by the wicking method using van Oss parameters							
mNm^{-1}		γ_S^{Tot}	γ_S^{LW}	γ_S^{AB}	γ_S^+	γ_S^-	γ_S^+ / γ_S^-	r^2
App Control	29.6	24.4	5.16	2.2	3.0	0.72	0.93
150	30.1	24.4	5.64	1.4	5.8	0.24	0.93
200	30.2	25.5	4.72	3.6	1.6	2.31	0.95
250	38.1	27.0	11.2	9.1	3.4	2.7	0.94
Ozark Control	28.8	22.9	5.9	2.1	4.2	0.50	0.55
150	30.1	25.3	4.8	0.8	6.8	0.12	0.87
200	28.1	24.6	3.6	4.9	0.6	7.62	0.25
250	28.6	25.7	2.9	3.1	0.7	4.54	0.74

Table 8. Surface energies calculated for water-formamide pair.

		Water Formamide Pair				
	γ_S^{Tot}	γ_S^{LW}	γ_S^+	γ_S^-	γ_S^+ / γ_S^-	γ_S^{AB}
Appalachian control	29.26	24.39	1.43	4.15	0.34	4.87
150	30.70	24.45	2.43	4.02	0.60	6.25
200	30.11	25.47	3.75	1.43	2.62	4.63
250	32.92	26.96	11.61	0.76	15.18	5.96
Ozark control	29.00	22.87	3.30	2.84	1.16	6.12
150	24.76	24.11	0.01	12.10	0.00	0.65
200	28.88	24.56	1.27	3.66	0.35	4.31
250	29.95	26.85	1.93	1.24	1.56	3.10

Table 9. Surface energies calculated for water-ethylene glycol pair.

		Water Ethylene Glycol Pair				
	γ_S^{Tot}	γ_S^{LW}	γ_S^+	γ_S^-	γ_S^+ / γ_S^-	γ_S^{AB}
Appalachian control	29.58	24.39	3.04	2.22	1.37	5.19
150	28.97	24.45	0.68	7.51	0.09	4.52
200	30.37	25.47	2.62	2.29	1.14	4.90
250	27.78	26.96	7.21	0.02	313.70	0.81
Ozark control	27.59	22.87	6.72	0.83	8.10	4.72
150	30.49	24.11	3.07	3.31	0.93	6.38
200	25.88	24.56	7.87	0.06	143.06	1.32
250	28.65	26.85	7.98	0.10	78.34	1.80

For the acid-base surface energies calculated by the three-liquid approach of van Oss (2002), a minimum in value for the water-formamide pair is not observed in the Appalachian oak while it occurs at 150 ^{o}C in the Ozark oak. The results for this pair show a higher acidity for the Ozark control relative to the Appalachian and less acidity at the higher thermal treatments for the Ozark oak. For the water-ethylene glycol pair shown in table 9, the Ozark oak shows higher acidity and acid-base ratios throughout compared to the Appalachian oak. With the exception of the water-formamide pair, all surface energy results derived from contact angle data indicate a higher acidity and acid-base ratio for the Ozark oak. These results are consistent with acid-base ratios calculated from XPS data. Examination of the contact angle data for the Ozark oak with formamide in table 5 indicates unusual behavior that possibly is a result of an interaction.

Contact angle data of a grain neutral spirit and white spirit against the Ozark oak is shown in table 10. The white spirit exhibits the greatest interaction on the thermally treated ozark oak at 250 ^{o}C. The white spirit (60% Ethanol) has Lewis acid-base parameters that are presumably between those of pure water and pure ethanol, which are described in table 2 in section 3.3. The increased interaction occurring at the 250 ^{o}C thermal treatment for the Ozark oak may result from a combination of decreased acidity observed in the Ozark oak surface shown in tables 6 and 7 coupled with the increased acidity of the water alcohol mixture due to the water component.

Table 10. Contact angle of alcohols on thermally treated Ozark oak.

Properties of Grain Neutral Spirits and White Spirits against Thermally Treated Ozark Oak				
sample	GNS		WS	
surface tension, mNm^{-1}	20		26	
	contact angle	work of adhesion	contact angle	work of adhesion
control	29.2	38	85	28
150	28.1	39	82.9	29
200	28.5	37	82.5	29
250	28.9	37	74.6	33

5.6 Analysis of XPS and Surface Energy Acid-Base Ratios

Comparison of the acid-base ratio from surface energy to the O/C and acid-base ratio obtained from XPS in Figures 46 and 47 show that the Appalachian and Ozark oak behave quite differently. The poor fit of the Ozark data using both sets of surface energy parameters compared to acid-base from XPS indicates that the surface and subsurface composition of the Ozark oak are different in terms of acid-base ratio with depth, in particular in the region of the minimums around 150 and 200 °C. The variability in properties in this region is very likely due to a greater concentration gradient with depth for the Ozark oak. The Appalachian oak follows a closer relationship with the two acid-base parameters and XPS than the Ozark oak. A comparison of acid-base ratio changes by XPS in Figures 44 and 45 show that the Ozark oak exhibits the greatest change in acid-base ratio upon extraction, which is indicative of a greater concentration gradient. The same observation also holds for the O/C ratio changes upon extraction shown earlier in Figures 29 and 30 for the Ozark oak relative to the Appalachian oak.

The greater inactivation of the Ozark oak surface, as measured by the lower acidic surface energy and higher contact angle in formamide (Table 5), indicates that a barrier exists in the Ozark oak, preventing formation and release of acidic components during the thermal degradation process.

5.7 Titration Analysis of White Oak Extract After Six Weeks of Aging

The results in table 11 summarize the acid strength of the extract in terms of the pK_a and equivalents of 0.02 N NaOH required per gram of solid. A normalized concentration factor is shown in table 11 since masses of solid sample blocks were not equivalent in mass. The results show higher extractable acidity, Veq/gram, for the Appalachian oak control than the Ozark oak, which is most likely due to free fatty acids that may not have been apparent in the surface analysis. The Ozark oak gave lower pK_a values at the higher thermal treatment, which is consistent with higher acid-base ratios in XPS and by surface energy analysis relative to the Appalachian oak.

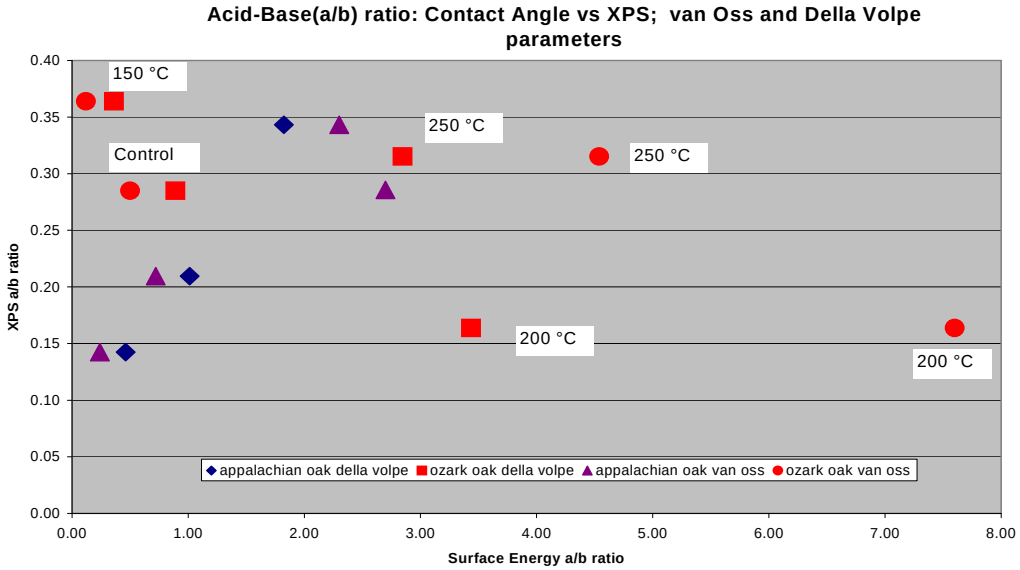


Figure 46. Acid-base (a/b) ratio of XPS versus surface energy.

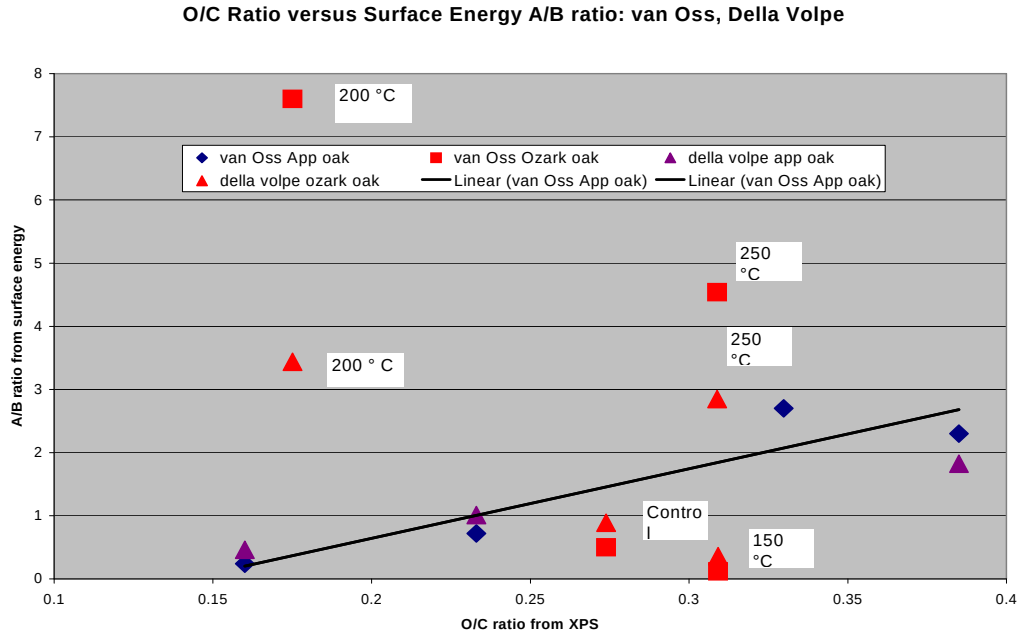


Figure 47. O/C ratio versus surface energy a/b ratio.

Table 11: Summary of titration data on Appalachian and Ozark oak.

	pKa	Veq/gram	ml/gm	mass	Concentration factor
Appalachian Control	4.98	0.20	5.80	8.62	1.25
150	5.17	0.12	5.50	9.09	1.31
200	5.12	0.11	5.41	9.25	1.34
250	5.50	0.10	6.62	7.55	1.09
Ozark Control	5.45	0.12	5.32	9.4	1.36
150	5.06	0.11	5.41	9.24	1.34
200	5.16	0.13	6.90	7.25	1.05
250	5.07	0.10	7.23	6.92	1.00

5.8 Gas Chromatographic Analysis of White Spirit Extract of the Thermally Treated Oaks

Gas chromatography of the white spirit extract of the thermally treated oaks was used to verify the relationship between the acidic properties of the surface and the acidic composition of the extract. Figure 48 shows a chromatogram of several acidic and flavor compounds found in distilled spirits. The retention times for the compounds shown are quite stable and can be used to identify compounds formed and their relative amounts. The lower molecular weight acetic and proprionic acids appear first while the lauric acid (C12) and stearic (C20) appear at much longer retention times. The retention times of the compounds identified in figure 12 in section 2.2 are shown graphically in figure 48. They are the cis and trans lactones (esters) at retention times of approximately 6.4 and 6.9 minutes , the aromatic alcohol eugenol is at around 8.8 minutes, and the aromatic aldehyde vanillin at 11.6 minutes. The column retention characteristics are such that lower molar mass fatty acids come off first while higher molar mass fatty acids come off at longer retention times. Esters and aromatic alcohols, such as whiskey lactones and eugenol, come off in the mid-range retention times. Aromatic aldehydes, such as vanillin, come off at the longer retention times. The compounds below were calibrated to

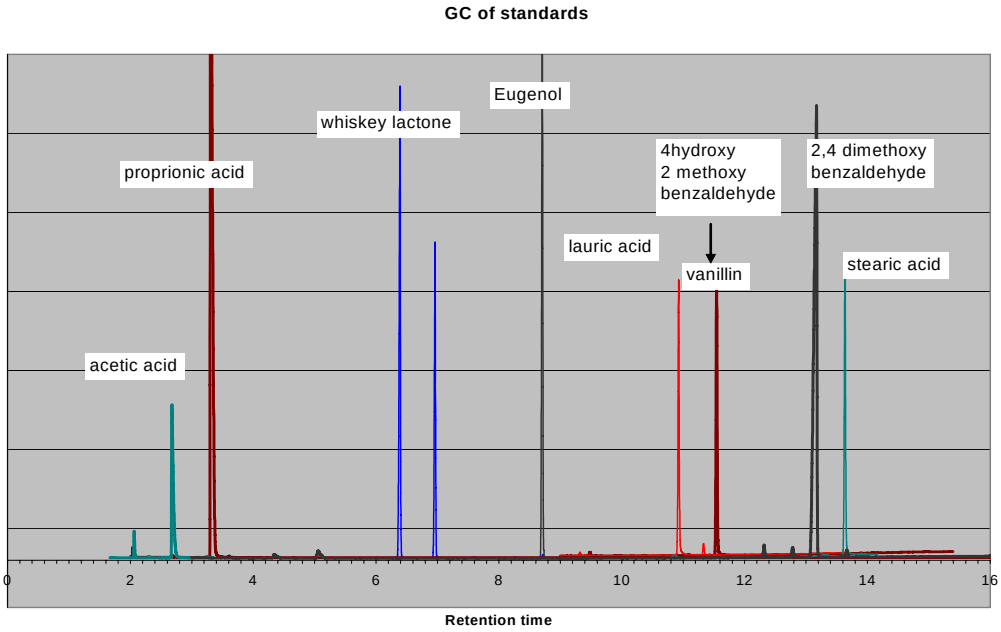


Figure 48. Gas chromatogram of flavor standards.

concentration standards using area percents obtained from the instrumentation software. The concentrations for several compounds for the extracted thermally treated oaks are summarized in table 12. An acid-to-base ratio was calculated for the spirit extract using acetic acid, cis and trans lactone, and stearic acid as acidic components and eugenol and vanillin as the basic components. The ratios are also summarized in table 12.

Figure 49 shows the gas chromatogram of the Ozark control and white spirits. Many compounds are present in the white spirits that also are present in the extracted sample of the Ozark control. The white spirit was subtracted as background in the subsequent chromatograms for both oaks to provide a clearer picture of the relative changes occurring upon extraction.

Table 12. Concentrations of components for thermally treated oak extracts.

mg/L	acetic acid	cis lactone	trans lactone	eugenol	vanillin	stearic acid	a/b ratio	total acids
retention time, min	2.67	6.25-6.35	6.8-6.95	8.69	11.52	13.6-13.9		mgL^{-1}
Appalachian control	697.9	50.9	22.8	0.4	0.4	20.8	984.6	792.3
Ozark control	483.5	57.9	44.6	2.9	1.0	45.0	159.0	631.0
Appalachian 150	692.8	74.7	19.1	1.2	1.0	26.8	364.1	813.4
Ozark 150	454.2	38.1	17.5	1.3	1.0	28.2	231.6	538.0
Appalachian 200	406.0	17.4	12.9	1.5	1.0	15.1	183.8	451.4
Ozark 200	216.7	22.8	16.2	1.3	12.4	41.3	21.6	297.0
Appalachian 250	127.7	20.0	12.5	1.1	1.4	9.1	67.6	169.4
Ozark 250	256.8	8.7	10.9	1.9	3.6	6.8	52.3	283.3

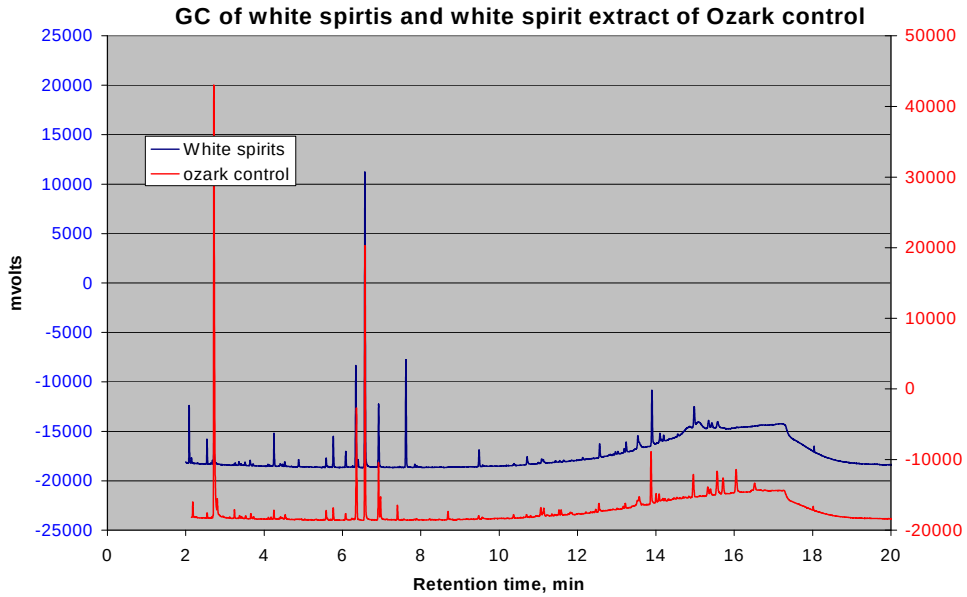


Figure 49. Gas chromatogram of Ozark oak control and white spirits after 6 weeks aging.

Figures 50 and 51 show the gas chromatograms of the Ozark and Appalachian oak control extracts after six weeks of aging and white spirits subtraction. From table 12, the acetic acid concentrations are 698 mgL^{-1} for the Appalachian oak and 483 mgL^{-1} for the Ozark oak. Titration analysis in table 11 showed a pK_a of 4.98 for the Appalachian oak versus 5.55 for the Ozark oak, clearly indicating a higher acidity for the former. Acid-base ratio from XPS after extraction in figure 44 of 0.30 for the Appalachian oak versus 0.25 for the Ozark oak is in agreement with the above observations. Similarly, the O/C ratios of 0.39 and 0.33 in Figures 29 and 30 for the Appalachian and Ozark oaks are in agreement with the higher acidity of the Appalachian oak by GC and titration analysis. Surface energy analysis of the acid-base ratio in tables 6 and 7 is also in agreement with the higher acidity of the Appalachian oak.

Figures 52 and 53 show the gas chromatograms for the Ozark and Appalachian oaks at the 150 ^{o}C thermal treatments. This temperature range corresponds to the minimum acid-base ratio from surface energy calculations summarized in tables 6, 7, and 9. The gas chromatograms for the Appalachian oak at 150 ^{o}C show greater contribution of the acetic acid and lactones than does the Ozark oak, which is indicative of higher acidity relative to basicity. Table 12 shows the Appalachian Oak has higher acidity and acid-base ratio from gas chromatography data at 813 versus 538 mgL^{-1} and 364 versus 231. The XPS data shows a greater acid-base ratio change for the Appalachian oak, from 0.15 to 0.30 versus 0.25 to 0.35 for the Ozark oak in Figures 44 and 45. Oxygen to carbon (O/C) ratio changes are much greater for the Appalachian oak and do not change for the Ozark oak as shown earlier in Figures 29 and 30. Surface energy and titration data in tables 6, 7, 9, and 11 support the somewhat higher acidity level for the Appalachian versus Ozark oak in this thermal treatment range.

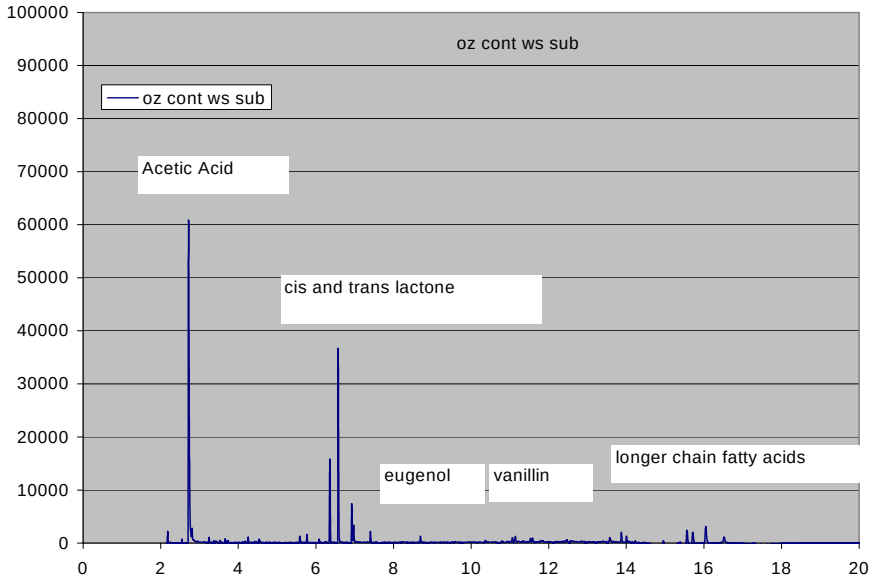


Figure 50. Gas chromatogram of Ozark control after white spirits subtraction.

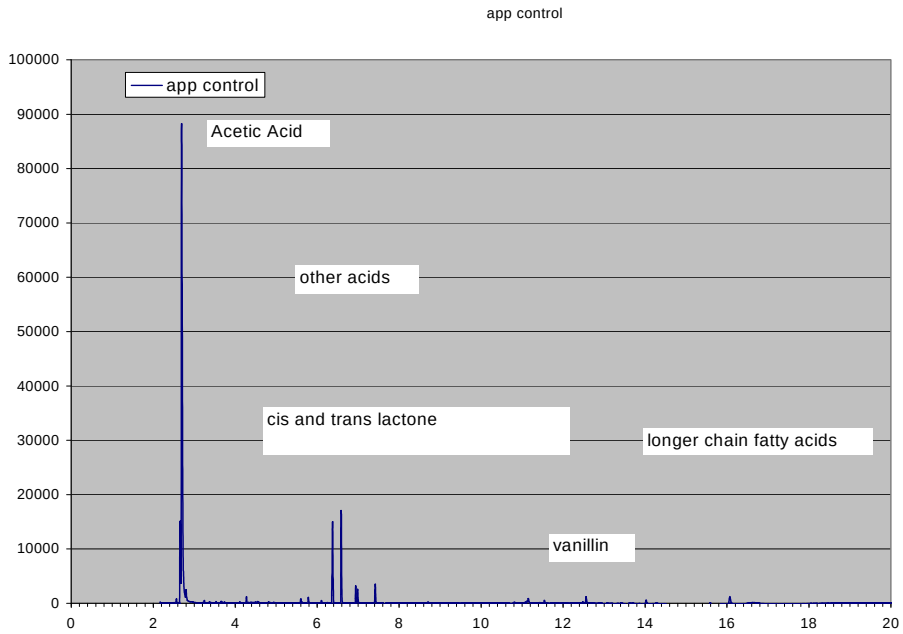


Figure 51. Gas chromatogram of Appalachian control after white spirits subtraction.

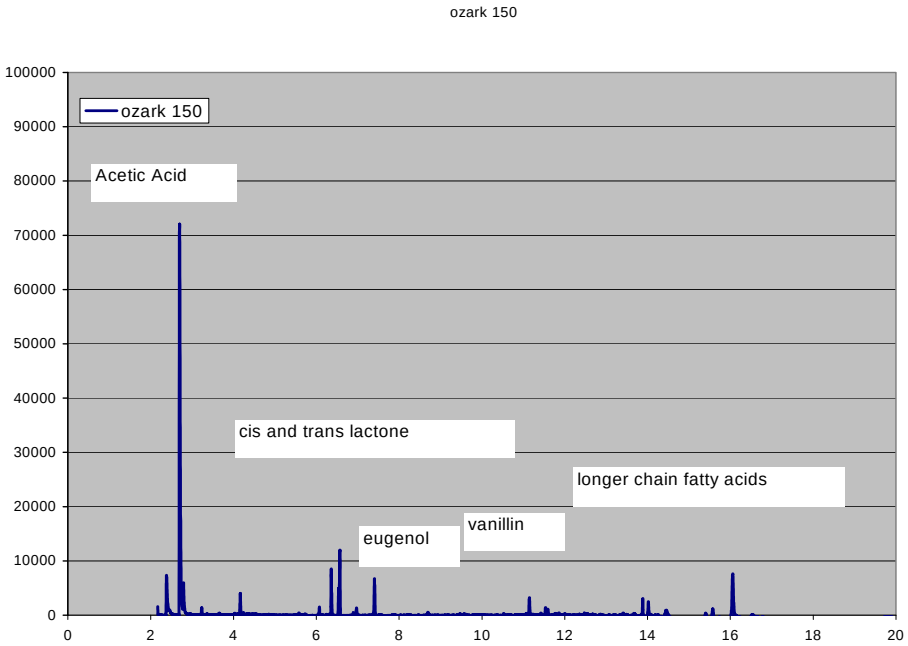


Figure 52. Gas chromatogram of Ozark 150 °C after WS subtraction.

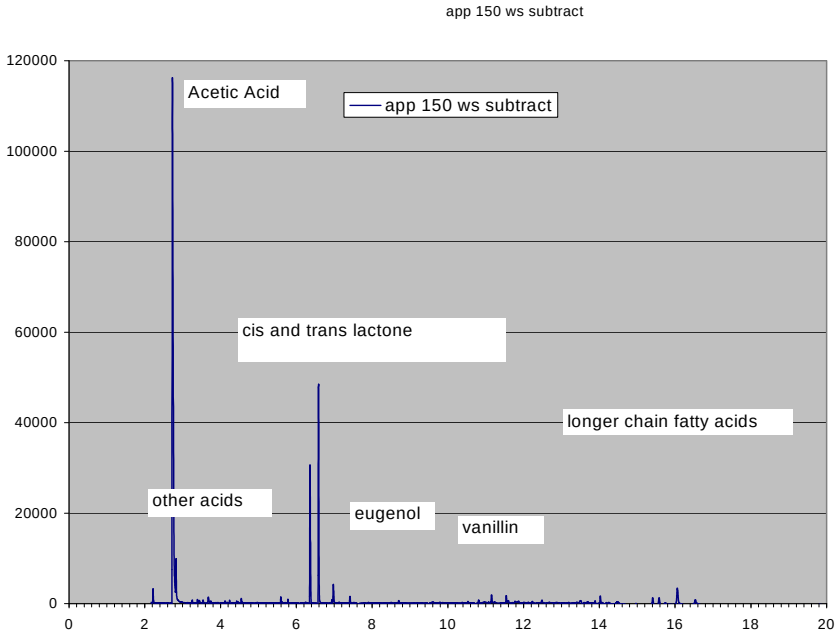


Figure 53. Gas chromatogram of Appalachian 150 °C after WS subtraction.

Figures 54 and 55 show the chromatograms for the Ozark and Appalachian oak extracts after 200 ^{o}C thermal treatments. The total acids and a/b ratio for the Appalachian and Ozark oaks are summarized in table 12. The peak at the 14.6 minute retention time could not be identified for the Ozark oak, but a higher chain fatty acid is probable. The 200 ^{o}C thermal treatments correspond to the minimum in O/C and acid-base ratios from XPS for the unextracted Ozark oak while for the Appalachian oak these values are increasing. Upon extraction, the fatty acid concentration and the acid-base ratio for the Ozark oak increase from 5 to 8 percent and from 0.15 to 0.53 as shown in Figures 41 and 45. Tables 6, 7, 9 and 11 show a higher acid-base ratio from surface energy and titration data for the Ozark oak although the pK_A values are comparable. The chromatograms show increased peak activity from the acid resolved column for the Ozark oak relative to the Appalachian oak. The Appalachian oak still has an intense acetic acid peak, making it difficult to quantify the relative acidity from chromatographic data. The titration data in table 11 show higher equivalent acid content, Veq, for the Ozark oak relative to the Appalachian oak.

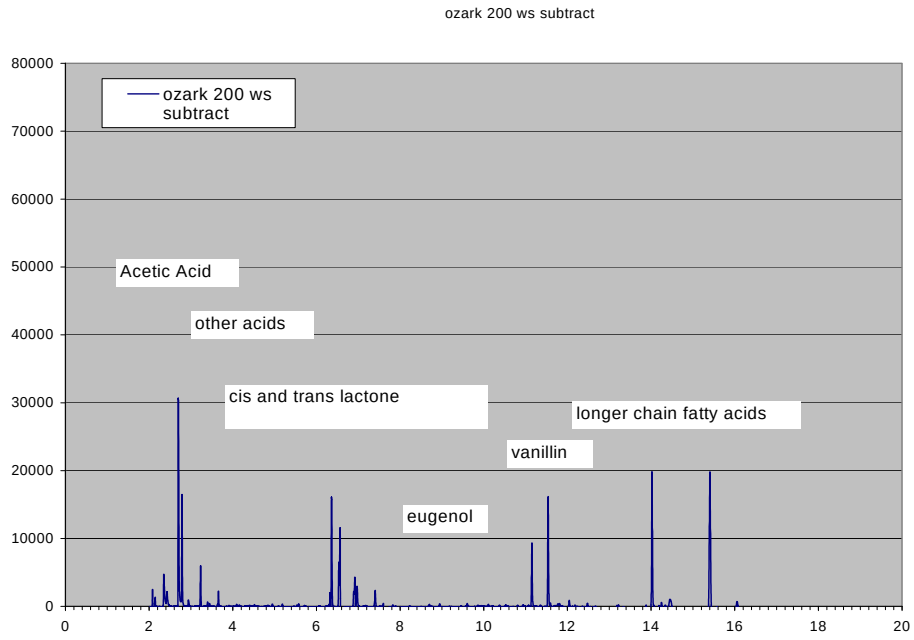


Figure 54. Gas chromatogram of Ozark 200 °C after WS subtraction.

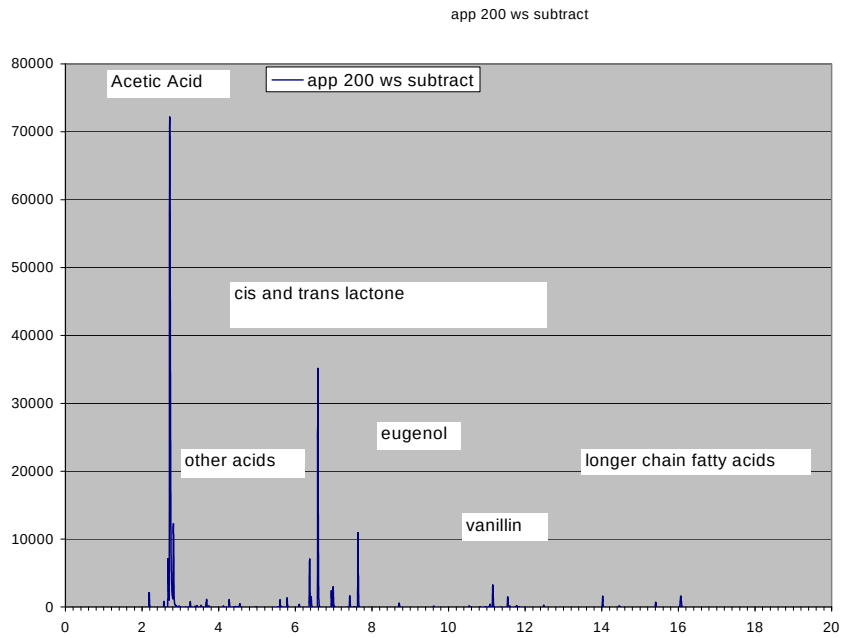


Figure 55. Gas chromatogram of Appalachian 200 °C after WS subtraction.

Figures 56 and 57 show the chromatograms for the two oak extracts after 250 ^{o}C thermal treatments. The total acid content from gas chromatography in table 12 shows higher acid content for the Ozark oak, which is in line with the greater increase in acid-base ratio from XPS in Figures 44 and 45 and in O/C ratio in Figures 29 and 30 for the two oaks. The Ozark oak clearly shows more activity than the Appalachian oak in terms of products coming off the acid resolved column. Also, surface energy and titration data in tables 6, 7, 9 and 11 show higher acid-base ratios and pKa values for the Ozark oak. This information, coupled with the increase in aromatic C0 peaks, is indicative of more phenolic-type alcohols that tend to be more acidic.

Figure 58 shows the gas chromatogram of a mature spirit after several years of aging. Peaks for acetic acid, eugenol, and vanillin are present along with others that appear in the higher thermal treatment extracts shown previously. The gas chromatogram in figure 59 of heavy char extracted with white spirits for six weeks shows more intense bands than the matured spirit. The extract sample was carried out at the lab scale and concentration differences would be expected. The overall volatile acid, ester, and aromatic aldehyde chromatographic fingerprint of the matured spirit is quite

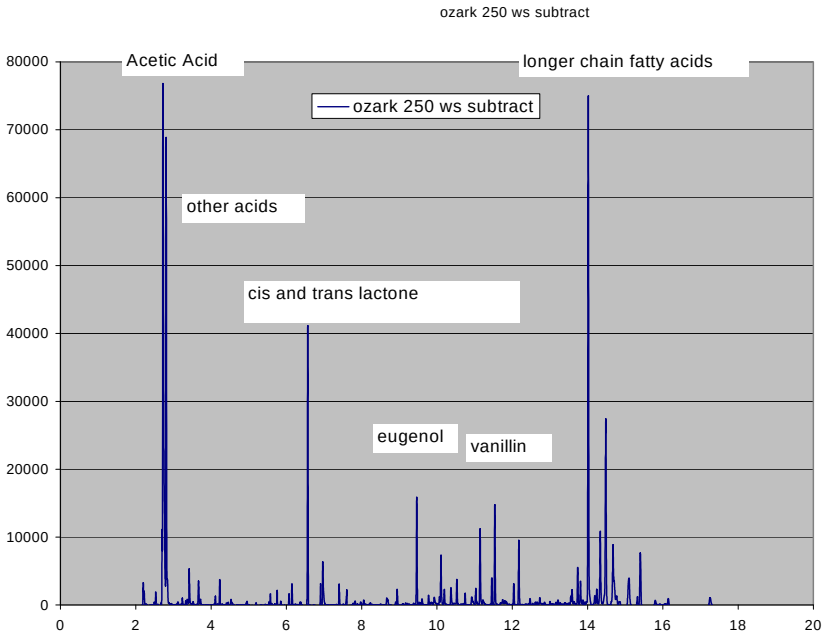


Figure 56. Gas chromatogram of Ozark 250 °C after WS subtraction.

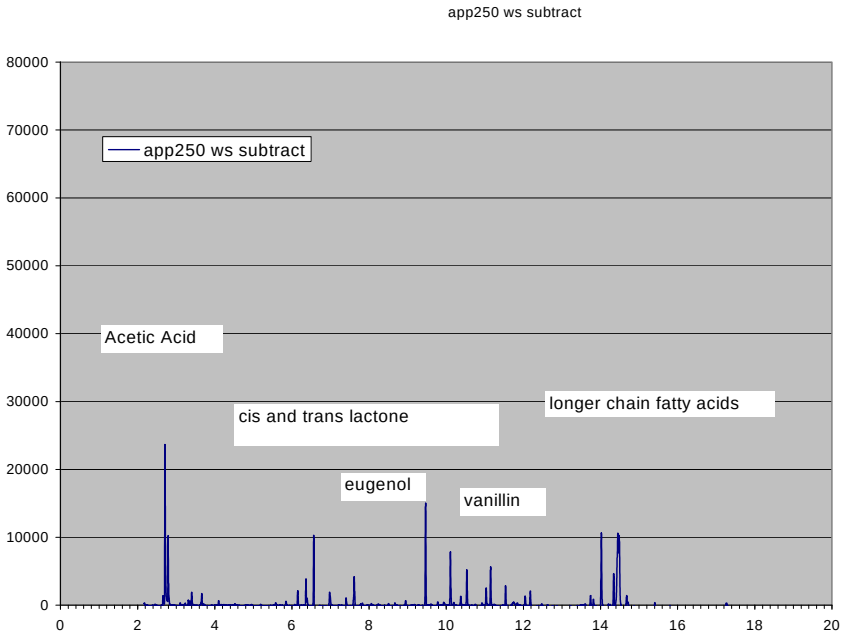


Figure 57. Gas chromatogram of Appalachian 250 °C after WS subtraction.

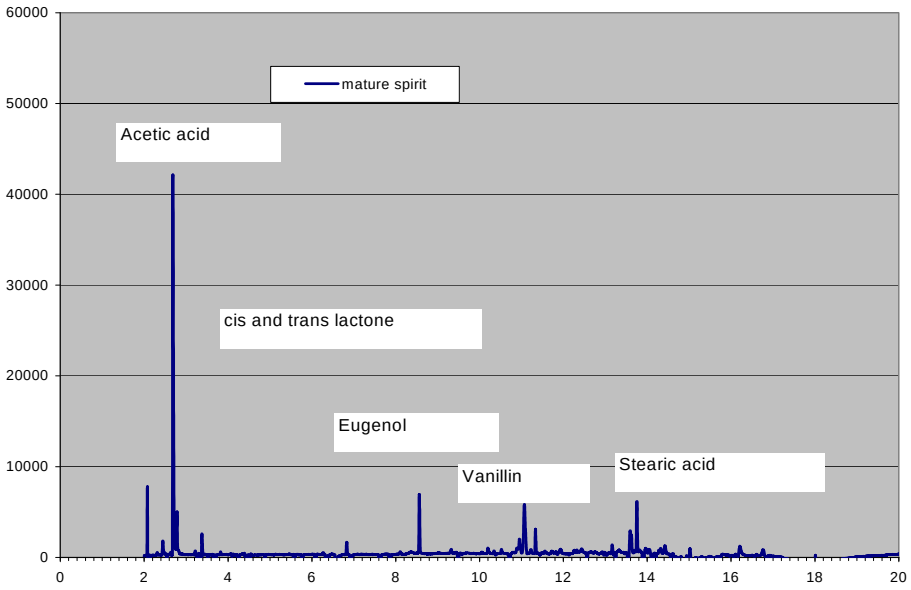


Figure 58. Gas chromatogram of a mature spirit.

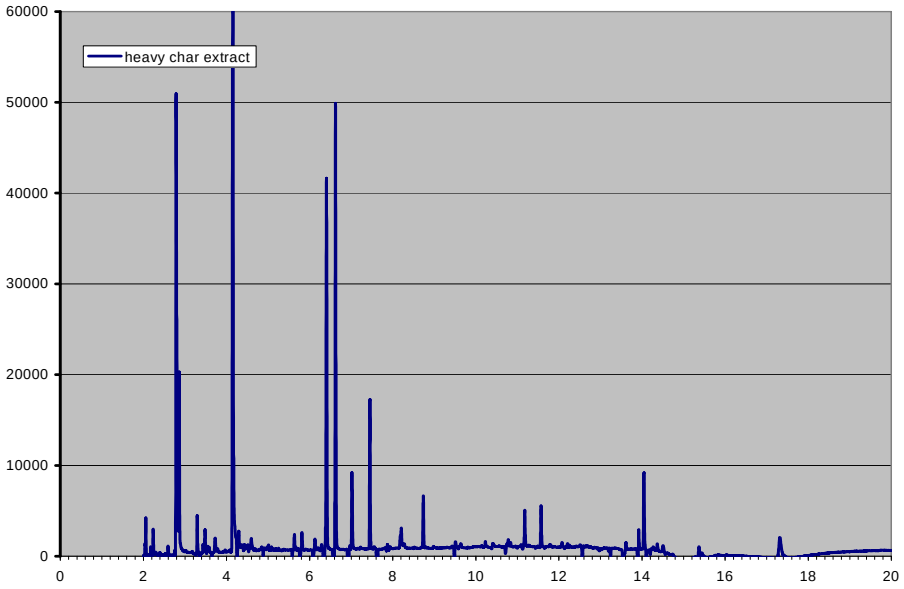


Figure 59. Gas chromatogram of charred white oak after extraction.

similar in components present to the white spirit extract of the charred white oak with the exception of the lactone peaks.

The white spirit extract composition obtained from gas chromatography is compared graphically for the thermally treated Ozark and Appalachian oaks in Figures 60-63. For the control in figure 60, the Ozark oak has higher lactones and stearic acid. Table 12 shows a much higher level of acetic acid for the Appalachian oak control. At the 150 °C thermal treatment in figure 61, the Appalachian oak has higher acetic acid and other components than does the Ozark oak. For both treatments at the lower temperatures, the increase in acid/base ratio is highest for the Appalachian oak, as shown earlier in Figures 44 and 45. The thermal treatments at 200 ° C and 250 ° C in Figures 56, 62 and 63 clearly show increased levels of aroma compounds for the Ozark oak in comparison to the Appalachian oak. Several compounds for the Ozark oak at the 250 °C thermal treatment were not identified.

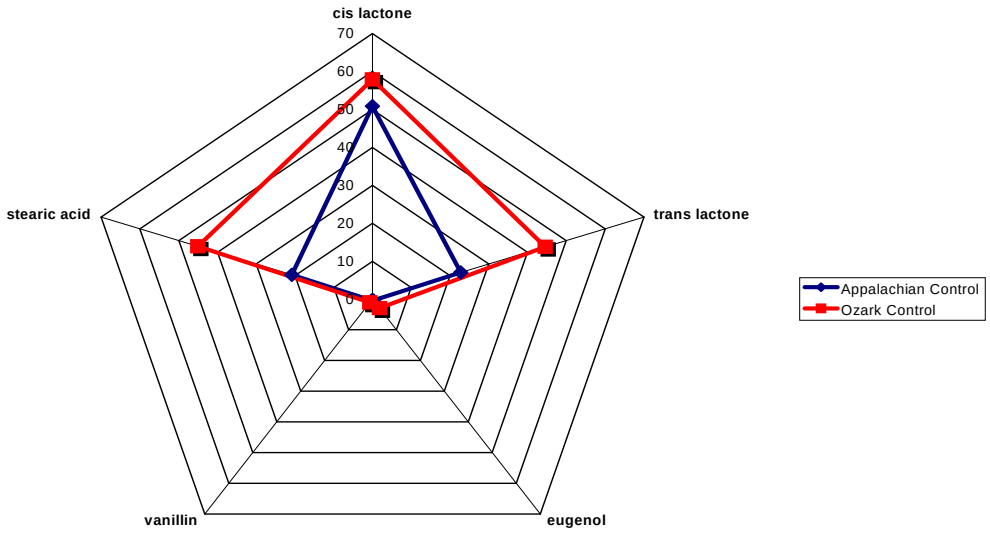


Figure 60. Spider chart of extract components for control.

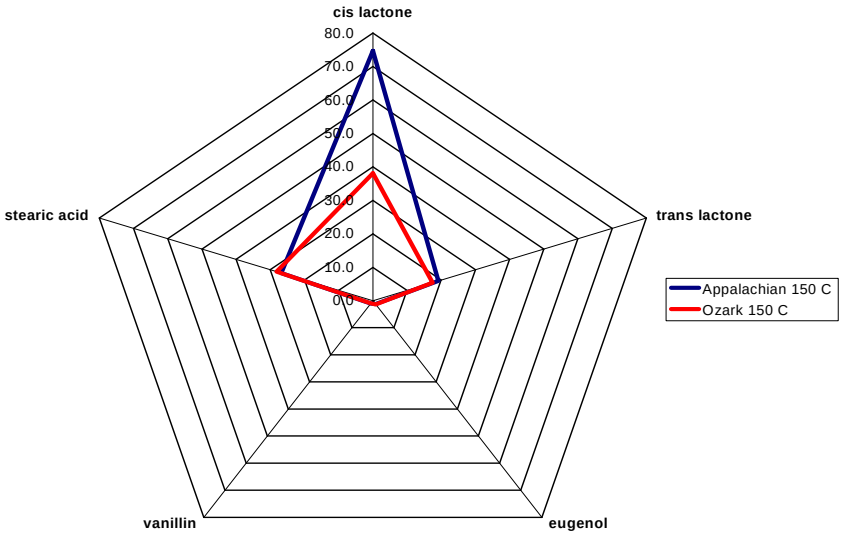


Figure 61. Spider chart for extract components at 150 °C.

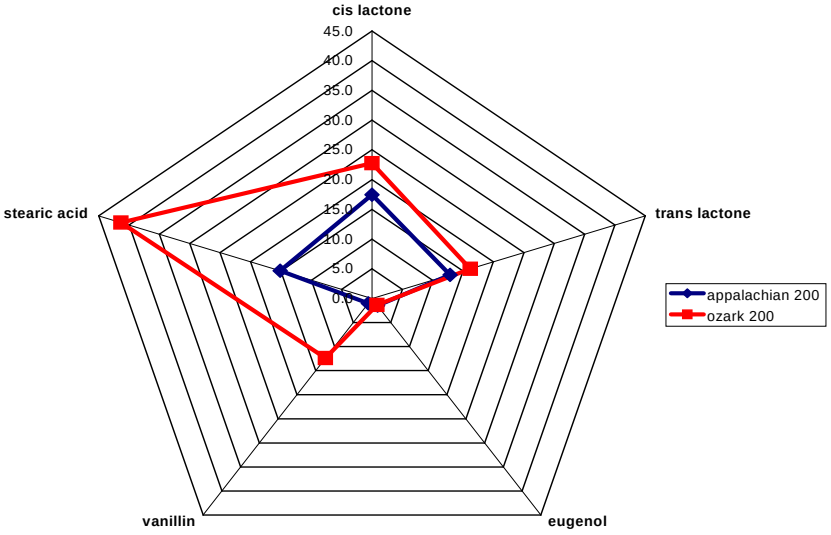


Figure 62. Spider chart for extract components at 200 °C.

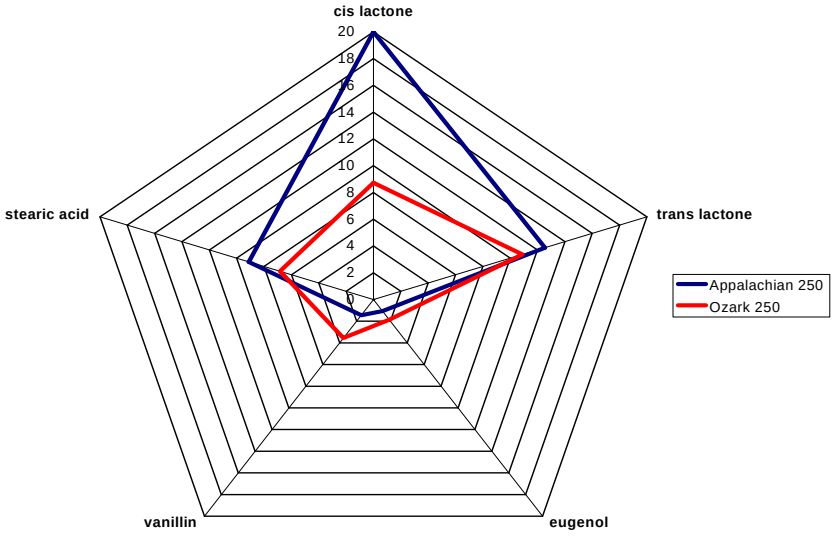


Figure 63. Spider chart for extract components at 250 °C.

5.9 Relationship Between Surface Composition, Surface Energy, and Spirit Extract Composition

The relationship between surface composition, surface energy, and extract composition can be represented by a comparison of the solid surface energy parameters, compositional data from XPS, and liquid composition of the extract from gas chromatography. Figure 64 shows a plot of the acid-base surface energy ratio from XPS versus the acid-base surface energy ratio for the spirit extract summarized in table 12. The data show a scattered inverse relationship between the acid-base ratio from surface energy and liquid composition. Two explanations can be given for the behavior at either extreme. The low acid-base ratio of the solid surface corresponds to low thermal treatments where the primary process is extraction of fatty acids and other acidic compounds, resulting in a higher extract liquid acid-base ratio. The higher acid-base ratio corresponds to higher thermal treatment. In this region, the extractive fatty acid

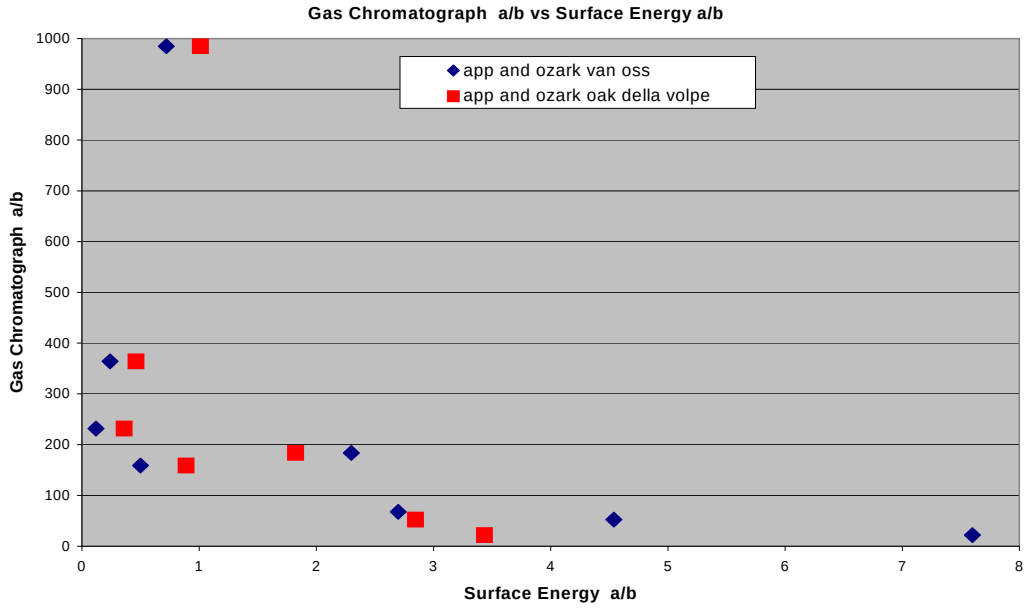


Figure 64. Extract a/b ratio versus surface energy a/b ratio.

materials have been degraded and are not as available for removal. Also, fatty acid and other surface oxygen components formed at the surface during oxidation are responsible for increased interaction of the liquid with the surface due to acid-base interactions. The increased surface oxygen content and acid base sites obtained with thermal treatment are more capable of acid-base interaction with the aqueous white spirit. Vanillin and eugenol could be formed directly in degradation from the thermolysis of lignin as shown in Figures 10 and 11, or some type of interaction of the white spirit with the phenoxy and phenethyl type intermediates may be required for its conversion. The latter type of reaction promotes more of the aromatic compounds such as vanillin and eugenol, as indicated by their higher levels in conjunction with a more acidic surface. The increase in surface acidity observed in XPS data in Figures 44 and 45 at the higher thermal treatments would occur due to removal of the more basic groups. Compositional data in Figures 40 and 41 show a reduction in carbon and increase in alcohol, fatty acid, and carbonyl upon extraction at the two highest temperatures with the carbonyl increasing the least.

Figure 65 compares the relationship between surface composition (acid-base and O/C) from XPS to the acid base spirit composition obtained from gas chromatography. While the data are scattered, they generally indicate that an increase in active oxygen groups results in an increase in acidic groups in the extract. The samples at the lower thermal treatments are giving much higher acidity due to higher levels of acidic extractives such as acetic acid and lactones as summarized in table 12.

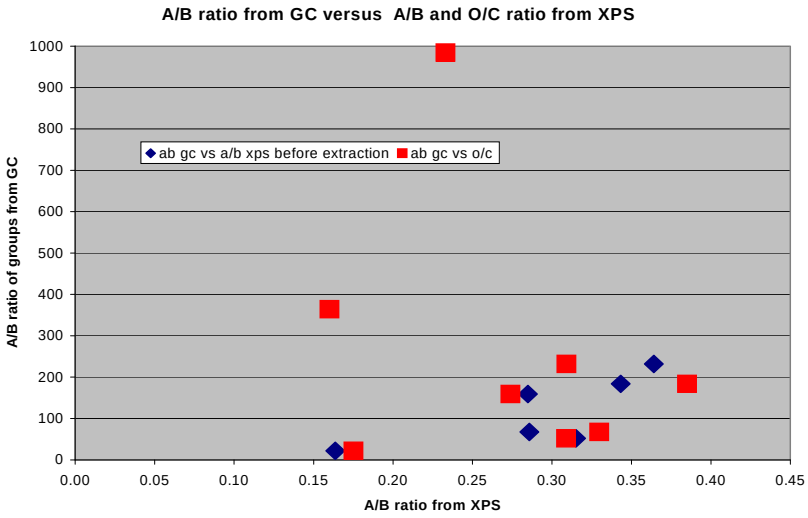


Figure 65. Extract a/b ratio versus a/b and O/C ratio from XPS.

6.0 Conclusions

The surface composition and surface energy of thermally treated white oak were investigated and compared to the volatile acid, ester, and aromatic aldehyde composition of white spirit extracts. By relating the oxygen-to-carbon ratio changes caused by thermal treatment and extraction to changes in cellulose, lignin, and extractive levels, it was possible to assign compositional changes in relation to changes in wood components. Measurements of changes in wood surface composition with thermal modification and spirit interaction aid in understanding how oxidative degradation pathways of oak wood and lignin can contribute to spirit composition.

The analytical techniques presented show that increases in surface concentration of specific functional groups upon extraction relate to their increased concentration in the spirit. Additionally, increases in surface acidity of the oaks upon extraction correspond to increased acidity of the spirit based on titration analysis. An acid-base ratio obtained from the thermally modified wood functional group composition was compared to the acid-base surface energy using the wicking method of contact angle analysis. The results were nearly linear for the Appalachian oak and very scattered for the Ozark oak. The high scatter observed in the Ozark oak may be a result of different depths of investigation with contact angles versus XPS as previously discussed. The temperatures for the minimum O/C and acid-base ratio were different from those observed for surface energy analysis of the Ozark oak. The changes in acid-base ratios upon extraction, contact angle with the interacting spirit, and surface energy analysis show that increased surface activity and interaction result in a changing product distribution that favors more aromatic aldehyde type compounds at the higher temperatures. When compared to the Appalachian oak, the Ozark oak showed higher levels of acidic groups relative to basic groups after thermal modification and extraction. Surface energy analysis showed a reduction in basic groups with increasing thermal treatment for both oaks with the greatest decrease occurring for the Appalachian oak.

The surface analytical data provided by the two techniques proved to be consistent with the relative amount of acidic products formed in extracts of the thermally modified oaks obtained by gas chromatography. The results show that for the Appalachian and Ozark oaks the surface oxygen groups initially decrease with thermal treatment in the 150 and 200 ° C range and then increase at higher temperatures. Higher acidic-basic functional group ratios and surface oxygen levels were obtained upon thermal treatment and extraction for the Ozark oak. The higher surface oxygen contents correspond to increased interaction of the white spirits with the thermally treated oak as measured by decreasing contact angle with the white spirits, increased acidity from titration, and increased volatile acid, ester, and aromatic aldehyde component concentration in the spirit extract from gas chromatography. For the Appalachian oak at 250 ° C, smaller increases in the surface oxygen content with thermal treatment and extraction correspond to a surface that does not wick water and is hydrophobic. Its lack of reactivity corresponds to decreased release of acidic components in the maturing extract as evidenced by gas chromatography results. The data support higher levels of aroma-type compounds produced by the Ozark oak upon thermal treatment and extraction. These results are consistent with the fact that the Ozark oak is preferred by spirit manufacturers.

Surface composition analysis is an important tool for determining how surface modifications affect wood's acid-base surface properties and interaction with liquids. As such, it can significantly improve understanding of thermally treated wood's impact on the composition of the maturing spirit. Experiments that probe the influence of surface modification on the relative degree of oxidation of the wood and the resulting product mix in the maturing spirit would be useful for accessing whether wood from different sources can be tailored to obtain certain spirit compositions. The relative degree of oxidation of the wood could perhaps be increased through ozonolysis followed by thermal treatments that vary in rate and duration. Application of solid state NMR when coupled with XPS could help differentiate the influence of oxidation kinetics on the relative proportion of aromatic aldehyde molecules and its precursors. Such studies

would be useful in learning how to tailor oak surface modification treatments to obtain desirable spirit composition.

List of References

Arjona-Gonzalez, D., Gallero-Gonzalez, V., Pablos, F. and Gonzalez, G. Authentication and differentiation of Irish whiskeys by higher-alcohol congener analysis. Analytica Chimica Acta, 1999, 381:257-264.

Baker, F.S., Daley, R.A., Bradley, R.H., J. Chem. Tech. Biotech., 2005, 80:878-883.

Berg, J.C. Chapter 2. Role of Acid-Base Interactions in Wetting and Related Phenomena. *Wettability*. Marcel Dekker, New York, 1993, 75-148.

Berg, J.C. The importance of acid-base interactions in wetting, coating, adhesion and related phenomena. Nord. Pulp Paper Res. J, 1993, 8(1):75-85.

Boruff, C.S. and Rittschof, L.A. Effects of barreling proof on the aging of American whiskeys. Agriculture and Food Chemistry, Vol. 7, No. 9, September 1959.

Braun, J.L., Holtmann, K.M. and Kadla, J.F. Lignin-based carbon fibers: Oxidative thermostabilization of kraft lignin. Carbon, 2005, 43:385-394.

Briggs, D. and Beamson, G. Primary and secondary oxygen-induced C 1s binding energy shifts in X-ray photoelectron spectroscopy of polymers. Anal. Chem., 1992, 64:1729-36.

Britt, P.F., Buchannan A.C. and Malcolm, E.A. Thermolysis of phenethyl phenyl ether-a model for ether linkages in lignin and low rank coal. J. Org Chem., 1995, 60(20): 6523-6536.

Britt, P.F., Buchannan A.C. and Malcolm, E.A. Impact of restricted mass transport on pyrolysis pathways for aryl ether containing lignin model compounds. Energy Fuels, 2000, 14(6):1314-1322.

Coates, J. Interpretation of Infrared Spectra, A Practical Approach. *Encyclopedia of Analytical Chemistry.* John Wiley and Sons Ltd., 2002.

Conner, J.M., Paterson, A. and Piggot, J.R. Changes in wood extractives from oak cask staves through maturation of scotch malt whisky. J. Sci Food Agric, 1993, 62:169-174.

Conner, J.M., Paterson, A. and Piggot, J.R. Release of distillate flavor compounds in scotch malt whiskey, J. Sci Food Agric, 1999, 79:1015-1020.

Crouch, S.R. and Holler, F.J. *Applications of Microsoft Excel in Analytical Chemistry.* Brooks/Cole, Belmont, CA, 2004.

de Meijer, M., Haemers, S., Cobben, W. and Miitz, H., Surface energy determination of wood: Comparison of methods and wood species, Langmuir, 2000, 16:9352-9359.

Della Volpe, C and Siboni, S. Some reflections on acid-base solid surface free energy theories. J. Colloid Interface Sci., 1997, 195:121-136.

Doussot, F., Pardon, P., Dedier, J. and De Jeso, B. Individual, species and geographic origin influence on cooperage oak extractible content (Quercus robur L. and Quercus petraea Liebl.), Analusis, 2000, 28:960-965.

Fowkes, F.M. Acid-base interactions in polymer adhesion. *Phyicochemical Aspects of Polymer Surfaces*. Vol. 2. Ed. K.L. Mittal. Plenum Press, New York, 1983, 583-603.

Fowkes, F.M. Additivity of intermolecular forces at interfaces. I. Determination of the contribution to surface and interfacial tensions of dispersion forces in various liquids. J. Phys. Chem., 1963, 67:2538-2541.

Fowkes, F.M., Kaczinski, M.B. and Dwight, D.W. Characterization of polymer surface sites with contact angles of test solutions. I. Phenol and iodine adsorption from CH2I2. Langmuir, 1991, 7:2464-2470.

Fowkes, F.M. and Mostafa, M.A. Acid-base interactions in polymer adsorption. Ind. Eng. Chem. Prod. Res. Dev., 1978, 17(1):3-7.

Fowkes, F.M., Tischler, D.O., Wolfe, J.A., Lannigan, L.A., Ademu-John, C.M. and Halliwell, M.J. Acid-Base complexes of polymers. J. Polym. Sci.Polym. Chem. Ed., 1984, 22:547-566.

Gardner, D.J. Application of the Lifshitz-van der Waals/acid-base approach to determine wood surface tension components. Wood Fiber Sci., 1996, 28(4):422-428.

Gindl, M and Tschegg, S. Significance of the acidity of wood to the surface free energy components of different wood species. Langmuir, 2002, 18:3209-3212.

Gomez-Plaza, E., Perez-Prieto, L., Fernandez, J. and Lopez-Rica, J. The effect of successive uses of oak barrels on the extraction of oak-related volatile compounds from wine. Internat. J. Food Sci. Tech., 2004, 39:1069-1078.

Hojo, M., Suzuki, M. and Ueda, T. Solute effects on the interaction between water and ethanol in aged whiskey, J. Agric. Food Chem., 2004, 52:5359-5365.

Holmes-Farley, S.R., Reamey, R.H., Nuzzo, T.J., McCarthy, G. and Whitesides, G.M. Wetting of functionalized polyethylene film having ionizable organic acids and bases at the polymer-water interface: Relations between functional group polarity, extent of ionization, and contact angle with water. Langmuir, 1988, 4:921-937.

Holmes-Farley, S.R. and Whitesides, G.M. Fluorescence properties of dansyl groups covalently bonded to the surface of oxidatively functionalized low-density polyethylene film. Langmuir, 1986, 2:266-281.

Holmes-Farley, S.R. and Whitesides, G.M., Reactivity of carboxylic acid and ester groups in the functionalized interfacial region of polyethylene carboxylic acid (PE-CO2H) derivatives: Differentiation of the functional, Langmuir, 1987, 3:62-76.

Jaic, M., Stevanovic-Janezik, T. and Dekanski A. Comparison of surface properties of beech and oakwood as determined by ESCA method. Holz Roh-Werkst, 1996, 54(1):37.

Li, K. and Reeve, D. Sample contamination in analysis of wood pulp fibers with X-ray photoelectron spectroscopy. J. Wood Chem. and Tech., 2004, 24(3):183-200.

Liu, F.P. and Rials, T.G. Relationship of wood surface energy to surface composition. Langmuir, 1998, 14:536-541.

March, J. and Smith, M. *March's Advanced Organic Chemistry*. Fifth Edition. John Wiley and Sons Ltd., 2001.

Maga, J.A. The Contribution of Wood to the Flavour of Alcoholic Beverages. Food. Rev. Internat., 1989, 5:39-99.

Miller, R. B. Structure of Wood. *Wood Handbook-Wood as an Engineering Material*. Gen Tech. Rep., FPL-GTR-113. U.S. Department of Agriculture, Forest Service, Forest Products Laboratory, Madison, WI, 1999.

Mosedale, J.R. and Puech, J.L. Wood maturation of distilled beverages. Trends in Food Sci. and Tech., 1998, 9:95-101.

Nishimiya, K., Hata, T., Imamura, Y. and Ishihara, S. Analysis of chemical structure of wood charcoal by X-ray photoelectron spectroscopy, J. Wood. Sci., 1998, 44:56-61.

Nishimura, K., Ohnishi, M., Masuda, M., Koga, K. and Matsuyama, R. *Flavour of Distilled Beverages*. Ed. J.R. Piggott. Ellis Horwood, Chichester, England, 1983, 242.

NIST Database. National Institute of Standards and Technology, U.S. Secretary of Commerce, 2003.

Nzokou, P. and Kamden, P.D. X-ray photoelectron spectroscopy study of red oak, black cherry, and red pine- extracted wood surfaces. Surf. Interface Anal., 2005, 37:689-694.

Palviainen, J. On the optical metrology of wood ultrastructure. Dissertation 39. University of Joensuu, Department of Physics, Vaisala Laboratory, 2003.

Reazin, G.H. Chemical mechanisms of whiskey maturation. Am. J. Enol.Vitic., 1981, 32(4).

Reid, K.J. and Swan, J.S. Assessment of scotch whisky quality by pyrolysis-mass spectrometry and the subsequent correlation of quality with the oak wood cask. J. Anal. and Appl. Pyrolysis, 1993, 25:49-62.

Riviere, J.C. and Myhra, S. *Handbook of Surface and Interface Analysis*. Marcel Dekker, Inc., New York, 1998.

Rudan-Tasic, D. and Klofutar, C. Gran's plots for end point detection in potentiometric titration of wine. Analusis, 1998, 26, 25-28.

Sernek, M., Kamke, F. and Glasser, G. Comparative analysis of inactivated wood surface. Holzforschung, 2004, 58:22-31.

Shchukarev, A., Sundberg, B., Mellerowicz and Persson, P. XPS study of living tree. Surf.Interface Anal., 2002, 34:284-288.

Shen, Q., Mikkola, P. and Rosenholm, J.B. Quantitative characterization of subsurface acid-base properties of wood by XPS and Fowkes theory. Colloids Surfaces:Physiochem. Eng. Aspects, 1998, 145:235-241.

Sielbold, A., Walliser, A., Nardin, M.N., Oppliger, M. and Schultz, J. Capillary rise for thermodynamic characterization of solid particle surface. J. Colloid and Interface Sci., 1997, 186:60-70.

Sinn, G., Reiterer, A. and Stanzl-Tschegg. Surface analysis of different wood species using X-Ray photoelectron spectroscopy (XPS). J. Materials Sci., 2001, 36:4673-4680.

Sorrel, T.N., *Organic Chemistry*, University Science Books, Sausalito, CA, 1997, 227.

Stark, N.M. and Matuana, L. M. Polymer Degradation and Stability, 2004, 86:1-9.

van Oss, C.J., Chadhury, M.K. and Good, R.J. Monopolar surfaces. Advanc. Colloid Interface Sci., 1987, 28:35-64.

van Oss, C.J., Giese, R.F., Li, Z., Murphy, K., Norris, J., Chadhury, M.K. and Good, R.J. Determination of contact angles and pore sizes of porous media by column and thin-layer wicking. J. Adhesion Sci. Tech., 1992, 6(4):413-428.

van Oss, C.J. Use of the combined Lifshitz-van der Waals and Lewis acid-base approaches in determining apolar and polar contributions to surface and interfacial tensions and free energies. J. Adhesion Sci. Tech., 2002, 16(6):669-677.

Walinder, M., Wetting phenomena on wood. Doctoral Thesis. KTH-Royal Institute of Technology, Stockholm, Sweden, 2000.

Wheeler, E.A. WPS, North Carolina State University, Raleigh, 1996.

Zisman, W.A. Ind. Eng. Chem., 1963, 55:19-38.

Appendix

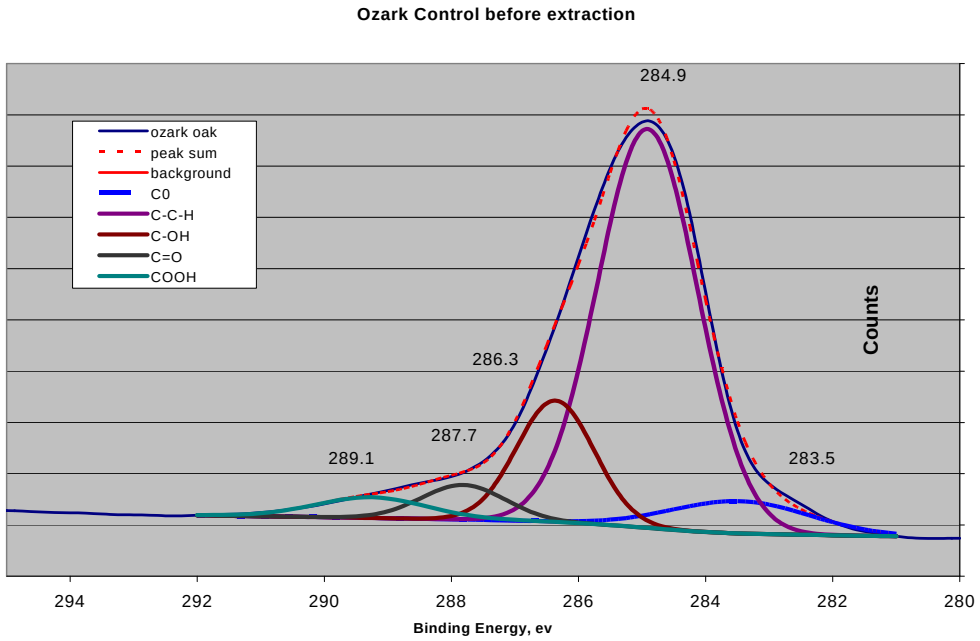


Figure A. 1. XPS scan of Ozark control before extraction

.

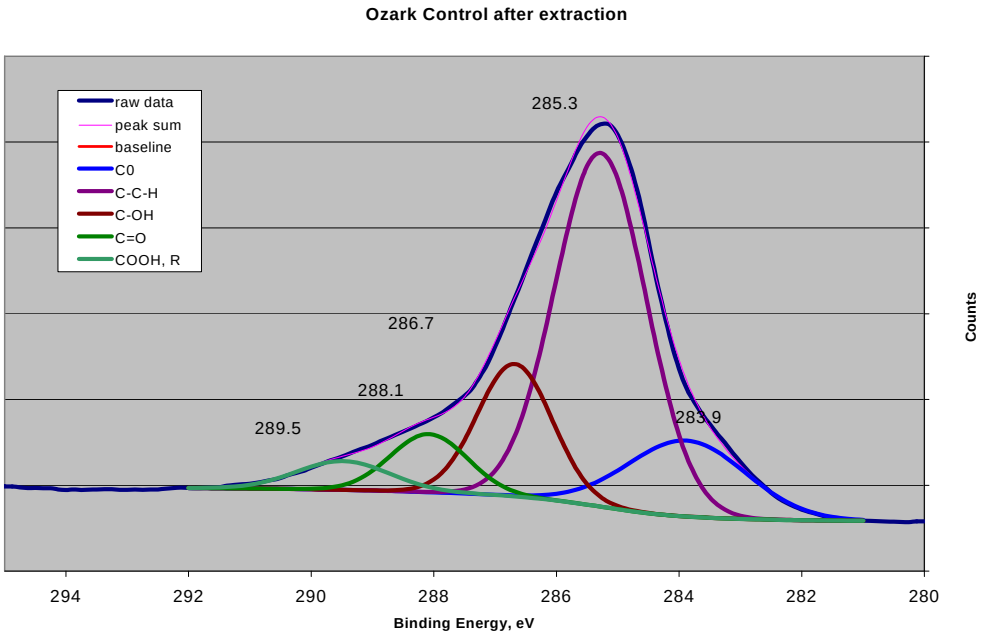


Figure A. 2. XPS of Ozark control after extraction

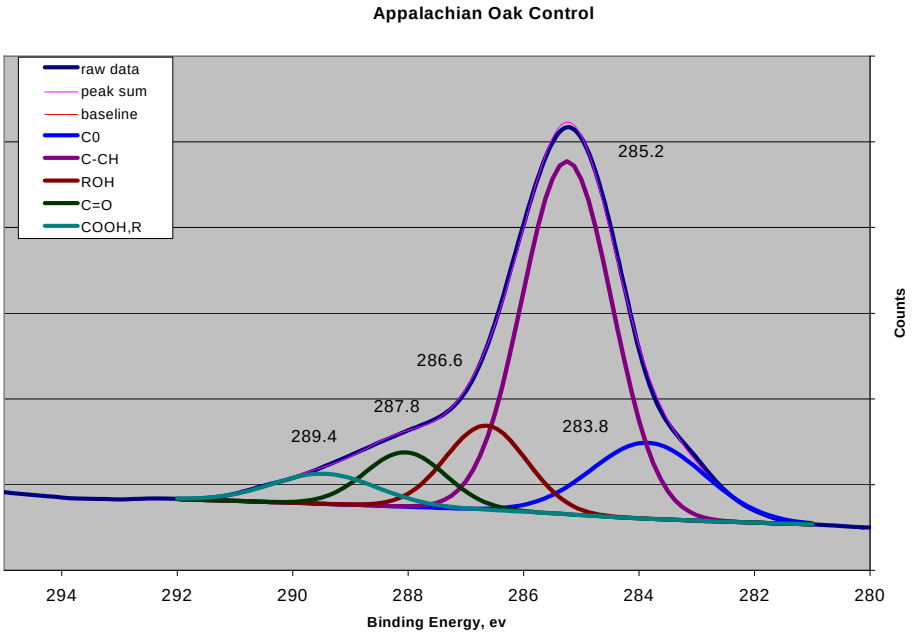


Figure A. 3. Appalachian oak control before extraction.

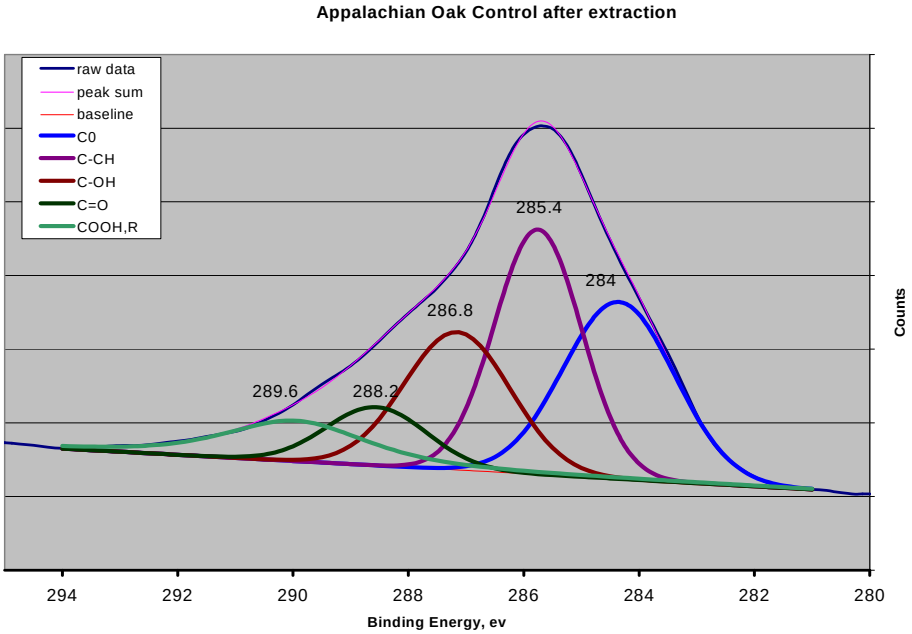


Figure A. 4. Appalachian oak after extraction.

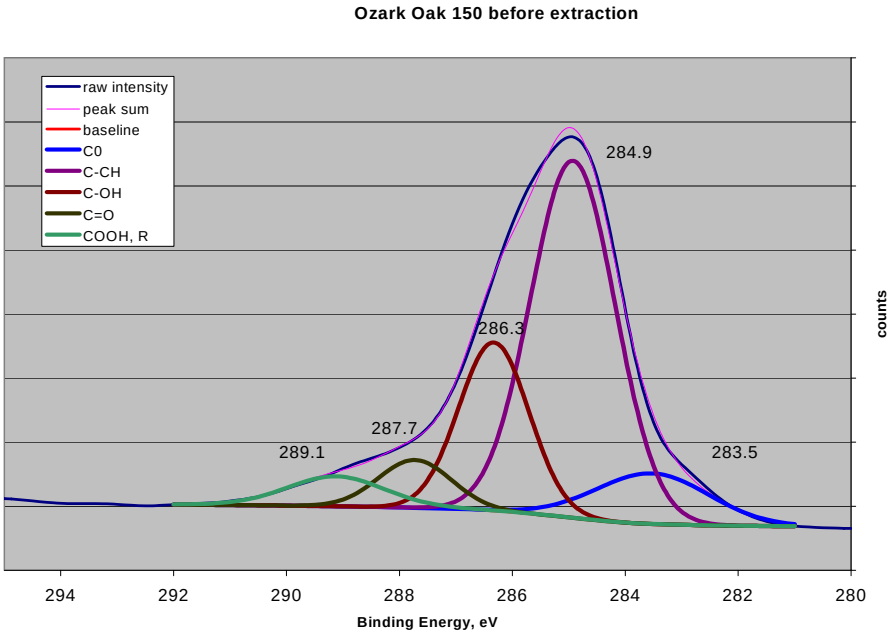


Figure A. 5. Ozark oak 150 °C before extraction.

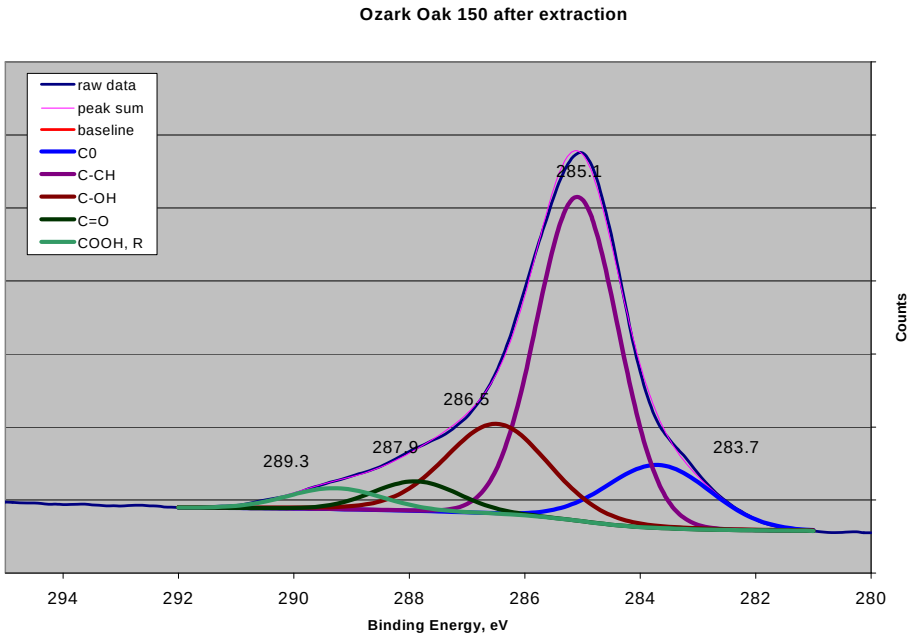


Figure A. 6. Ozark oak 150 °C after extraction

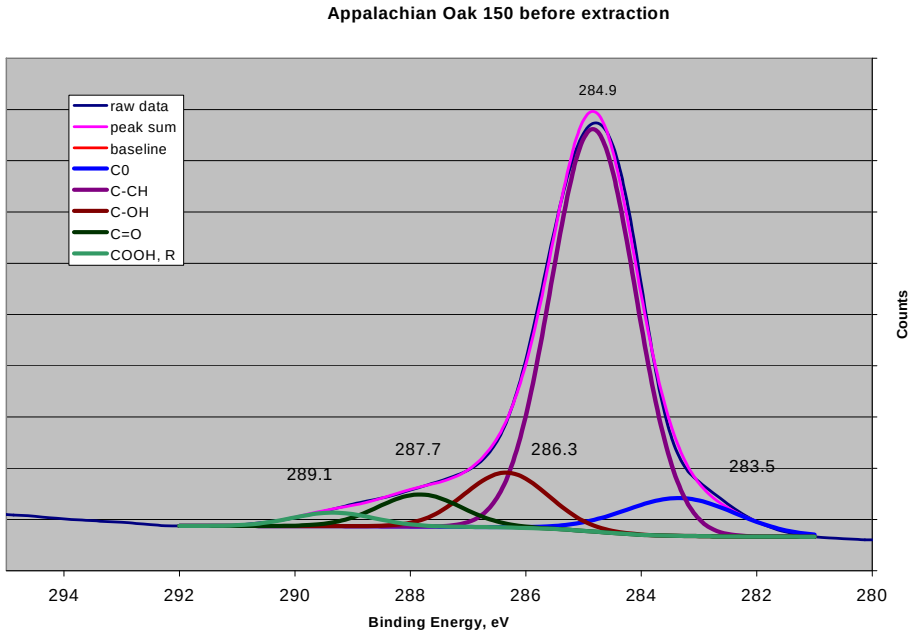


Figure A. 7. Appalachian oak 150 °C before extraction.

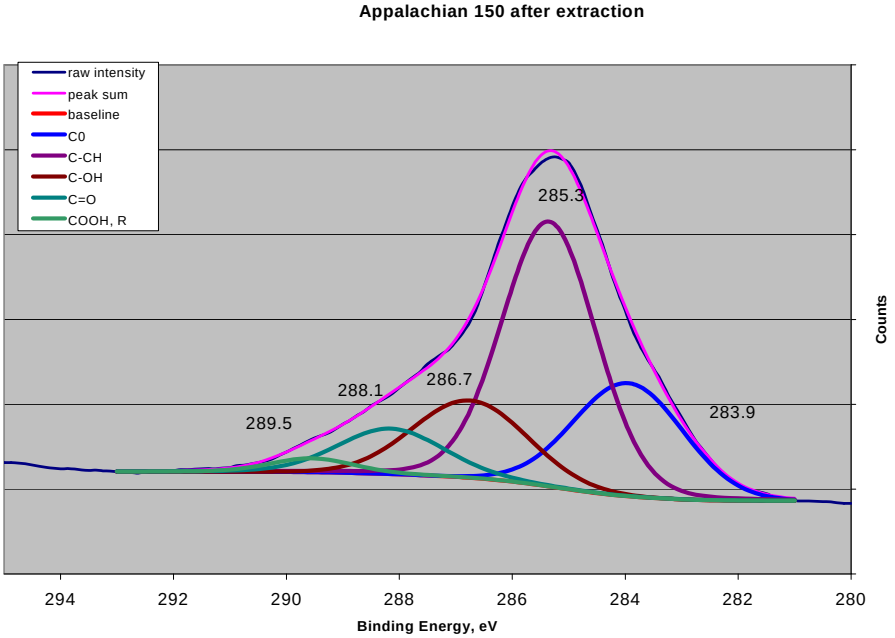


Figure A. 8. Appalachian oak 150 °C after extraction.

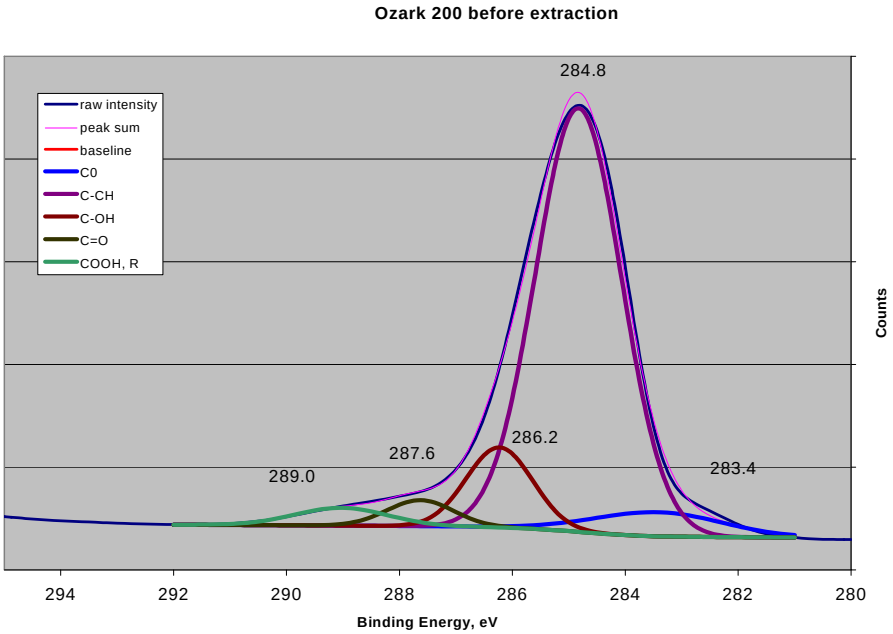


Figure A. 9. Ozark oak 200 °C before extraction.

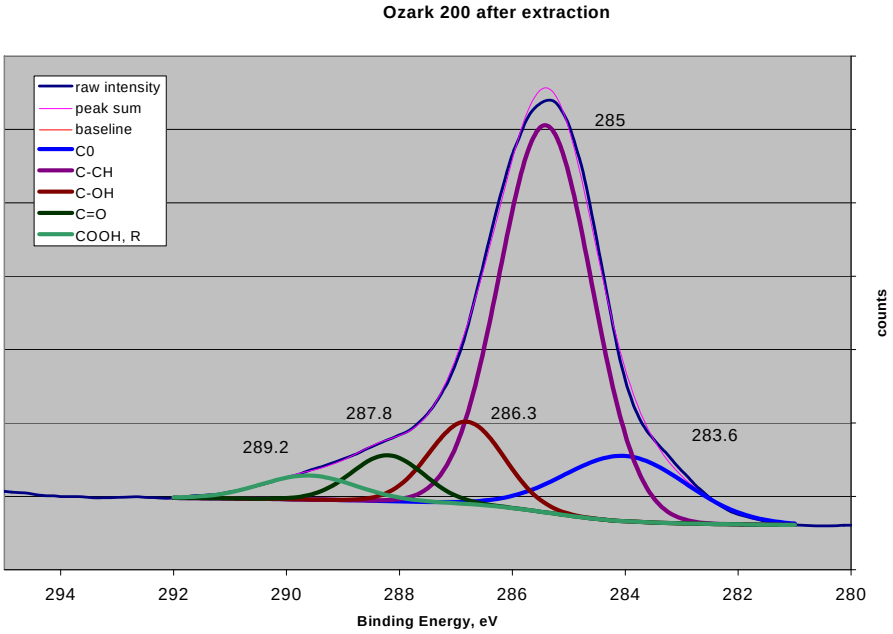


Figure A. 10. Ozark oak 200 °C after extraction.

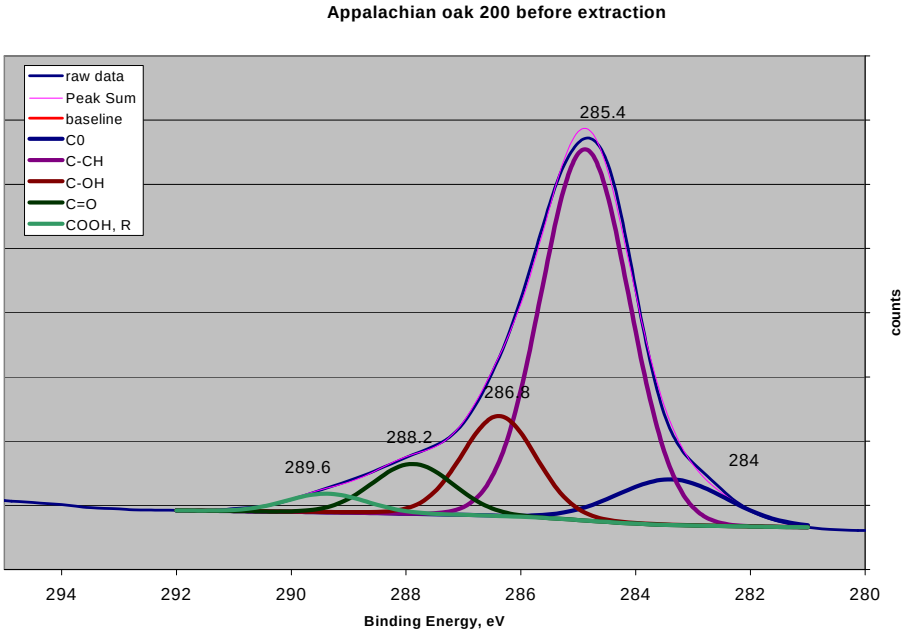


Figure A. 11. Appalachian oak 200 °C before extraction.

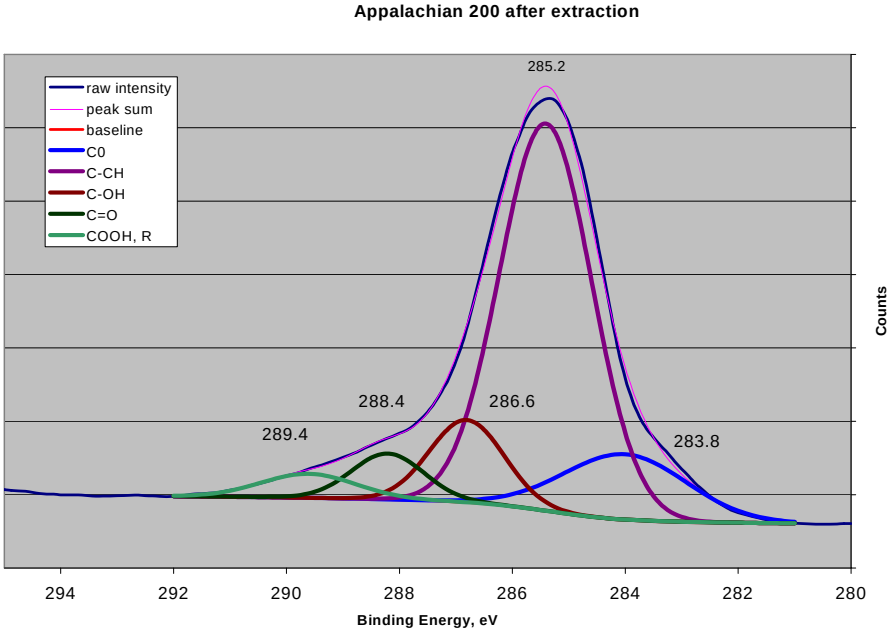


Figure A. 12. Appalachian oak 200 °C after extraction.

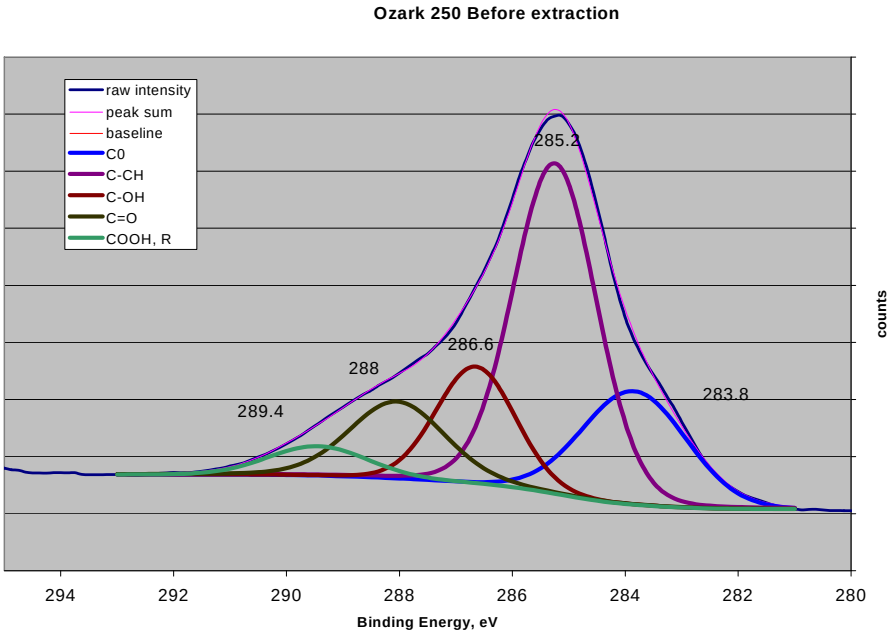


Figure A. 13. Ozark oak 250 °C before extraction.

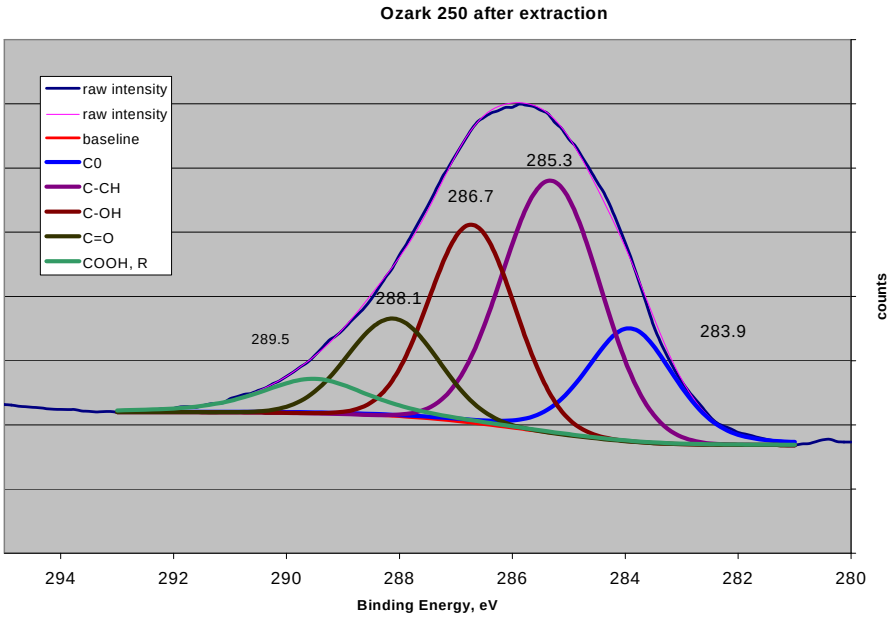


Figure A. 14. Ozark oak 250 °C after extraction.

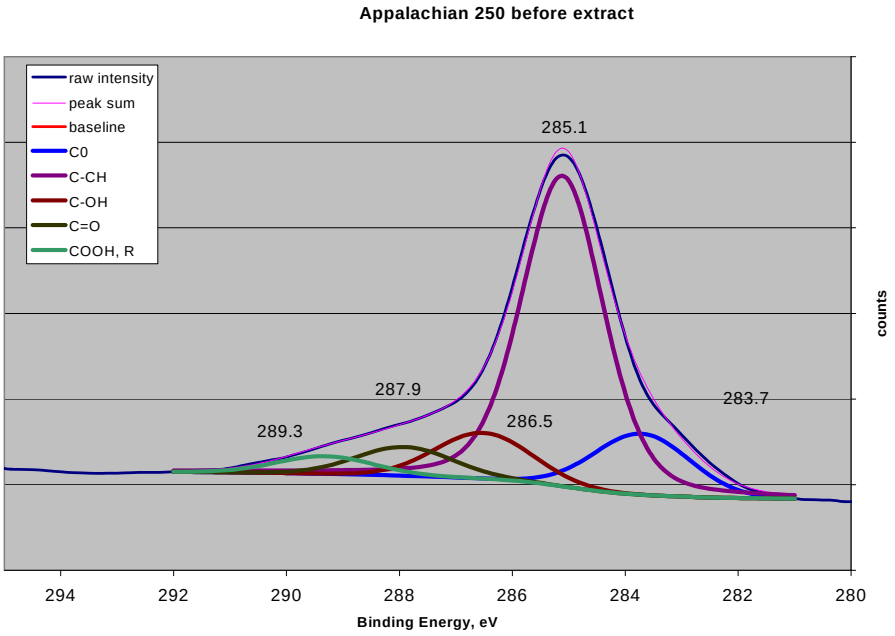


Figure A. 15. Appalachian oak 250 °C before extraction

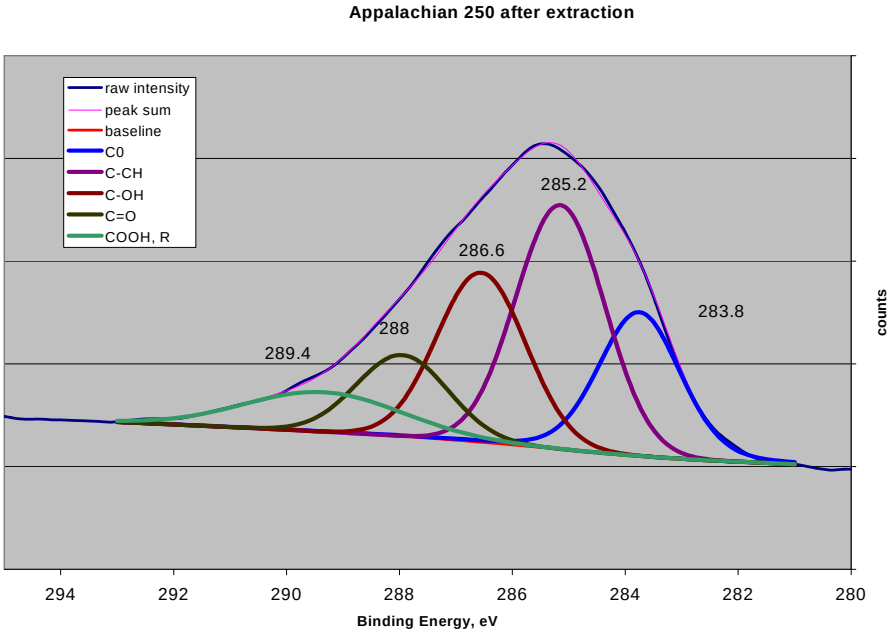


Figure A. 16. Appalachian oak 250 °C after extraction.

Table A. 1. Appalachian oak XPS Peak Positions

	average peak position		std	average percent	std
CO	App	283.8	0.07	0.15	0.01
C1		285.2	0.08	0.60	0.02
C2		286.6	0.08	0.12	0.00
C3		288.0	0.08	0.08	0.00
C4		289.4	0.08	0.05	0.01
CO	App extract	284.0	0.27	0.24	0.03
C1		285.4	0.27	0.42	0.03
C2		286.8	0.27	0.18	0.01
C3		288.2	0.27	0.11	0.01
C4		289.6	0.27	0.04	0.03
CO	App 150	283.5	0.13	0.09	0.01
C1		284.9	0.13	0.73	0.03
C2		286.3	0.13	0.09	0.02
C3		287.7	0.13	0.05	0.01
C4		289.1	0.14	0.03	0.00
CO	App 150 extract	283.9	0.06	0.23	0.01
C1		285.3	0.07	0.43	0.03
C2		286.7	0.07	0.20	0.03
C3		288.1	0.07	0.10	0.01
C4		289.5	0.07	0.03	0.01
CO	App 200	284.0	0.20	0.18	0.03
C1		285.4	0.20	0.45	0.03
C2		286.8	0.20	0.21	0.03
C3		288.2	0.20	0.12	0.02
C4		289.6	0.20	0.05	0.01
CO	App 200 extract	283.8	0.16	0.11	0.03
C1		285.2	0.16	0.66	0.02
C2		286.6	0.16	0.14	0.02
C3		288.0	0.16	0.05	0.01
C4		289.4	0.16	0.04	0.00
CO	App 250	283.7	0.01	0.19	0.01
C1		285.1	0.01	0.55	0.02
C2		286.5	0.01	0.17	0.02
C3		287.9	0.01	0.04	0.02
C4		289.3	0.01	0.05	0.01
CO	App 250 ext	283.8	0.11	0.21	0.01
C1		285.2	0.11	0.39	0.03
C2		286.6	0.11	0.21	0.03
C3		288.0	0.11	0.11	0.02
C4		289.4	0.11	0.08	0.03

Table A. 2. Ozark oak XPS Peak Positions

		average peak pos	std	average area	std
CO	Ozark Cont	283.5	0.01	0.08	0.00
C1		284.9	0.01	0.65	0.01
C2		286.3	0.01	0.18	0.00
C3		287.7	0.01	0.04	0.00
C4		289.1	0.01	0.05	0.00
CO	Ozark Ext Cont	283.9	0.04	0.16	0.00
C1		285.3	0.04	0.56	0.01
C2		286.7	0.04	0.16	0.01
C3		288.1	0.04	0.08	0.00
C4		289.5	0.04	0.04	0.00
CO	Ozark 150	283.9	0.04	0.10	0.00
C1		285.3	0.04	0.56	0.01
C2		286.7	0.04	0.21	0.01
C3		288.1	0.04	0.07	0.00
C4		289.5	0.04	0.05	0.00
CO	Ozark 150 ext	283.5	0.01	0.13	0.01
C1		284.9	0.01	0.53	0.03
C2		286.3	0.01	0.28	0.04
C3		287.7	0.01	0.03	0.02
C4		289.1	0.01	0.03	0.01
CO	Ozark 200	283.7	0.05	0.07	0.00
C1		285.1	0.05	0.75	0.00
C2		286.5	0.05	0.11	0.00
C3		287.9	0.05	0.04	0.00
C4		289.3	0.05	0.03	0.00
CO	Ozark 200 extract	283.7	0.05	0.09	0.02
C1		285.1	0.05	0.48	0.03
C2		286.5	0.05	0.27	0.03
C3		287.9	0.05	0.08	0.02
C4		289.3	0.05	0.08	0.01
CO	Ozark 250	283.4	0.00	0.20	0.01
C1		284.8	0.00	0.46	0.02
C2		286.2	0.00	0.18	0.02
C3		287.6	0.00	0.11	0.00
C4		289.0	0.00	0.06	0.01
CO	Ozark 250 ext	283.6	0.24	0.16	0.02
C1		285.0	0.24	0.38	0.01
C2		286.4	0.24	0.26	0.00
C3		287.8	0.24	0.14	0.01
C4		289.2	0.24	0.07	0.00

Vita

Roy Douglas Wilcox was born in Dallas, Texas, attended primary school in Los Angeles, California, and graduated from North Iredell High School in North Carolina. He received a Bachelor of Arts degree in chemistry from Appalachian State University, Boone, North Carolina, and a Master of Science degree in chemistry from the University of Tennessee, Knoxville. He then worked for twelve years at Baroid Drilling Fluids, Inc., which is now a division of Halliburton Corporation, in Houston, Texas. As a senior scientist and later the industry liaison manager, he developed products, received a patent, and published papers in professional technical journals.

After moving back to Knoxville, he worked in technical management for Singleton Laboratories and Midlab, Inc., and received a Master of Education from the University of Tennessee. He is currently teaching chemistry at Lincoln Memorial University, Harrogate, Tennessee.